

Refined topological vertex with ON-planes

Sung-Soo Kim, Xing-Yue Wei

*School of Physics, University of Electronic Science and Technology of China,
No. 2006 Xiyuan Ave, West Hi-Tech Zone, Chengdu, Sichuan 611731, China*

E-mail: sungsoo.kim@uestc.edu.cn, xingyue_wei@std.uestc.edu.cn

ABSTRACT: We propose refined topological vertex formalism for 5-brane systems with ON-planes by introducing a new vertex associated with reflection over an ON-plane, which gives rise to new vertex and edge factors. We test our proposal against various 5d $\mathcal{N} = 1$ gauge theories which can be realized as 5-brane webs with ON-planes, which include D -type quiver theories. In particular, we compute the refined partition functions for 6d E-string theory on a circle as well as 5d SU(3) theory at the Chern-Simons level 9, which can be realized as 5-brane webs with two ON-planes. Our results completely agree with the known results.

Contents

1	Introduction	1
2	Refined topological vertex with ON-planes	3
2.1	5-brane web	3
2.2	Topological vertex	4
2.3	Refined topological vertex with ON-planes	7
3	Examples	16
3.1	5d SU(2)+4F	17
3.2	5d SU(2)+8F: E-string theory as 5d affine D_4 quiver	24
3.3	5d SU(3) theory at CS level 7	28
3.4	5d SU(3) theory at CS level 9	38
4	Conclusion	42
A	Characters	43
B	Reflected 5-brane web with $C^{\mathbf{R}}$ and $\tilde{f}^{\mathbf{R}}$.	44

1 Introduction

String theory and M-theory have provided various useful tools for studying supersymmetric field theories. For example, 5-brane webs in Type IIB string theory [1, 2] and M-theory compactified on a Calabi-Yau threefold [3–5] have shed light on uncovering various noble aspects for supersymmetric theories of eight supercharges in five and six dimensions (5d/6d). In particular, 5-brane webs have been a useful tool for better understanding of 5d superconformal theories qualitatively as well as quantitatively. Different gauge theories can be described by different brane systems with or without introduction of orientifold planes. Their interplay through Hanany-Witten transitions, resolutions of an orientifold $O7^-$ -plane to two 7-branes, and S-duality has revealed various gauge theory descriptions.

Many 6d theories on a circle with or without a twist are represented on a 5-brane web as a 5d KK theory. 5d SU(2) gauge theory with 8 hypermultiplets in the fundamental representation is an interesting example of a KK theory for 6d E-string theory on a circle [6–8]. As discussed in [9], the corresponding 5-brane web has a repeated spiral configuration called Tao web diagram, which gives rise to a constant

period related to the radius of the compactification circle. This hence provides a diagrammatic characteristic of KK spectrum of the theory. The E-string theory can also be described by an affine D_4 quiver which consists of an $SU(2)$ node in the middle and four “ $SU(1)$ ” nodes at each quadrivalent leg. This is a realization of 6d (D_4, D_4) conformal matter theory. Such quiver theories are described as a 5-brane web with two ON-planes. An ON-plane is the S-dual orientifold of an O5-plane [10–13]. ON-planes are even more useful than just describing a D -type quiver theory, as $SU(3)$ gauge theory at higher Chern-Simons levels can be constructed with ON-planes [14].

With such various 5-brane systems, one can compute their BPS spectrum. In fact, there has been various progress on computing partition functions of 5d/6d $\mathcal{N} = 1$ supersymmetric gauge theories. For instance, the ADHM method [15–21], the Ding-Iohara-Miki algebra [22–25], topological vertex [26–30] and blowup equation [31–40]. In particular, the blowup method can be applied to theories without 5-brane configurations or any Lagrangian descriptions [39, 40].

In this paper, we attempt to develop and generalize the topological vertex which is a computation tool based on 5-brane webs as they provide intuitive pictures, and we confirm our result with known results obtained by other methods. Topological vertex works very well for toric 5-brane webs but it has some challenges for non-toric webs with orientifolds. For $O7^-$ cases, one can resolve an $O7^-$ -plane into two 7-branes [41] and hence it leads to a non-toric 5-brane web without the orientifold plane. In such case, we can obtain the partition function as the Higgsing [42–44]. For the O5 case [13, 14, 45–48], on the other hand, the application of topological vertex was first proposed in [49] and further developed in [50–53]. The 5-brane transition on an O5-plane where two 5-branes intersect gives rise to a phase where they can be smoothly connected to the mirror images reflected due to the O5-plane. But these are only available for unrefined cases, where the sum of two Omega deformation parameters is set to zero, $\epsilon_1 + \epsilon_2 = 0$. Generalization toward the refined topological vertex is still a difficult task. The main difficulty comes from the Omega deformation parameters assigned to the original web and the reflected web which are not compatible with topological vertex formulation with conventional choice of the preferred direction which is parallel to O5-plane. To avoid this difficulty, we, instead, consider the ON case, which one can regard as an S-dual of O5-plane [13, 54, 55]. It has a technical advantage for generalizing to the refined case, as the preferred direction is perpendicular to an ON-plane.

A 5-brane web with an ON-plane describes a D -type quiver. For such 5-brane configurations with ON-planes, we propose new refined vertex and edge factors so that they account for the 5-brane system reflected over an ON-plane, as a generalization of unrefined topological vertex formalism [49].¹ In fact, these new factors are

¹There is an algebraic construction for a D -type quiver based on the DIM algebra [56, 57], which may lead to refined topological vertex. Our proposal is different from this as it is a generalization

not just a computational device, it is another set of vertex and edge factors which is equally applicable for computation of the partition function. For instance, we explicitly show that one can use our new factors to obtain the same partition function based on a 5-brane web without an ON-plane. We demonstrate our proposal with various theories where ON-planes are used for constructing the corresponding 5-brane systems, which include the $SU(2)$ theory with 8 flavors and the $SU(3)$ theory at the CS level 7 and 9. We also present the exact form of one- and two-instanton partition function for these theories. In particular, the refined partition function for the $SU(3)$ theory at the CS level 9 is recently computed based on the blowup equation [39] and our prescription perfectly reproduces this result.

The organization of the paper is as follows: In section 2, we start with reviewing the refined topological vertex and propose a new vertex factor that accounts the reflection due to an ON-plane. In section 3, we apply the proposed refined topological vertex to various gauge theories which can be realized with one or two ON-plane(s). We discuss $SU(2) + 4\mathbf{F}$ as an instructive example, and then compute the partition functions for the E-string on a circle and 5d $SU(3)$ gauge theory at the Chern-Simons levels 7 and 9. We summarize our result in section 4. In Appendix A, we list the characters of global symmetries discussed in the main text. In Appendix B, we discuss how one can obtain the partition function of a 5-brane web without ON-planes by only using the new vertex and edge factors.

2 Refined topological vertex with ON-planes

In this section, we discuss salient feature of the refined topological vertex [28] and then we generalize it to 5-brane systems with ON-planes.

2.1 5-brane web

A large class of 5d $\mathcal{N} = 1$ supersymmetric theories can be realized through 5-brane webs in Type IIB string theory. With the convention that $(1, 0)$ 5-brane refers to D5-brane and $(0, 1)$ 5-brane refers to NS5-brane, 5d $\mathcal{N} = 1$ supersymmetric field theories form a charge conserving configuration of various (p, q) 5-branes. A simple web diagram is given in Figure 1, where D5-branes are extended along $x^0, x^1, x^2, x^3, x^4, x^6$ while NS5-branes are extended along $x^0, x^1, x^2, x^3, x^4, x^5$ and 5-brane webs are given in a (x^5, x^6) -plane called the (p, q) -plane, as summarized in Table 1.

of the unrefined topological vertex to the refined one.

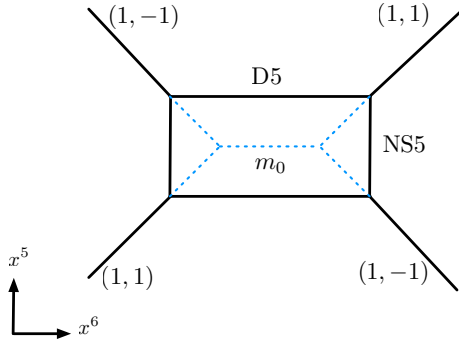


Figure 1. A 5-brane web for the $SU(2)_0$ gauge theory.

	0	1	2	3	4	5	6	7	8	9
NS5 / ON	×	×	×	×	×	×				
D5 / O5	×	×	×	×	×		×			
(p, q)	×	×	×	×	×	ϑ	ϑ			
7-brane / O7	×	×	×	×	×			×	×	×

Table 1. Worldvolume configuration of 5-brane webs. The occupation of each brane is marked with \times or ϑ , where a (p_1, q_1) 5-brane appears as a line on the (p, q) -plane with the slope given by $\vartheta = \tan^{-1}(q_1/p_1)$.

In Figure 1, a 5-brane web for 5d $SU(2)_0$ gauge theory of the vanishing discrete theta parameter is drawn. Here, the Kähler parameter along the NS5-brane connecting two D5-branes is associated with the Coulomb branch moduli, while the Kähler parameter between two NS5-branes is associated with a product of the instanton factor and the Coulomb branch parameter. More precisely, the instanton factor is given by $u = e^{-\beta m_0}$, where m_0 is the inverse gauge coupling squared and corresponds to the distance between two NS5 branes at trivial Kähler parameter for the Coulomb branch moduli as shown in Figure 1. In a similar fashion, the instanton factor for gauge theories of higher rank is defined. One can introduce 7-branes such that the external 5-branes are attached. With these 7-branes, one can explicitly show various dualities by the Hanany-Witten moves. 5-brane webs also provide a way to compute the BPS spectrum of the theory through topological vertex [27, 28], which we shall discuss in the next subsection.

2.2 Topological vertex

The refined topological vertex is a powerful way of computing the partition functions of 5d supersymmetric gauge theories on the Ω background, $\mathbb{R}_{\epsilon_1, \epsilon_2}^4 \times S^1$. With the fugacity of Ω -deformation parameters $\mathfrak{q} = e^{-\beta\epsilon_1}$ and $\mathfrak{t} = e^{\beta\epsilon_2}$, the partition function Z is given as a sum of the Young diagrams λ, μ, ν, \dots along edge factors and vertex

factors for a given 5-brane web,

$$Z = \sum_{\lambda, \mu, \nu, \dots} \left(\prod \text{edge factor} \right) \left(\prod \text{vertex factor} \right). \quad (2.1)$$

Here, following the convention used in [58], the edge factor and vertex factor are defined as follows. For all the internal edges of a 5-brane web, we associate each edge with a Kähler parameter Q , an arrow, and a Young diagram (or integer partition) $\mu = (\mu_1, \mu_2, \dots, \mu_{\ell(\mu)})$, where flopping the arrow corresponds to the transpose μ^t of the associated Young diagram μ . The edge factor is then given as

$$(-Q)^{|\mu|} \mathfrak{f}_\mu^{\mathbf{n}}, \quad (2.2)$$

where the framing factor function \mathfrak{f}_μ takes the form: along the preferred direction,

$$\mathfrak{f}_\mu \rightarrow f_\mu(\mathbf{t}, \mathbf{q}) = (-1)^{|\mu|} \mathbf{t}^{\frac{\|\mu^t\|^2}{2}} \mathbf{q}^{-\frac{\|\mu\|^2}{2}} = f_{\mu^t}(\mathbf{q}, \mathbf{t})^{-1}, \quad (2.3)$$

and along the non-preferred directions,

$$\mathfrak{f}_\mu \rightarrow \tilde{f}_\mu(\mathbf{t}, \mathbf{q}) = (-1)^{|\mu|} \mathbf{t}^{\frac{\|\mu^t\|^2 + |\mu|}{2}} \mathbf{q}^{-\frac{\|\mu\|^2 + |\mu|}{2}} = \tilde{f}_{\mu^t}(\mathbf{q}, \mathbf{t})^{-1}, \quad (2.4)$$

where

$$|\mu| = \sum_{i=1}^{\ell(\mu)} \mu_i, \quad \|\mu\|^2 = \sum_{i=1}^{\ell(\mu)} \mu_i^2, \quad (2.5)$$

and the power \mathbf{n} is defined as $\mathbf{n} = v_{\text{in}} \wedge v_{\text{out}} = p_1 q_2 - p_2 q_1$ for a pair of charges $v_{\text{in}} = (p_1, q_1)$ and $v_{\text{out}} = (p_2, q_2)$ which are connected to the edge of Q , where v_{in} and v_{out} are two dimensional vectors $(\pm p, \pm q)$ associated with the (p, q) charge of the corresponding brane with \pm signs chosen to be compatible with the directions of the vectors.

The vertex factor is assigned to each vertex of three out-going edges with three Young diagrams λ, μ, ν in clockwise direction where the last Young diagram ν is reserved for Young diagram on the edge of the preferred direction, and it is defined as

$$C_{\lambda\mu\nu}(\mathbf{t}, \mathbf{q}) = \mathbf{q}^{\frac{\|\mu\|^2 + \|\nu\|^2}{2}} \mathbf{t}^{-\frac{\|\mu^t\|^2}{2}} \tilde{Z}_\nu(\mathbf{t}, \mathbf{q}) \sum_{\eta} \left(\frac{\mathbf{q}}{\mathbf{t}} \right)^{\frac{|\eta| + |\lambda| - |\mu|}{2}} s_{\lambda^t/\eta}(\mathbf{t}^{-\rho} \mathbf{q}^{-\nu}) s_{\mu/\eta}(\mathbf{q}^{-\rho} \mathbf{t}^{-\nu^t}), \quad (2.6)$$

where \mathbf{t} and \mathbf{q} are assigned to the edge associated with λ and μ , respectively, and

$$\tilde{Z}_\nu(\mathbf{t}, \mathbf{q}) = \prod_{i=1}^{\ell(\nu)} \prod_{j=1}^{\nu_i} (1 - \mathbf{t}^{\nu_j^t - i + 1} \mathbf{q}^{\nu_i - j})^{-1}, \quad (2.7)$$

and $s_{\sigma/\eta}(\mathbf{x})$ are the skew-Schur functions of an infinite vector \mathbf{x} , e.g., $\mathbf{t}^{-\rho}\mathbf{q}^{-\nu} = (\mathbf{t}^{\frac{1}{2}}\mathbf{q}^{-\nu_1}, \mathbf{t}^{\frac{3}{2}}\mathbf{q}^{-\nu_2}, \dots)$.

We list some special functions that are useful in actual computation:

$$\mathcal{R}_{\lambda\mu}(Q; \mathbf{t}, \mathbf{q}) := \prod_{i,j=1}^{\infty} \left(1 - Q\mathbf{t}^{i-\frac{1}{2}-\lambda_j}\mathbf{q}^{j-\frac{1}{2}-\mu_i}\right) = \mathcal{M}(Q\sqrt{\frac{\mathbf{t}}{\mathbf{q}}}; \mathbf{t}, \mathbf{q})^{-1} \mathcal{N}_{\lambda^t\mu}(Q\sqrt{\frac{\mathbf{t}}{\mathbf{q}}}; \mathbf{t}, \mathbf{q}), \quad (2.8)$$

$$\mathcal{M}(Q; \mathbf{t}, \mathbf{q}) := \prod_{i,j=1}^{\infty} (1 - Q\mathbf{t}^{i-1}\mathbf{q}^j)^{-1}, \quad (2.9)$$

$$\begin{aligned} \mathcal{N}_{\lambda\mu}(Q; \mathbf{t}, \mathbf{q}) &:= \prod_{i,j=1}^{\infty} \frac{1 - Q\mathbf{t}^{i-1-\lambda_j^t}\mathbf{q}^{j-\mu_i}}{1 - Q\mathbf{t}^{i-1}\mathbf{q}^j} \\ &= \prod_{(i,j) \in \lambda} (1 - Q\mathbf{t}^{\mu_j^t - i}\mathbf{q}^{\lambda_i - j + 1}) \prod_{(i,j) \in \mu} (1 - Q\mathbf{t}^{-\lambda_j^t + i - 1}\mathbf{q}^{-\mu_i + j}). \end{aligned} \quad (2.10)$$

To evaluate the Young diagram sums along non-preferred directions, one needs to repeatedly use the Cauchy identities²

$$\begin{aligned} &\sum_{\lambda} Q^{|\lambda|} s_{\lambda/\mu_1}(Q_1\mathbf{t}^{-\rho}\mathbf{q}^{-\nu_1}) s_{\lambda^t/\mu_2}(Q_2\mathbf{q}^{-\rho}\mathbf{t}^{-\nu_2}) \\ &= \mathcal{R}_{\nu_2\nu_1}(-QQ_1Q_2) \sum_{\lambda} Q^{|\lambda|} s_{\mu_2^t/\lambda}(QQ_1\mathbf{t}^{-\rho}\mathbf{q}^{-\nu_1}) s_{\mu_1^t/\lambda^t}(QQ_2\mathbf{q}^{-\rho}\mathbf{t}^{-\nu_2}). \end{aligned} \quad (2.11)$$

$$\begin{aligned} &\sum_{\lambda} Q^{|\lambda|} s_{\lambda/\mu_1}(Q_1\mathbf{t}^{-\rho}\mathbf{q}^{-\nu_1}) s_{\lambda/\mu_2}(Q_2\mathbf{q}^{-\rho}\mathbf{t}^{-\nu_2}) \\ &= \mathcal{R}_{\nu_2\nu_1}(QQ_1Q_2)^{-1} \sum_{\lambda} Q^{|\lambda|} s_{\mu_2/\lambda}(QQ_1\mathbf{t}^{-\rho}\mathbf{q}^{-\nu_1}) s_{\mu_1/\lambda}(QQ_2\mathbf{q}^{-\rho}\mathbf{t}^{-\nu_2}). \end{aligned} \quad (2.12)$$

Conventions. In the rest of the paper except for the beginning of section 2.3, to avoid the cluttering of the 5-brane diagrams, we use the following convention when assigning \mathbf{t} , \mathbf{q} , arrows, and Young diagrams:

- (1) The preferred direction is always along the horizontal edges and the arrows associated with it are chosen to point toward the left. The arrows along non-preferred directions are chosen to point upward.
- (2) The Ω -deformation parameters $\mathbf{q} = e^{-\beta\epsilon_1}$, $\mathbf{t} = e^{\beta\epsilon_2}$ are assigned such that \mathbf{t} 's are always placed above the edges associated with the preferred direction, while \mathbf{q} 's are placed below the edges associated with the preferred direction.
- (3) We use the Greek letters μ, ν, \dots to denote the Young diagrams. If an edge is labelled by a Young diagram, say α , then we also call the edge as edge α or brane α for simplicity.

²These identities are slightly modified from the ones in [58].

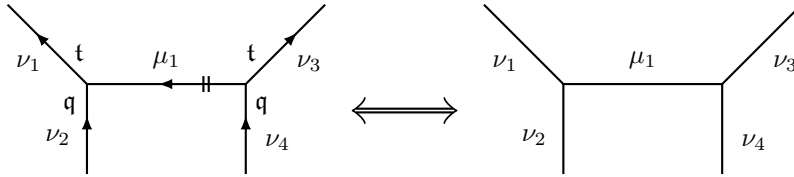


Figure 2. Convention for assignment of the arrows and the Ω -deformation parameters throughout the paper.

For instance, the 5-brane web on the right-hand side of Figure 2 should be understood as the 5-brane web with the assignments given on the left-hand side.

We also define

$$\mathcal{R}_{\lambda\mu}(Q) \equiv \mathcal{R}_{\lambda\mu}(Q; \mathbf{t}, \mathbf{q}), \quad \mathcal{N}_{\lambda\mu}(Q) \equiv \mathcal{N}_{\lambda\mu}(Q; \mathbf{t}, \mathbf{q}), \quad \mathcal{M}(Q) \equiv \mathcal{M}(Q; \mathbf{t}, \mathbf{q}) \quad (2.13)$$

for simplicity. The products of several Kähler parameters are expressed as a shorthand notation, for example, $Q_{i,j^2,k} \equiv Q_i Q_j^2 Q_k$. On the other hand, $\mu_{i,j,k}$ means μ_i, μ_j, μ_k for short which we will use occasionally.

2.3 Refined topological vertex with ON-planes

The refined topological vertex formalism discussed in the previous section works well with those 5-brane webs which do not involve orientifold planes like O5-, O7⁺-, or ON-planes. It is also applicable for 5-brane web systems with O7⁻-planes, as an O7⁻-plane can be resolved into a pair of two 7-branes, [1, -1], [1, 1] 7-branes or [2, -1], [0, 1] 7-branes [41]. Such 5-brane configuration with the resolved 7-branes can be understood as the Higgsing [42, 59]. In this subsection, we attempt to generalize the refined topological vertex to be applicable for 5-brane webs with orientifold planes. As discussed, unrefined topological vertex formalism with O5/ON-planes was introduced. Let us first discuss some of relevant features of this formalism and generalize them to refined topological vertex with an orientifold plane.

To this end, we first recall the unrefined case with an O5-plane (or an ON-plane) [49]. For the unrefined case, $\mathbf{t} = \mathbf{q} = g$, one introduces the vertex factor for the reflected image due to the orientifold plane where the Young diagrams of the vertex factor for the reflected image are all transposed. The vertex factor for the reflected images satisfies the following reflection identity

$$C_{\mu^t \lambda^t \nu^t} = (-1)^{|\lambda|+|\mu|+|\nu|} f_\lambda(g) f_\mu(g) f_\nu(g) C_{\lambda\mu\nu} . \quad (2.14)$$

This is an important identity as it gives rise to the relation between the vertex factor for the reflected image of 5-branes due to an O5/ON-plane and that defined on 5-brane web without O5/ON-plane. It is therefore natural to generalize the reflection identity (2.14) to the refined case.

New vertex factor. We introduce the following refined vertex factor for reflected image of a 5-brane web with an ON-plane or an O5-plane:

$$C_{\lambda\mu\nu}^{\text{R}}(\mathbf{t}, \mathbf{q}) = \mathbf{q}^{\frac{\|\mu\|^2 + \|\nu\|^2}{2}} \mathbf{t}^{-\frac{\|\mu^t\|^2}{2}} \tilde{Z}_\nu(\mathbf{t}, \mathbf{q}) \sum_{\eta} \left(\frac{\mathbf{q}}{\mathbf{t}} \right)^{\frac{-|\eta| + |\lambda| - |\mu|}{2}} s_{\lambda^t/\eta}(\mathbf{t}^{-\rho} \mathbf{q}^{-\nu}) s_{\mu/\eta}(\mathbf{q}^{-\rho} \mathbf{t}^{-\nu^t}). \quad (2.15)$$

Here, we used the superscript ^R to denote that this new vertex factor is associated with the reflected image and also to distinguish the conventional vertex factor C . Compared with the vertex factor C in (2.6), C^{R} has the opposite sign in front of $|\eta|$ appearing in the power of $\frac{\mathbf{q}}{\mathbf{t}}$. We note that these two kinds of vertex factors are related by the following relation

$$C_{\nu^t \mu^t \sigma^t}^{\text{R}}(\mathbf{q}, \mathbf{t}) = (-1)^{|\mu| + |\nu| + |\sigma|} f_{\mu}(\mathbf{t}, \mathbf{q}) f_{\nu}(\mathbf{t}, \mathbf{q}) f_{\sigma}(\mathbf{t}, \mathbf{q}) \frac{\tilde{Z}_{\sigma^t}(\mathbf{q}, \mathbf{t})}{\tilde{Z}_{\sigma}(\mathbf{t}, \mathbf{q})} C_{\mu\nu\sigma}(\mathbf{t}, \mathbf{q}), \quad (2.16)$$

or equivalently,

$$C_{\mu\nu\sigma}(\mathbf{t}, \mathbf{q}) = (-1)^{|\nu^t| + |\mu^t| + |\sigma^t|} f_{\nu^t}(\mathbf{q}, \mathbf{t}) f_{\mu^t}(\mathbf{q}, \mathbf{t}) f_{\sigma^t}(\mathbf{q}, \mathbf{t}) \frac{\tilde{Z}_{\sigma}(\mathbf{t}, \mathbf{q})}{\tilde{Z}_{\sigma^t}(\mathbf{q}, \mathbf{t})} C_{\nu^t \mu^t \sigma^t}^{\text{R}}(\mathbf{q}, \mathbf{t}), \quad (2.17)$$

which is a refined version of the reflection identity (2.14). It is straightforward to check that in the unrefined limit, the reflected vertex C^{R} reduces to the usual C , and the refined reflection identities (2.16) and (2.17) become the unrefined identity (2.14). In Figure 3, the assignments of Young diagrams and \mathbf{t}, \mathbf{q} associated with the new vertex factor C^{R} are depicted in comparison with those for the usual vertex factor C . As discussed earlier, in usual refined topological vertex formalism, the Young diagrams of $C_{\mu\nu\sigma}(\mathbf{t}, \mathbf{q})$ are assigned clockwise with the last one being the preferred direction. We follow the same rule for the new vertex factor C^{R} . Likewise, the assignments of \mathbf{t}, \mathbf{q} in the reflected image are also given clockwise as in Figure 3. So, for the vertex factor $C_{\nu^t \mu^t \sigma^t}^{\text{R}}(\mathbf{q}, \mathbf{t})$ in the reflected image, Young diagrams and \mathbf{t}, \mathbf{q} are treated in the same way as those in the usual C vertex function as illustrated in Figure 3.

We note that when a Young diagram along the non-preferred direction of C^{R} is of an empty set, C^{R} is equal to C as the vertex factor is only nonzero for $\eta = \emptyset$. Unlike the unrefined case, both vertex factors C and C^{R} are necessary for the refined case. As a 5-brane configuration away from an ON-plane looks like usual web without an ON-plane, only vertices near an ON-plane are related to C^{R} . Even more, we claim that C^{R} 's appear only on the strips of NS-branes that are next to an ON-plane and all other vertices are assigned with C 's.

We also note that as shown in Figure 3(b), the assignments of \mathbf{t}, \mathbf{q} are exchanged in the reflected image of the vertex over an O5-plane which makes it more difficult to deal with in refined topological vertex formalism, so from now on we only consider cases with ON-planes in this paper.

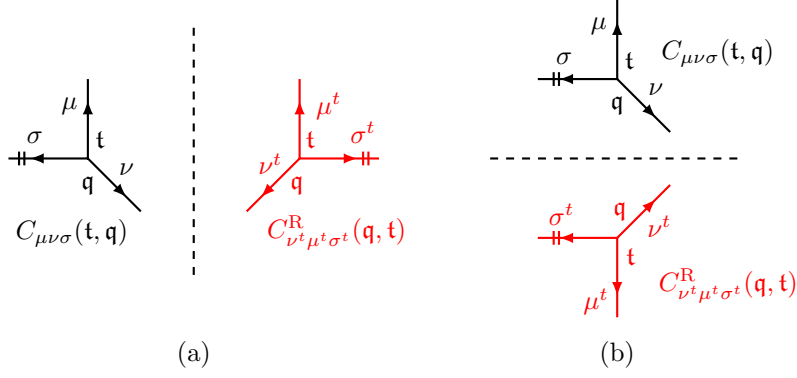


Figure 3. The usual vertex factor C and the reflected vertex factor C^R . (a) is for the case of ON-plane reflection and (b) is for the case of O5-plane reflection.

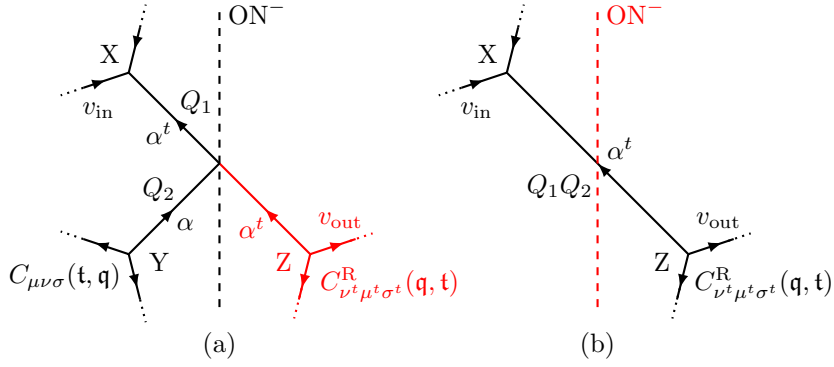


Figure 4. Reflection of the brane α by the ON-plane.

New Edge factors. Together with the new vertex factor C^R , new edge factors naturally follow in the refined topological vertex with ON-plane. Consider 5-brane configuration near an ON-plane, as depicted in Figure 4. Figure 4(a) represents typical 5-brane configuration with an ON-plane. On the other hand, Figure 4(b) represents a 5-brane configuration with half of 5-brane webs being reflected over an ON-plane so that the corresponding 5-brane web appears to be smoothly connected as if there is no ON-plane. Here the new vertex factor C^R is introduced and the corresponding Young diagram is transposed accordingly.

To be more general, we introduce generic vertices X, Y, and Z in Figure 4 which are associated with either usual vertex factor C or the reflected vertex factor C^R and denote them by C_X, C_Y and C_Z . Let us first consider the case where C_Y is the usual vertex factor $C_Y = C$, which is the case depicted in Figure 4(a). We will consider the case where C_Y is associated with C^R later. To be more specific, C_Y is $C_{\mu\nu\sigma}(\mathbf{t}, \mathbf{q})$ where σ is assumed to be along the preferred direction. We also introduce the Young diagram α which is one of the Young diagrams μ, ν, σ associated with the vertex factor $C_{\mu\nu\sigma}(\mathbf{t}, \mathbf{q})$, *i.e.*, $\alpha \in \{\mu, \nu, \sigma\}$. Depending on whether α is along the preferred

direction or not, we will have different new edge factors. Note that Z in Figure 4(b) is the reflected vertex of Y in Figure 4(a). As we consider the case $C_Y = C_{\mu\nu\sigma}(\mathbf{t}, \mathbf{q})$, the vertex factor associated with Z is given as $C_Z = C_{\nu^t\mu^t\sigma^t}^{\mathbf{R}}(\mathbf{q}, \mathbf{t})$.

We now write the edge factor for the edge associated with the Young diagram α^t (of the Kähler parameter Q_1Q_2) in Figure 4(b), which is the edge connecting the vertices X and Z. As Z is the reflected image of Y, this would lead to how to define or construct the edge factor associated with Y. The product of the edge factor and vertex factors associated with the edge between X and Z can be written as

$$\begin{aligned} & C_X \cdot (-Q_1Q_2)^{|\alpha^t|} \mathcal{F}_{\alpha^t} \cdot C_Z \\ &= C_X \cdot (-Q_1Q_2)^{|\alpha^t|} \mathcal{F}_{\alpha^t} \cdot C_{\nu^t\mu^t\sigma^t}^{\mathbf{R}}(\mathbf{q}, \mathbf{t}) \\ &= C_X \cdot (+Q_1Q_2)^{|\alpha|} \left(\mathcal{F}_{\alpha^t} f_{\alpha}(\mathbf{t}, \mathbf{q}) \right) \left(\frac{\tilde{Z}_{\sigma^t}(\mathbf{q}, \mathbf{t})}{\tilde{Z}_{\sigma}(\mathbf{t}, \mathbf{q})} \right)^{\delta_{\alpha\sigma}} \cdot C_{\mu\nu\sigma}(\mathbf{t}, \mathbf{q}) \cdot (\dots), \end{aligned} \quad (2.18)$$

where we denote by \mathcal{F}_{α^t} the framing factor associated with Q_1Q_2 . In the second equality, we used (2.15) to express $C^{\mathbf{R}}$ into usual vertex factor C . As we are only interested in finding new edge factor involving α , we neglect irrelevant α -independent parts by putting them into the ellipsis (\dots) in (2.18). If the Young diagram α is along the preferred diction, namely $\alpha = \sigma$, then $\delta_{\alpha\sigma} = 1$; otherwise $\delta_{\alpha\sigma} = 0$. Notice that $C_{\mu\nu\sigma}(\mathbf{t}, \mathbf{q})$ in (2.18) is nothing but C_Y . This hence leads to the edge factor between the vertices X and Y in Figure 4(a). The new edge is then given by

$$(+Q_1Q_2)^{|\alpha|} (f_{\alpha}(\mathbf{t}, \mathbf{q}) \mathcal{F}_{\alpha^t}) \left(\frac{\tilde{Z}_{\sigma^t}(\mathbf{q}, \mathbf{t})}{\tilde{Z}_{\sigma}(\mathbf{t}, \mathbf{q})} \right)^{\delta_{\alpha\sigma}}, \quad \alpha \in \{\mu, \nu, \sigma\}. \quad (2.19)$$

We note that so far we consider the case where $C_Z = C^{\mathbf{R}}$. In general, C_Z can also be of the usual vertex factor C . Of course, if C_X and C_Z are all of C , then the framing factor \mathcal{F}_{α^t} is simply $f_{\alpha^t}^{\mathbf{n}}$ or $\tilde{f}_{\alpha^t}^{\mathbf{n}}$. We will also discuss other C_X and C_Z cases later.

Consider also the case $C_Y = C_{\mu\nu\sigma}^{\mathbf{R}}(\mathbf{t}, \mathbf{q})$, which means $C_Z = C_{\nu^t\mu^t\sigma^t}(\mathbf{q}, \mathbf{t})$ accordingly. In this case, by repeating a similar calculation as (2.18) taking into account (2.17), one finds that the resulting edge factor is still the same form as (2.19). When the order of \mathbf{t}, \mathbf{q} in the argument of Y exchanges, namely $C_Y = C_{\dots}^{\mathbf{R}}(\mathbf{q}, \mathbf{t})$, the edge factor also correspondingly changes to

$$(+Q_1Q_2)^{|\alpha|} (f_{\alpha}(\mathbf{q}, \mathbf{t}) \mathcal{F}_{\alpha^t}) \left(\frac{\tilde{Z}_{\sigma^t}(\mathbf{t}, \mathbf{q})}{\tilde{Z}_{\sigma}(\mathbf{q}, \mathbf{t})} \right)^{\delta_{\alpha\sigma}}, \quad \alpha \in \{\mu, \nu, \sigma\}. \quad (2.20)$$

We note that the analysis above is based on Figure 4 in which the ON-plane is on the right-hand side. If an ON-plane is on the left-hand side, we can still do the similar analysis which yields that the edge factor is still given as the form of (2.19) or (2.20).

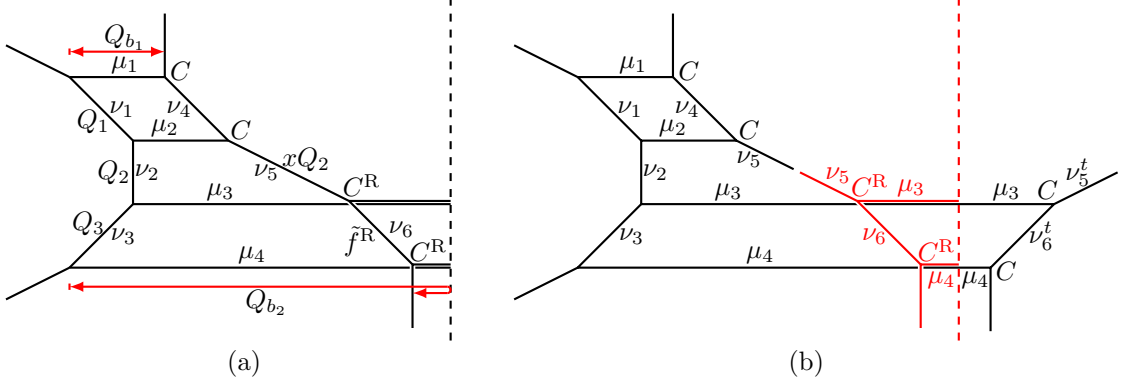


Figure 5. 5-brane webs with an ON^- -plane for $D_2(N_1, N_2)$ gauge theory with $N_1 = 2, N_2 = 2$.

Now that we have described how new edge factor appears when we consider the edge associated with the 5-brane being reflected by an ON -plane, we try to apply our prescription to actual computations involving an ON -plane. As a simple example, a 5-brane configuration is given in Figure 5 which may look like a 5-brane web for a single gauge theory, though it is merely two copies of $\text{SU}(2)$ theories without bifundamental matter. For purposes of expediency, we call such theory the “ $D_2(N_1, N_2)$ ” theory which is a linear sum of $\text{SU}(N_1)$ and $\text{SU}(N_2)$ gauge theories. For simplicity, first we consider the case when $N_1 = 2$ and $N_2 = 2$, as given in Figure Figure 5. Here, the Young diagrams μ_1, μ_2 label the two color D5-branes for one $\text{SU}(2)$ and the Young diagrams μ_3, μ_4 label the two color D5-branes for the other $\text{SU}(2)$. As discussed earlier, a 5-brane configuration with an ON -plane like Figure 5(a) can be realized by folding the right part of a 5-brane configuration in Figure 5(b) to the left and then by gluing the edges in the middle. The 5-brane configuration before the folding is all equipped with the conventional vertex factors C because the diagram contains two copies of normal $\text{SU}(2)$ webs. After the folding, on the other hand, the two vertices are reflected and they become C^{R} on the left. The edge factor between this two vertices also changes due to the folding. The edge factor between the two C 's on the right of the ON -plane together with the two C 's in Figure 5(b) are given by

$$\begin{aligned}
& C_{\nu_5^t \nu_6 \mu_3}(\mathbf{t}, \mathbf{q}) \cdot (-Q_3)^{|\nu_6|} \tilde{f}_{\nu_6^t}^{-1}(\mathbf{q}, \mathbf{t}) \cdot C_{\nu_6^t \varnothing \mu_4}(\mathbf{t}, \mathbf{q}) \\
&= C_{\nu_6^t \nu_5 \mu_3^t}^{\text{R}}(\mathbf{q}, \mathbf{t}) \cdot (-Q_3)^{|\nu_6|} \left(\frac{\mathbf{t}}{\mathbf{q}} \right)^{\frac{|\nu_6|}{2}} f_{\nu_6}(\mathbf{q}, \mathbf{t}) \cdot C_{\varnothing \nu_6 \mu_4^t}^{\text{R}}(\mathbf{q}, \mathbf{t}) \cdot (\cdots) \\
&= C_{\nu_6^t \nu_5 \mu_3^t}^{\text{R}}(\mathbf{q}, \mathbf{t}) \cdot (-Q_3)^{|\nu_6|} \tilde{f}_{\nu_6}^{\text{R}}(\mathbf{q}, \mathbf{t}) \cdot C_{\varnothing \nu_6 \mu_4^t}^{\text{R}}(\mathbf{q}, \mathbf{t}) \cdot (\cdots) .
\end{aligned} \tag{2.21}$$

In the second line of the above equation, (2.17) is used and edge factors that do not involve ν_6 are put into the ellipsis. In the third line, we have defined

$$\tilde{f}_{\mu}^{\text{R}}(\mathbf{q}, \mathbf{t}) \equiv (-1)^{|\mu|} \mathbf{q}^{\frac{\|\mu^t\|^2 - |\mu|}{2}} \mathbf{t}^{-\frac{\|\mu\|^2 - |\mu|}{2}} , \tag{2.22}$$

which plays the role of the new framing factor function for edge that connects two C^R vertices, and one can check that this definition is also consistent for the case when ON-plane is on the left of the web diagram. So

$$(-Q_3)^{|\nu_6|} \tilde{f}_{\nu_6}^R(\mathbf{q}, \mathbf{t}) \quad (2.23)$$

is the edge factor of edge ν_6 in Figure 5(a). As \tilde{f}^R is the reflected correspondence of the normal \tilde{f} , one may think whether there is also a reflected correspondence of the preferred direction framing factor f , but actually one can check that the reflected correspondence is the same as the normal f .

The edge ν_5 is the glued edge which has two different kinds of vertices at its two ends. The framing factor of this edge is zero due to $\mathbf{n} = 0$, but we still need to modify the edge factor in order to get the correct partition function. It turns out that a multiplier x needs to be added to the Kähler parameter Q_2 of ν_5 . Then we compute the partition function of the web diagram in Figure 5(a) with the prescription that we discussed,

$$\begin{aligned} Z^{D_2(2,2)} &= C_{\nu_1^t \emptyset \mu_1^t}(\mathbf{q}, \mathbf{t}) C_{\nu_2^t \nu_1 \mu_2^t}(\mathbf{q}, \mathbf{t}) C_{\nu_3^t \nu_2 \mu_3^t}(\mathbf{q}, \mathbf{t}) C_{\emptyset \nu_3 \mu_4^t}(\mathbf{q}, \mathbf{t}) C_{\emptyset \nu_4^t \mu_1}(\mathbf{t}, \mathbf{q}) \\ &\quad \times C_{\nu_4 \nu_5^t \mu_2}(\mathbf{t}, \mathbf{q}) C_{\nu_6^t \nu_5 \mu_3^t}^R(\mathbf{q}, \mathbf{t}) C_{\emptyset \nu_6 \mu_4^t}^R(\mathbf{q}, \mathbf{t}) (-Q_1)^{|\nu_1|} \tilde{f}_{\nu_1}(\mathbf{q}, \mathbf{t}) (-Q_2)^{|\nu_2|} \tilde{f}_{\nu_2}(\mathbf{q}, \mathbf{t}) \\ &\quad \times (-Q_3)^{|\nu_3|} \tilde{f}_{\nu_3}(\mathbf{q}, \mathbf{t}) (-Q_1)^{|\nu_4|} \tilde{f}_{\nu_4}(\mathbf{q}, \mathbf{t})^{-1} (-xQ_2)^{|\nu_5|} (-Q_3)^{|\nu_6|} \tilde{f}_{\nu_6}^R(\mathbf{q}, \mathbf{t}) \\ &\quad \times (-Q_{b1})^{|\mu_1|} f_{\mu_1}(\mathbf{t}, \mathbf{q})^{-1} (-Q_{b1})^{|\mu_2|} f_{\mu_2}(\mathbf{t}, \mathbf{q}) (+Q_{b2})^{|\mu_3|} f_{\mu_3}(\mathbf{t}, \mathbf{q})^{-1} \\ &\quad \times f_{\mu_5^t}(\mathbf{q}, \mathbf{t}) \frac{\tilde{Z}_{\mu_3}(\mathbf{t}, \mathbf{q})}{\tilde{Z}_{\mu_3^t}(\mathbf{q}, \mathbf{t})} (+Q_{b2})^{|\mu_4|} f_{\mu_4}(\mathbf{t}, \mathbf{q}) f_{\mu_4^t}(\mathbf{q}, \mathbf{t}) \frac{\tilde{Z}_{\mu_4}(\mathbf{t}, \mathbf{q})}{\tilde{Z}_{\mu_4^t}(\mathbf{q}, \mathbf{t})}. \end{aligned} \quad (2.24)$$

Using the extended Cauchy identities repeatedly, we can sum over the non-preferred direction Young diagrams along the vertical strips, we obtain

$$\begin{aligned} Z^{D_2(2,2)} &= \mathbf{q}^{||\mu_1||^2 + ||\mu_3||^2} \mathbf{t}^{||\mu_2^t||^2 + ||\mu_4^t||^2} Q_{b1}^{|\mu_1| + |\mu_2|} Q_{b2}^{|\mu_3| + |\mu_4|} \prod_{i=1}^4 \tilde{Z}_{\mu_i}(\mathbf{t}, \mathbf{q}) \tilde{Z}_{\mu_i^t}(\mathbf{q}, \mathbf{t}) \\ &\quad \times \mathcal{R}_{\mu_1^t \mu_3}(xQ_1Q_2) \mathcal{R}_{\mu_1^t \mu_4}(xQ_1Q_2Q_3) \mathcal{R}_{\mu_2^t \mu_3}(xQ_2) \mathcal{R}_{\mu_2^t \mu_4}(xQ_2Q_3) \\ &\quad \times \left(\mathcal{R}_{\mu_1^t \mu_2}(\sqrt{\frac{\mathbf{q}}{\mathbf{t}}}Q_1) \mathcal{R}_{\mu_1^t \mu_2}(\sqrt{\frac{\mathbf{t}}{\mathbf{q}}}Q_1) \mathcal{R}_{\mu_1^t \mu_3}(\sqrt{\frac{\mathbf{q}}{\mathbf{t}}}Q_1Q_2) \mathcal{R}_{\mu_1^t \mu_4}(\sqrt{\frac{\mathbf{q}}{\mathbf{t}}}Q_1Q_2Q_3) \right. \\ &\quad \left. \times \mathcal{R}_{\mu_2^t \mu_3}(\sqrt{\frac{\mathbf{q}}{\mathbf{t}}}Q_2) \mathcal{R}_{\mu_2^t \mu_4}(\sqrt{\frac{\mathbf{q}}{\mathbf{t}}}Q_2Q_3) \mathcal{R}_{\mu_3^t \mu_4}(\sqrt{\frac{\mathbf{q}}{\mathbf{t}}}Q_3) \mathcal{R}_{\mu_3^t \mu_4}(\sqrt{\frac{\mathbf{t}}{\mathbf{q}}}Q_3) \right)^{-1}. \end{aligned} \quad (2.25)$$

By fixing

$$x = \sqrt{\frac{\mathbf{q}}{\mathbf{t}}}, \quad (2.26)$$

the factors $\mathcal{R}_{\mu_i^t \mu_j}$ with $i = 1, 2$ and $j = 3, 4$ which are the bifundamental contributions cancel, and the result turns out to be the correct partition function of $D_2(2, 2)$ gauge

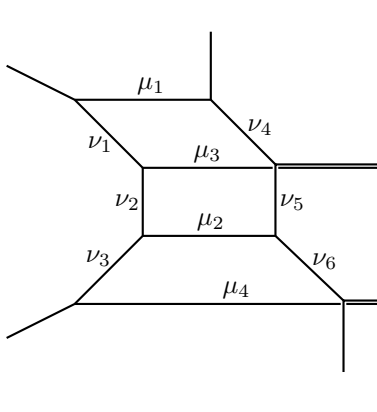


Figure 6. 5-brane configuration for $D_2(2, 2)$ gauge theory of overlapping sub webs.

theory. So the new edge factor for the edge ν_5 is

$$\left(-\sqrt{\frac{\mathfrak{q}}{\mathfrak{t}}}Q_2\right)^{|\nu_5|}, \quad (2.27)$$

and we indicate this edge factor in the figures as $\sqrt{\frac{\mathfrak{q}}{\mathfrak{t}}}Q_2$ for short.

The two $SU(2)$ nodes in Figure 5(a) are drawn in the way that their sub webs do not overlap with each other. If we move the color brane μ_3 upward passing the color brane μ_2 , we then end up with Figure 6 in which the sub webs of the two $SU(2)$ nodes overlap. Our refined topological vertex prescription does not work well in this kind of overlapping case. If we simply assume the vertices on the strip of NS-branes next to the ON-plane to be C or C^R or some modified vertices which are obtained by changing the coefficients of $|\eta|, |\lambda|, |\mu|$ in the power of $\frac{\mathfrak{q}}{\mathfrak{t}}$ in (2.15) and multiply the Kähler parameters of $\nu_{4,5,6}$ by some $\mathfrak{t}, \mathfrak{q}$ factors as we have done in fixing the x , then after summing over Young diagrams in the non-preferred direction, we always end up with non-vanishing bifundamental contributions or incorrect vector contributions³. We suspect that when μ_3 is moved upward passing μ_2 the two vertices C and C^R are entangled and the entangled vertices are hard to determine. So in this paper, we will always use separated sub webs which do not overlap for computation.

From Figure 5(a) we can “flop” the lower C^R vertex⁴ or both the C^R vertices into the ON-plane and reflect back, then we obtain Figure 7(a) and 7(b) respectively. Correspondingly, the vertices and edge factors also change due to the flopping, we

³The correct vector contribution should have the form of $\left(\mathcal{R}_{\alpha^t\beta}(Q\sqrt{\frac{\mathfrak{q}}{\mathfrak{t}}})\mathcal{R}_{\alpha^t\beta}(Q\sqrt{\frac{\mathfrak{t}}{\mathfrak{q}}})\right)^{-1}$ where Q is the Kähler “distance” from the color brane α to β with the vertical position of brane α being higher than β .

⁴By “flop”, we mean that we deform 5-brane web near an ON-plane such that the shape of the 5-brane web is changed so that the horizontal Kähler parameter from the ON-plane to the corresponding vertex becomes its inverse. More precisely, the position on the ON-plane is shifted toward the 5-brane web.

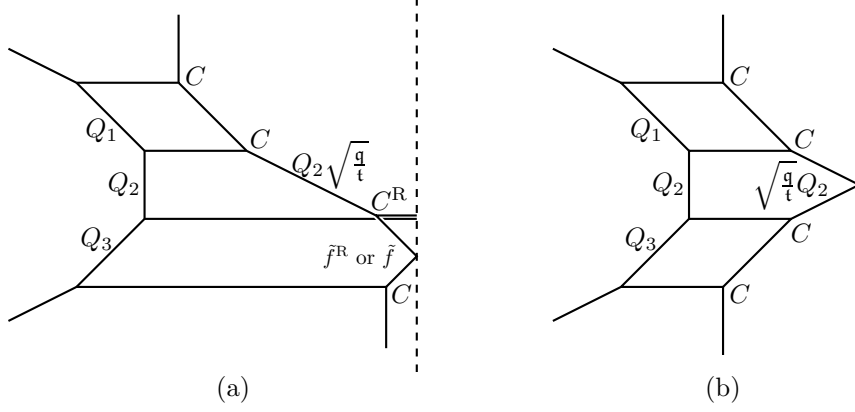


Figure 7. Two 5-brane webs for $D_2(2,2)$ gauge theory which are related by a series of flops.

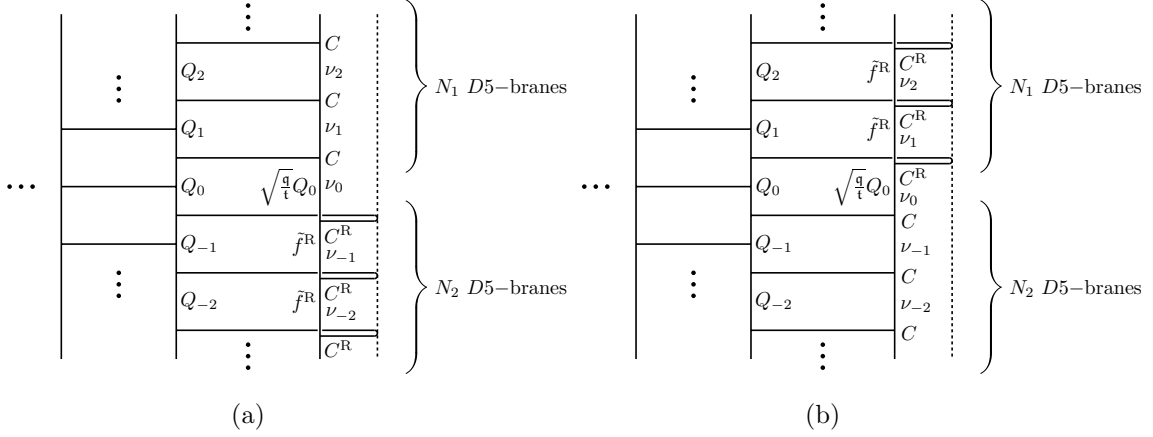


Figure 8. 5-brane configurations for general D -type quiver gauge theory with an ON-plane located on the right.

have labelled them in Figure 7. Note that when using (2.19) or (2.20) to determine the edge factor of the reflected brane that connects C and C^R in Figure 7(a), if we choose C as the vertex that is reflected by the ON-plane, then we should use \tilde{f}^R as the framing factor function for \mathcal{F} , if we choose C^R as the vertex that is reflected by the ON-plane, then we should use \tilde{f} as the framing factor function for \mathcal{F} . The derivation is just like the previous derivations that we have done in finding out the edge factors, so we omit it here.

A general D -type quiver gauge theory with $SU(N_1)$ and $SU(N_2)$ gauge groups at its bivalent nodes is illustrated in Figure 8(a), the sub webs of the two SU nodes do not overlap. The analysis for refinement we have done in the $D_2(2,2)$ case can be easily generalized to this case, here we just state the result without proof. Along the strip of NS5-branes next to the ON-plane, we multiply the factor $\sqrt{q/t}$ to Q_0

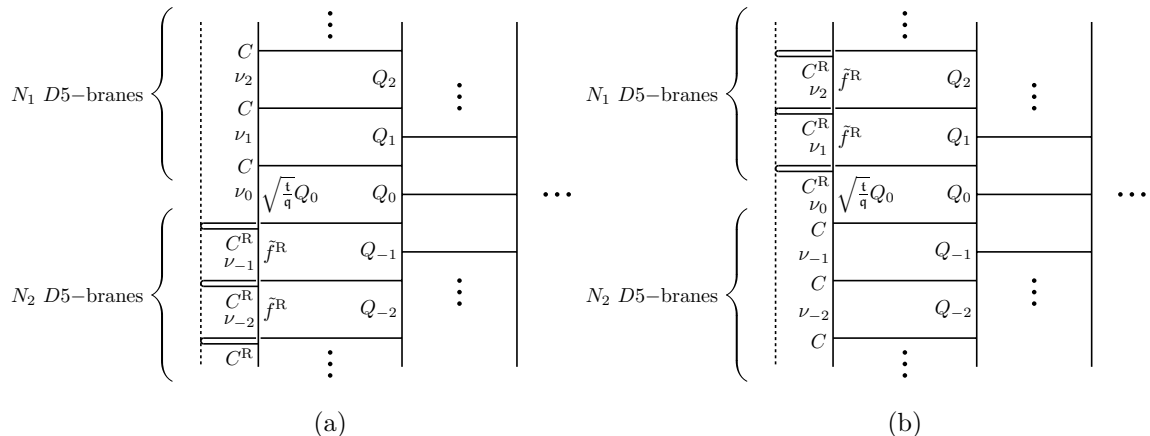


Figure 9. 5-brane webs for general D -type quiver gauge theory with an ON-plane located on the left.

of ν_0 which is between the two SU nodes, all the vertices and framing factors in the $SU(N_2)$ nodes are C^R and \tilde{f}^R . If we flop the vertices C^R into the ON-plane and reflect back, the vertices will become C , as illustrated in Figure 7.

Summary of our proposal on topological vertex with an ON-plane. 5-brane configurations can be viewed as consisting of vertical strips of NS5-branes glued by horizontal D5-branes with vertex factors and non-preferred direction edge factors living on vertical strips and preferred direction edge factors living on D5-branes. Away from ON-planes, such factors are the same as the usual vertex and edge factors as in the cases without ON-planes. We propose that new vertex and edge factors are only presented on the strips of NS5-branes next to an ON-plane with the following steps:

- (1) **Deform 5-brane webs so that bivalent sub webs have no overlapping phase.** 5-brane web with an ON-plane describes a D -type quiver which has an SU gauge theory node at each bivalent leg. A typical 5-brane web with an ON-plane for such quiver may be drawn in a way that two sub webs for each SU gauge theory look overlapping as depicted in Figure 10(a). Such overlapping phase can be deformed to yield two sub webs which do not have any overlapping phase as in Figure 10(b). In order for the topological vertex with an ON-plane to be applied, we require that 5-brane configuration should have no overlapping phase.
- (2) **Apply C^R, \tilde{f}^R along the strip next to ON-planes.** If the prescription (1) is satisfied, we claim that there are two kinds of vertices that we need to assign on the strip next to an ON-plane. One is the usual

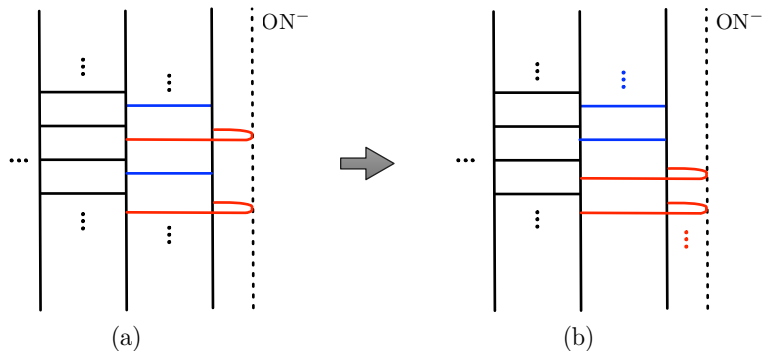


Figure 10. Two phases of 5-brane webs with an ON-plane: (a) Overlapping phase of two bivalent SU gauge groups of a D -type quiver (b) Split phase of SU gauge groups of a D -type quiver. D5-branes in red and D5-branes in blue correspond to each SU gauge theory of two ends of bivalent node.

topological vertex factor C , the other one is the reflected refined topological vertex factor C^R defined in (2.15). The framing factor for the edges that connect C^R 's is the new framing factor \tilde{f}^R defined in (2.22). If we draw the web diagram in the standard way like Figure 8 or Figure 9, then the assignment of the vertex and framing factors on the strip should follow that in Figure 8(a) or Figure 8(b) when the ON-plane is on the right-hand side, and should follow that in Figure 9(a) or Figure 9(b) when the ON-plane is on the left-hand side.

- (3) **Dress additional $\mathfrak{t}, \mathfrak{q}$ factors on the edge connecting two SU sub webs.** $\sqrt{\frac{\mathfrak{q}}{\mathfrak{t}}}$ or $\sqrt{\frac{\mathfrak{t}}{\mathfrak{q}}}$ needs to be multiplied to the Kähler parameters of the edges that connect the two SU nodes which is illustrated in Figure 8 and Figure 9.
- (4) **Introduce the new reflected edge factor to the edge reflected by an ON-plane.**

For edges that are reflected by an ON-plane as in Figure 4(a), the corresponding edge factor is given by (2.19) when the reflected vertex is associated with the vertex factor of $C(\mathfrak{t}, \mathfrak{q})$ or $C^R(\mathfrak{t}, \mathfrak{q})$. When the reflected vertex is of $C(\mathfrak{q}, \mathfrak{t})$ or $C^R(\mathfrak{q}, \mathfrak{t})$, the corresponding edge factor is given by (2.20).

We also remark that we can “flop” the vertices into the ON-planes to obtain diagrams like those given in Figure 7. For such cases, C and C^R become C^R and C respectively after flopping, and the edge factors also change according to the edge factors presented in Figure 7.

3 Examples

In this section, we demonstrate how to apply the refined topological vertex with ON-planes that we proposed in the previous section with instructive examples as

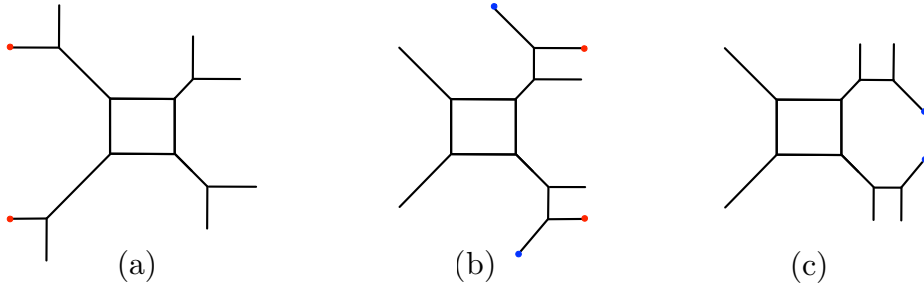


Figure 11. 5-brane webs for $SU(2)+4\mathbf{F}$. (a) A typical 5-brane web. (b) Performing Hanany-Witten moves to the left. (c) A 5-brane configuration as a D_3 -type quiver, “ $SU(1)$ – $SU(2)$ –“ $SU(1)$ ”, after further Hanany-Witten moves.

well as some rank-2 theories whose ADHM construction is not known. We provide computational details.

3.1 5d $SU(2)+4\mathbf{F}$

5d $\mathcal{N} = 1$ $SU(2)$ gauge theory with four hypermultiplets in the fundamental representation ($SU(2) + 4\mathbf{F}$) is a proper instructive example for applying topological vertex with ON-planes as its refined partition function is well known and also this theory can be regarded as a quiver “ $SU(1)$ – $SU(2)$ –“ $SU(1)$ ”. A typical 5-brane configuration for $SU(2)+4\mathbf{F}$ is depicted in Figure 11(a). It is easy to see that Hanany-Witten moves can deform the 5-brane configuration so that it can be viewed as “ $SU(1)$ – $SU(2)$ –“ $SU(1)$ ” as in Figure 11(c), where an “ $SU(1)$ ” is made out of one D5-brane suspended between two NS5-branes that does not have Coulomb branch but has the coupling [60]. One can see that together with the bifundamental degrees of freedom connecting $SU(2)$ and “ $SU(1)$ ”, “ $SU(1)$ – $SU(2)$ –“ $SU(1)$ ” captures the same degrees of freedom as those of $SU(2)+4\mathbf{F}$. As it can be also seen as a D_3 -type quiver, the $SU(2)+4\mathbf{F}$ theory can be described with a 5-brane configuration with an ON-plane as given in Figure 12(a).

Following our proposal with ON-planes presented in the previous section, we assign the vertex factors C and C^R on 5-brane web as shown in Figure 12(a). In particular, C^R is assigned to the vertex on the strip next to an ON-plane, which can be viewed as a configuration by reflecting and gluing Figure 12(b) which is one of possible 5-brane configurations for $SU(2)+4\mathbf{F}$ as depicted in Figure 11. It follows from Figure 12 that the Kähler parameters for the masses of 4 flavors $M_i = e^{-\beta m_i}$, $i = 1, 2, 3, 4$ can be readily identified. For later convenience, we have defined the fourth mass with M_4^{-1} in Figure 12(a).

The partition function for $SU(2)+4\mathbf{F}$ based on our proposal in the previous section then takes the form:

$$Z^{SU(2)+4\mathbf{F}} = \sum_{\mu, \nu} C_{\nu_1^t \phi \mu_1^t}(\mathbf{q}, \mathbf{t}) C_{\phi \nu_1 \mu_2^t}(\mathbf{q}, \mathbf{t}) C_{\phi \nu_2^t \mu_1}(\mathbf{t}, \mathbf{q}) C_{\nu_3^t \nu_2 \mu_3^t}(\mathbf{q}, \mathbf{t}) C_{\nu_4^t \nu_3 \mu_4^t}(\mathbf{q}, \mathbf{t})$$

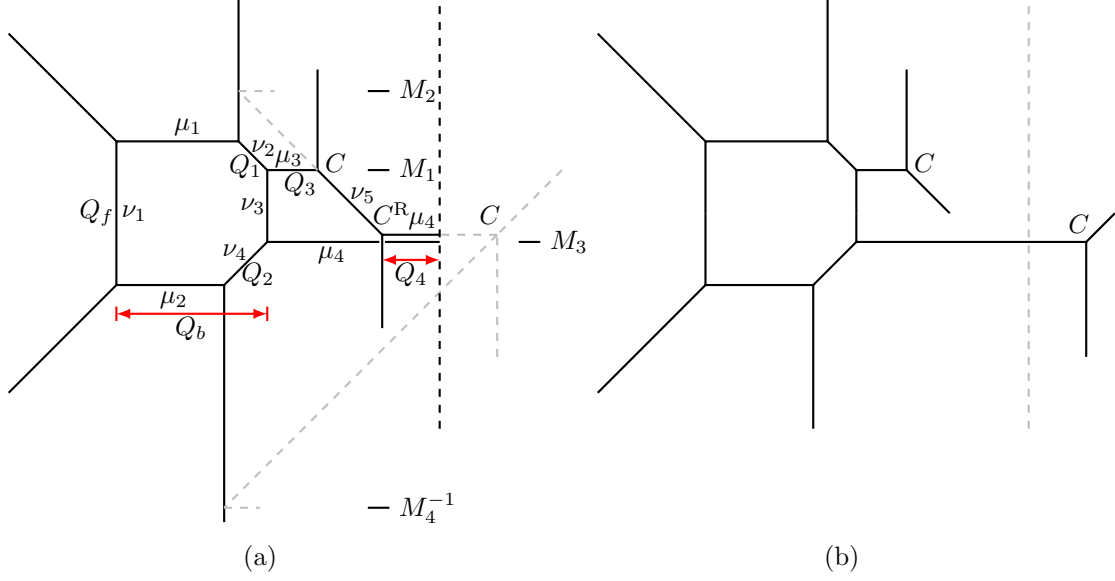


Figure 12. A 5-brane web for $SU(2)+4\mathbf{F}$ as a D_3 -quiver, $SU(1)-SU(2)-SU(1)$. The vertical dotted line represents an ON^- -plane.

$$\begin{aligned}
& \times C_{\nu_4 \emptyset \mu_2}(\mathbf{t}, \mathbf{q}) C_{\emptyset \nu_5^t \mu_3}(\mathbf{t}, \mathbf{q}) C_{\emptyset \nu_5^t \mu_4^t}^{\mathbf{R}}(\mathbf{q}, \mathbf{t}) (-Q_f)^{|\nu_1|} \tilde{f}_{\nu_1}(\mathbf{q}, \mathbf{t}) (-Q_1)^{|\nu_2|} \left(-\frac{Q_f}{Q_{1,2}}\right)^{|\nu_3|} \\
& \times \tilde{f}_{\nu_3}(\mathbf{q}, \mathbf{t}) (-Q_2)^{|\nu_4|} \left(-\frac{Q_f}{Q_{1,2}} \sqrt{\frac{\mathbf{q}}{\mathbf{t}}}\right)^{|\nu_5|} \left(-\frac{Q_b}{Q_1}\right)^{|\mu_1|} \left(-\frac{Q_b}{Q_2}\right)^{|\mu_2|} (-Q_3)^{|\mu_3|} \\
& \times \left(+\frac{Q_{f,3,4^2}}{Q_{1,2}}\right)^{|\mu_4|} f_{\mu_4^t}(\mathbf{q}, \mathbf{t}) \frac{\tilde{Z}_{\mu_4}(\mathbf{t}, \mathbf{q})}{\tilde{Z}_{\mu_4^t}(\mathbf{q}, \mathbf{t})}, \tag{3.1}
\end{aligned}$$

where $\boldsymbol{\mu}, \boldsymbol{\nu}$ means a collective notation for all Young diagrams associated with μ_i and ν_i , and we have used the shorthand notation $Q_{i,j,k^2} \equiv Q_i Q_j Q_k^2$. Recall that if an empty set is assigned to the new vertex factor $C^{\mathbf{R}}$ in the non-preferred direction, then $C^{\mathbf{R}}$ is equivalent to usual C . Hence, in this example, we have $C_{\emptyset \nu_5^t \mu_4^t}^{\mathbf{R}}(\mathbf{q}, \mathbf{t}) = C_{\emptyset \nu_5^t \mu_4^t}(\mathbf{q}, \mathbf{t})$. After simplifying the Young diagram sum $\boldsymbol{\nu}$ along the non-preferred directions, we obtain

$$\begin{aligned}
Z^{\text{SU}(2)+4\mathbf{F}} &= \sum_{\boldsymbol{\mu}} (-Q_3)^{|\mu_3|} \left(-\frac{Q_b}{Q_1}\right)^{|\mu_1|} \left(-\frac{Q_b}{Q_2}\right)^{|\mu_2|} \left(-\frac{Q_{3,4^2,f}}{Q_{1,2}}\right)^{|\mu_4|} \\
& \times \mathbf{q}^{\frac{1}{2} \sum_{i=1}^4 \|\mu_i\|^2} \mathbf{t}^{\frac{1}{2} \sum_{i=1}^4 \|\mu_i^t\|^2} \prod_{i=1}^4 \tilde{Z}_{\mu_i}(\mathbf{t}, \mathbf{q}) \tilde{Z}_{\mu_i^t}(\mathbf{q}, \mathbf{t}) \\
& \times \frac{\mathcal{R}_{\mu_1^t \mu_3}(Q_1) \mathcal{R}_{\mu_1^t \mu_4}(Q_2) \mathcal{R}_{\mu_3^t \mu_2}(Q_1) \mathcal{R}_{\mu_4^t \mu_2}(Q_2)}{\mathcal{R}_{\mu_1^t \mu_2}(Q_f \sqrt{\frac{\mathbf{q}}{\mathbf{t}}}) \mathcal{R}_{\mu_1^t \mu_2}(Q_f \sqrt{\frac{\mathbf{t}}{\mathbf{q}}})}. \tag{3.2}
\end{aligned}$$

We now express this partition function in terms of the gauge theory parameters. Based on the 5-brane web in Figure 12, one readily finds the map between the Kähler

parameters and the gauge theory parameters,

$$\begin{aligned} Q_b &= A^2 u \sqrt{\frac{M_3}{M_1 M_2 M_4}}, & Q_f &= A^2, \\ Q_1 &= \frac{A}{M_1}, & Q_2 &= A M_3, & Q_3 &= \frac{M_2}{A}, & Q_4 &= \sqrt{\frac{M_3 M_4}{M_1 M_2}}, \end{aligned} \quad (3.3)$$

where u is the instanton factor and A is the Coulomb branch parameter. By substituting (3.3) into (3.2) and using (2.8), we find

$$\mathcal{Z}^{\text{SU}(2)+4\mathbf{F}} = Z_M^{N_f=4} \sum_{\mu_1, \mu_2} Z_{\mu_1 \mu_2}^{N_f=4} \sum_{\mu_3} Z_{\mu_1 \mu_2 \mu_3}(M_1, M_2) \sum_{\mu_4} Z_{\mu_1 \mu_2 \mu_4}(M_3, M_4), \quad (3.4)$$

where

$$\begin{aligned} Z_M^{N_f=4} &= \frac{\mathcal{M}(A^2) \mathcal{M}(A^2 \frac{\mathbf{t}}{\mathbf{q}})}{\mathcal{M}(\frac{A}{M_1} \sqrt{\frac{\mathbf{t}}{\mathbf{q}}}) \mathcal{M}(A M_1 \sqrt{\frac{\mathbf{t}}{\mathbf{q}}}) \mathcal{M}(\frac{A}{M_3} \sqrt{\frac{\mathbf{t}}{\mathbf{q}}}) \mathcal{M}(A M_3 \sqrt{\frac{\mathbf{t}}{\mathbf{q}}})}, \quad (3.5) \\ Z_{\mu_1 \mu_2}^{N_f=4} &= \frac{\mathbf{q}^{\frac{\|\mu_1\|^2 + \|\mu_2\|^2}{2}} \mathbf{t}^{\frac{\|\mu_1^{\mathbf{t}}\|^2 + \|\mu_2^{\mathbf{t}}\|^2}{2}} (-A u)^{|\mu_1| + |\mu_2|} \tilde{Z}_{\mu_1}(\mathbf{t}, \mathbf{q}) \tilde{Z}_{\mu_1^{\mathbf{t}}}(\mathbf{q}, \mathbf{t}) \tilde{Z}_{\mu_2}(\mathbf{t}, \mathbf{q}) \tilde{Z}_{\mu_2^{\mathbf{t}}}(\mathbf{q}, \mathbf{t})}{\mathcal{N}_{\mu_1 \mu_2}(A^2) \mathcal{N}_{\mu_1 \mu_2}(A^2 \frac{\mathbf{t}}{\mathbf{q}})}, \quad (3.6) \end{aligned}$$

$$\begin{aligned} Z_{\mu_1 \mu_2 \mu_3}(M_1, M_2) &= \left(\sqrt{\frac{M_1}{M_2}} \right)^{|\mu_1|} \left(\sqrt{\frac{1}{M_1 M_2}} \right)^{|\mu_2|} \left(-\frac{M_2}{A} \right)^{|\mu_3|} \mathbf{q}^{\frac{\|\mu_3\|^2}{2}} \mathbf{t}^{\frac{\|\mu_3^{\mathbf{t}}\|^2}{2}} \\ &\quad \times \tilde{Z}_{\mu_3}(\mathbf{t}, \mathbf{q}) \tilde{Z}_{\mu_3^{\mathbf{t}}}(\mathbf{q}, \mathbf{t}) \mathcal{N}_{\mu_1 \mu_3}(\frac{A}{M_1} \sqrt{\frac{\mathbf{t}}{\mathbf{q}}}) \mathcal{N}_{\mu_3 \mu_2}(A M_1 \sqrt{\frac{\mathbf{t}}{\mathbf{q}}}), \quad (3.7) \end{aligned}$$

$$\begin{aligned} Z_{\mu_1 \mu_2 \mu_4}(M_3, M_4) &= \left(\sqrt{\frac{M_3}{M_4}} \right)^{|\mu_1|} \left(\sqrt{\frac{1}{M_3 M_4}} \right)^{|\mu_2|} \left(-\frac{M_4}{A} \right)^{|\mu_4|} \mathbf{q}^{\frac{\|\mu_4\|^2}{2}} \mathbf{t}^{\frac{\|\mu_4^{\mathbf{t}}\|^2}{2}} \\ &\quad \times \tilde{Z}_{\mu_4}(\mathbf{t}, \mathbf{q}) \tilde{Z}_{\mu_4^{\mathbf{t}}}(\mathbf{q}, \mathbf{t}) \mathcal{N}_{\mu_1 \mu_4}(\frac{A}{M_3} \sqrt{\frac{\mathbf{t}}{\mathbf{q}}}) \mathcal{N}_{\mu_4 \mu_2}(A M_3 \sqrt{\frac{\mathbf{t}}{\mathbf{q}}}). \quad (3.8) \end{aligned}$$

Here, we remark some technical points. The contribution of $Z_{\mu_1 \mu_2 \mu_3}(M_1, M_2)$ to the perturbative part of the partition function is $\sum_{\mu_3} Z_{\phi \phi \mu_3}(M_1, M_2)$, so we need to sum over all the Young diagrams μ_3 . This means that one sums over all the partitions associated with the Young diagram μ_3 from zero partition to infinite partitions. In order to compute such an infinite summation, we take the logarithm of $\sum_{\mu_3} Z_{\phi \phi \mu_3}(M_1, M_2)$ and then do a series expansion of it with respect to M_2 . Practically, one can sum over the Young diagrams μ_3 up to some finite box number as the upper bound such that for terms involving M_2 , lower order terms do not get corrected even though one increases the upper bound, while higher order terms do get corrected when the upper bound of $|\mu_3|$ increase, that is an artifact of a finite sum which will not be presented when we actually sum all the way to infinity. By using this trick, we are able to find the correct lower order expansion of $\sum_{\mu_3} Z_{\phi \phi \mu_3}(M_1, M_2)$, from the expansion we find that it has the following form as the Plethystic exponential,

$$\sum_{\mu_3} Z_{\phi \phi \mu_3}(M_1, M_2) = \text{PE} \left[\frac{-M_1 M_2 \sqrt{\mathbf{q} \mathbf{t}} - A^2 M_1 M_2 \sqrt{\mathbf{q} \mathbf{t}} + A M_2 (M_1^2 \mathbf{q} + \mathbf{t})}{A M_1 (1 - \mathbf{q})(1 - \mathbf{t})} \right]$$

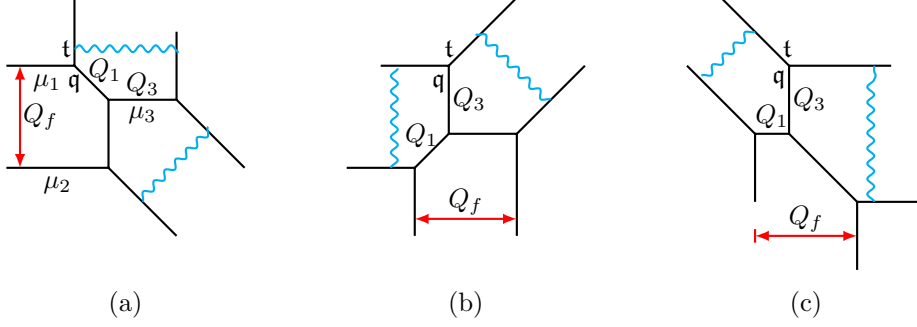


Figure 13. Sources of the extra factors.

$$= \frac{\mathcal{M}(M_1 M_2) \mathcal{M}\left(\frac{M_2 t}{M_1 q}\right)}{\mathcal{M}\left(\frac{M_2}{A} \sqrt{\frac{t}{q}}\right) \mathcal{M}\left(A M_2 \sqrt{\frac{t}{q}}\right)}. \quad (3.9)$$

Notice that $\mathcal{M}(M_1 M_2)$ and $\mathcal{M}\left(\frac{M_2 t}{M_1 q}\right)$ do not depend on the Coulomb branch parameter A , so they are the extra factors. In terms of Kähler parameters, they are given as $\mathcal{M}\left(\frac{Q_3 Q_f}{Q_1}\right)$ and $\mathcal{M}(Q_1 Q_3 \frac{t}{q})$ respectively. These extra factors can be also seen from 5-brane webs. For instance, $Q_1 Q_3$ is the distance between the two external parallel branes in the upper part of Figure 12(a), and hence it contributes to the extra factor $\mathcal{M}(Q_1 Q_3 \frac{t}{q})$. On the other hand, the extra factor $\mathcal{M}\left(\frac{Q_3 Q_f}{Q_1}\right)$ is not easy to directly see from Figure 12(a). We note that these two extra factors rather can be seen from Figure 13. The function $Z_{\mu_1 \mu_2 \mu_3}(M_1, M_2)$ is proportional to the topological string partition function of Figure 13(a). The extra factors $\mathcal{M}\left(\frac{Q_3 Q_f}{Q_1}\right)$, $\mathcal{M}(Q_1 Q_3 \frac{t}{q})$ correspond to the two (p, q) -strings in blue which connect the parallel external branes. Figure 13(b) is the S-dual of Figure 13(a), from Figure 13(b) it is easy to see the extra factor corresponding to the left vertical string which is $\mathcal{M}(Q_1 Q_3 \frac{t}{q})$. Figure 13(c) is obtained by an $SL(2, \mathbb{Z})$ transformation of Figure 13(b), from which we can easily see that the other extra factor $\mathcal{M}\left(\frac{Q_3 Q_f}{Q_1}\right)$ corresponds to the (p, q) -string in blue that is vertically expanded on the right side.

The same analysis applies to $\sum_{\mu_4} Z_{\emptyset \emptyset \mu_4}(M_3, M_4)$. Combining these results with (3.5), we finally obtain the full perturbative part⁵,

$$Z_{\text{pert}}^{\text{SU}(2)+4\text{F}} = \mathcal{M}(A^2) \mathcal{M}\left(A^2 \frac{t}{q}\right) \left[\mathcal{M}\left(\frac{A}{M_1} \sqrt{\frac{t}{q}}\right) \mathcal{M}\left(A M_1 \sqrt{\frac{t}{q}}\right) \mathcal{M}\left(\frac{A}{M_3} \sqrt{\frac{t}{q}}\right) \mathcal{M}\left(A M_3 \sqrt{\frac{t}{q}}\right) \right. \\ \left. \times \mathcal{M}\left(\frac{A}{M_2} \sqrt{\frac{t}{q}}\right) \mathcal{M}\left(A M_2 \sqrt{\frac{t}{q}}\right) \mathcal{M}\left(\frac{A}{M_4} \sqrt{\frac{t}{q}}\right) \mathcal{M}\left(A M_4 \sqrt{\frac{t}{q}}\right) \right]^{-1}. \quad (3.10)$$

Written as Plethystic exponential,

$$Z_{\text{pert}}^{\text{SU}(2)+4\text{F}} = \text{PE} \left[\frac{1}{(1-t)(1-q)} \left((q+t)A^2 - \chi_{\mathbf{8v}}^{\text{SO}(8)} \sqrt{qt}A \right) \right], \quad (3.11)$$

⁵After necessary flops: $\mathcal{M}(Q; t, q) \rightarrow \mathcal{M}\left(\frac{1}{Q}; q, t\right) = \mathcal{M}\left(\frac{1}{Q} \frac{t}{q}; t, q\right)$.

where $\chi_{\mathbf{8v}}^{\text{SO}(8)}$ is the character for the 8-dimensional vector representation of $\text{SO}(8)$. From here on, we use $\chi_{\mathbf{n}}^{\text{SO}(8)}$ to denote the character of the \mathbf{n} -dimensional representation of $\text{SO}(8)$, defined in Appendix A.

Extracting the perturbative part from (3.4), one finds that the instanton part can be expressed as

$$Z_{\text{inst}}^{\text{SU}(2)+4\mathbf{F}} = \sum_{\mu_1, \mu_2} Z_{\mu_1 \mu_2}^{N_f=4} \left(\frac{\sum_{\mu_3} Z_{\mu_1 \mu_2 \mu_3}(M_1, M_2)}{\sum_{\mu_3} Z_{\emptyset \emptyset \mu_3}(M_1, M_2)} \right) \left(\frac{\sum_{\mu_4} Z_{\mu_1 \mu_2 \mu_4}(M_3, M_4)}{\sum_{\mu_4} Z_{\emptyset \emptyset \mu_4}(M_3, M_4)} \right). \quad (3.12)$$

At first sight, it appears that we need to sum over all the Young diagrams associated with μ_3, μ_4 in order to obtain the coefficients of u at a fixed order because $Z_{\mu_1 \mu_2}^{N_f=4}$ is proportional to $u^{|\mu_1|+|\mu_2|}$. However, the sum is truncated at finite order. Recall that the $\text{SU}(2)+4\mathbf{F}$ theory has an $\text{SO}(8)$ global symmetry which can be further enhanced to $\text{SO}(10)$ [6, 61], and also notice that the individual factor $\frac{\sum_{\mu_3} \dots}{\sum_{\mu_3} \dots}$ in the parenthesis only involves M_1 and M_2 which is of an $\text{SO}(4) = \text{SU}(2) \times \text{SU}(2)$ symmetry, exchanging M_1 and M_1^{-1} as well as M_2 and M_2^{-1} . If we Taylor expand $\frac{\sum_{\mu_3} \dots}{\sum_{\mu_3} \dots}$ with respect to M_2 , the lowest order is $M_2^{-\frac{|\mu_1|+|\mu_2|}{2}}$, and it looks like the highest order could be infinity, but because of the symmetry between M_2 and M_2^{-1} , the highest order should be $M_2^{\frac{|\mu_1|+|\mu_2|}{2}}$, so higher order terms greater than $\frac{|\mu_1|+|\mu_2|}{2}$ would cancel with one another. We define $\mathcal{Z}_{\mu_1 \mu_2} \equiv \frac{\sum_{\mu_3} \dots}{\sum_{\mu_3} \dots}$ and rewrite it as follows,

$$\mathcal{Z}_{\mu_1 \mu_2}(M_1, M_2) \equiv \frac{\sum_{\mu_3} Z_{\mu_1 \mu_2 \mu_3}(M_1, M_2)}{\sum_{\mu_3} Z_{\emptyset \emptyset \mu_3}(M_1, M_2)} = \frac{\sum_{\mu_3} B_{\mu_1 \mu_2 \mu_3} M_2^{|\mu_3|}}{\sum_{\mu_3} D_{\mu_3} M_2^{|\mu_3|}} M_2^{-\frac{|\mu_1|+|\mu_2|}{2}}, \quad (3.13)$$

where unimportant coefficients are denoted by B, D for simplicity. The lowest order in the Taylor expansion of the fractional factor in (3.13) is 1 and the highest order should be $M_2^{|\mu_1|+|\mu_2|}$, we obtain the following formula:

$$\frac{\sum_{\mu_3} B_{\mu_1 \mu_2 \mu_3} M_2^{|\mu_3|}}{\sum_{\mu_3} D_{\mu_3} M_2^{|\mu_3|}} M_2^{-\frac{|\mu_1|+|\mu_2|}{2}} = \left(\frac{\sum_{\mu_3}^{\leq |\mu_1|+|\mu_2|} B_{\mu_1 \mu_2 \mu_3} M_2^{|\mu_3|}}{\sum_{\mu_3}^{\leq |\mu_1|+|\mu_2|} D_{\mu_3} M_2^{|\mu_3|}} \right) M_2^{-\frac{|\mu_1|+|\mu_2|}{2}}. \quad (3.14)$$

On the right-hand side we sum over Young diagrams no greater than $|\mu_1| + |\mu_2|$. The superscript of the big parentheses means that we only keep the terms whose M_2 orders are no greater than $|\mu_1| + |\mu_2|$ after Taylor expanding the fraction in the parentheses with respect to M_2 . In this way⁶, we can compute the sum over μ_3 exactly by summing over finite number of Young diagrams.

We note that one may find that even after we obtain the right-hand side of (3.14), the result is still not very compact, although we have a finite polynomial

⁶See also section 4.3.2 in [42] for a related discussion.

with M_2 . To obtain a compact expression, we further expand it with respect to the Coulomb branch parameter A , again by a naive analysis that the lowest order term should be $A^{-|\mu_1|-|\mu_2|}$ and the highest order term should be $A^{2|\mu_1|+2|\mu_2|}$, it turns out that the actual computation yields that the lowest order term is 1 and the highest order term is $A^{|\mu_1|+|\mu_2|}$, due to drastic cancellations in lower and higher orders. We list the results of $\mathcal{Z}_{\mu_1\mu_2}$'s for a few lower orders. For one-instanton partition function, the corresponding $\mathcal{Z}_{\mu_1\mu_2}$'s take the form

$$\begin{aligned}\mathcal{Z}_{\{1\},\emptyset}(M_1, M_2) &= \frac{M_1 + M_2}{\sqrt{M_1 M_2}} - \left(\frac{1}{\sqrt{M_1 M_2}} + \sqrt{M_1 M_2} \right) \sqrt{\frac{\mathfrak{q}}{\mathfrak{t}}} A, \\ \mathcal{Z}_{\emptyset,\{1\}}(M_1, M_2) &= \left(\frac{1}{\sqrt{M_1 M_2}} + \sqrt{M_1 M_2} \right) - \frac{M_1 + M_2}{\sqrt{M_1 M_2}} \sqrt{\frac{\mathfrak{t}}{\mathfrak{q}}} A.\end{aligned}\quad (3.15)$$

For two-instanton partition function, the corresponding $\mathcal{Z}_{\mu_1\mu_2}$'s are given by

$$\begin{aligned}\mathcal{Z}_{\{2\},\emptyset}(M_1, M_2) &= 1 + \mathfrak{q} + \frac{M_1}{M_2} + \frac{M_2}{M_1} - \left(\frac{1}{M_1} + \frac{1}{M_2} + M_1 + M_2 \right) \sqrt{\frac{\mathfrak{t}}{\mathfrak{q}}} (1 + \mathfrak{q}) A \\ &\quad + \left((1 + \mathfrak{q}) \frac{\mathfrak{q}}{\mathfrak{t}} + \left(\frac{1}{M_1 M_2} + M_1 M_2 \right) \frac{\mathfrak{q}^2}{\mathfrak{t}} \right) A^2, \\ \mathcal{Z}_{\{1,1\},\emptyset}(M_1, M_2) &= 1 + \frac{1}{\mathfrak{t}} + \frac{M_1}{M_2} + \frac{M_2}{M_1} - \left(\frac{1}{M_1} + \frac{1}{M_2} + M_1 + M_2 \right) \sqrt{\frac{\mathfrak{q}}{\mathfrak{t}}} \left(1 + \frac{1}{\mathfrak{t}} \right) A \\ &\quad + \left(\frac{\mathfrak{q} + \mathfrak{q}\mathfrak{t}}{\mathfrak{t}^2} + \left(\frac{1}{M_1 M_2} + M_1 M_2 \right) \frac{\mathfrak{q}}{\mathfrak{t}^2} \right) A^2, \\ \mathcal{Z}_{\{1\},\{1\}}(M_1, M_2) &= \frac{1}{M_1} + M_1 + \frac{1}{M_2} + M_2 - \left(\frac{(1 + \mathfrak{q})(1 + \mathfrak{t})}{\sqrt{\mathfrak{q}\mathfrak{t}}} \right. \\ &\quad \left. + \left(\frac{1}{M_1 M_2} + M_1 M_2 \right) \sqrt{\frac{\mathfrak{q}}{\mathfrak{t}}} + \left(\frac{M_1}{M_2} + \frac{M_2}{M_1} \right) \sqrt{\frac{\mathfrak{t}}{\mathfrak{q}}} \right) A \\ &\quad + \left(\frac{1}{M_1} + M_1 + \frac{1}{M_2} + M_2 \right) A^2, \\ \mathcal{Z}_{\emptyset,\{2\}}(M_1, M_2) &= 1 + \frac{1}{\mathfrak{q}} + \frac{1}{M_1 M_2} + M_1 M_2 - \left(\frac{1}{M_1} + M_1 + \frac{1}{M_2} + M_2 \right) \sqrt{\frac{\mathfrak{t}}{\mathfrak{q}}} \left(1 + \frac{1}{\mathfrak{q}} \right) A \\ &\quad + \left(\frac{\mathfrak{t} + \mathfrak{q}\mathfrak{t}}{\mathfrak{q}^2} + \left(\frac{M_1}{M_2} + \frac{M_2}{M_1} \right) \frac{\mathfrak{t}}{\mathfrak{q}^2} \right) A^2, \\ \mathcal{Z}_{\emptyset,\{1,1\}}(M_1, M_2) &= 1 + \mathfrak{t} + \frac{1}{M_1 M_2} + M_1 M_2 - \left(\frac{1}{M_1} + M_1 + \frac{1}{M_2} + M_2 \right) \sqrt{\frac{\mathfrak{t}}{\mathfrak{q}}} (1 + \mathfrak{t}) A \\ &\quad + \left(\frac{\mathfrak{t}}{\mathfrak{q}} + \left(1 + \frac{M_1}{M_2} + \frac{M_2}{M_1} \right) \frac{\mathfrak{t}^2}{\mathfrak{q}} \right) A^2.\end{aligned}\quad (3.16)$$

Now we rewrite the instanton partition function (3.12) as

$$\mathcal{Z}_{\text{inst}}^{\text{SU}(2)+4\mathbf{F}} = \sum_{\mu_1, \mu_2} \mathcal{Z}_{\mu_1\mu_2}^{N_f=4} \mathcal{Z}_{\mu_1\mu_2}(M_1, M_2) \mathcal{Z}_{\mu_1\mu_2}(M_3, M_4). \quad (3.17)$$

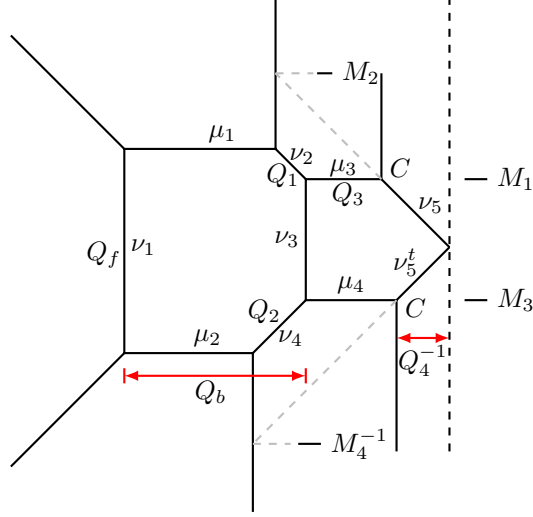


Figure 14. A 5-brane web for $SU(2)$ with 4 flavors by flopping.

By substituting the form of $\mathcal{Z}_{\mu_1\mu_2}(M_1, M_2)\mathcal{Z}_{\mu_1\mu_2}(M_3, M_4)$ at each order of the instanton, we can obtain the instanton partition function. For instance, the one-instanton partition function takes the following form up to A^2 ,

$$Z_{\text{inst}}^{\text{SU}(2)+4\mathbf{F}} = 1 + \left(-\frac{\sqrt{\mathbf{q}\mathbf{t}}\chi_{\mathbf{8s}}^{\text{SO}(8)}}{(1-\mathbf{q})(1-\mathbf{t})}A + \frac{(\mathbf{q}+\mathbf{t})\chi_{\mathbf{8c}}^{\text{SO}(8)}}{(1-\mathbf{q})(1-\mathbf{t})}A^2 + \mathcal{O}(A^3) \right) u + \mathcal{O}(u^2), \quad (3.18)$$

where $\chi_{\mathbf{8s}}^{\text{SO}(8)}$ and $\chi_{\mathbf{8c}}^{\text{SO}(8)}$ are respectively the character for the spinor and conjugate spinor representation of $SO(8)$, defined in Appendix A. The perturbative and one-instanton results given in (3.11) and (3.18) perfectly agree with the partition functions computed from the conventional 5-brane web diagram for $SU(2)+4\mathbf{F}$ without an ON-plane, as expected. The prescription of topological vertex in this example also coincide with the one that were found in [56] because $C^{\mathbf{R}}$ reduces to C in this case.

We also remark that there are other shape of 5-brane configurations than those that we discussed earlier. For instance, Figure 14 is another 5-brane diagram for $SU(2)+4\mathbf{F}$ which can be obtained by flopping the vertex associated with $C^{\mathbf{R}}$ in Figure 12(a) into the ON-plane and reflecting back. By our proposal, the corresponding topological string partition function is given by

$$\begin{aligned} Z^{\text{SU}(2)+4\mathbf{F}} &= \sum_{\mu, \nu} C_{\nu_1^t \phi \mu_1^t}(\mathbf{q}, \mathbf{t}) C_{\phi \nu_1 \mu_2^t}(\mathbf{q}, \mathbf{t}) C_{\phi \nu_2^t \mu_1}(\mathbf{t}, \mathbf{q}) C_{\nu_3^t \nu_2 \mu_3^t}(\mathbf{q}, \mathbf{t}) C_{\nu_4^t \nu_3 \mu_4^t}(\mathbf{q}, \mathbf{t}) \\ &\quad \times C_{\nu_4 \phi \mu_2}(\mathbf{t}, \mathbf{q}) C_{\phi \nu_5^t \mu_3}(\mathbf{t}, \mathbf{q}) C_{\nu_5^t \phi \mu_4}(\mathbf{t}, \mathbf{q}) (-Q_f)^{|\nu_1|} \tilde{f}_{\nu_1}(\mathbf{q}, \mathbf{t}) (-Q_1)^{|\nu_2|} \\ &\quad \times \left(-\frac{Q_f}{Q_{1,2}}\right)^{|\nu_3|} \tilde{f}_{\nu_3}(\mathbf{q}, \mathbf{t}) (-Q_2)^{|\nu_4|} \left(\frac{Q_f}{Q_{1,2}} \sqrt{\frac{\mathbf{q}}{\mathbf{t}}}\right)^{|\nu_5|} f_{\nu_5^t}(\mathbf{t}, \mathbf{q}) \left(-\frac{Q_b}{Q_1}\right)^{|\mu_1|} \\ &\quad \times \left(-\frac{Q_b}{Q_2}\right)^{|\mu_2|} (-Q_3)^{|\mu_3|} \left(-\frac{Q_{f,3,4^2}}{Q_{1,2}}\right)^{|\mu_4|}. \end{aligned} \quad (3.19)$$

After summing over ν , we obtain

$$\begin{aligned}
Z'^{SU(2)+4\mathbf{F}} &= \sum_{\mu} \left(-\frac{Q_b}{Q_1}\right)^{|\mu_1|} \left(-\frac{Q_b}{Q_2}\right)^{|\mu_2|} (-Q_3)^{|\mu_3|} \left(-\frac{Q_{f,3,4^2}}{Q_{1,2}}\right)^{|\mu_4|} \\
&\times \mathbf{q}^{\frac{1}{2}\sum_{i=1}^4 \|\mu_i\|^2} \mathbf{t}^{\frac{1}{2}\sum_{i=1}^4 \|\mu_i^t\|^2} \prod_{i=1}^4 \tilde{Z}_{\mu_i}(\mathbf{t}, \mathbf{q}) \tilde{Z}_{\mu_i^t}(\mathbf{q}, \mathbf{t}) \\
&\times \frac{\mathcal{R}_{\mu_1^t \mu_3}(Q_1) \mathcal{R}_{\mu_1^t \mu_4}\left(\frac{Q_f}{Q_2}\right) \mathcal{R}_{\mu_3^t \mu_2}\left(\frac{Q_f}{Q_1}\right) \mathcal{R}_{\mu_4^t \mu_2}(Q_2)}{\mathcal{R}_{\mu_1^t \mu_2}\left(Q_f \sqrt{\frac{\mathbf{q}}{\mathbf{t}}}\right) \mathcal{R}_{\mu_1^t \mu_2}\left(Q_f \sqrt{\frac{\mathbf{t}}{\mathbf{q}}}\right)}, \tag{3.20}
\end{aligned}$$

which is exactly the same as (3.2). This confirms that our proposal for the topological vertex with ON-planes also works well for the flopped diagrams.

3.2 5d $SU(2)+8\mathbf{F}$: E-string theory as 5d affine D_4 quiver

In this subsection, we apply our proposal to a 5-brane system with two ON-planes. As shown in the previous subsection, $SU(2)+4\mathbf{F}$ can be realized with an ON-plane. Now we add four more flavors to the 5-brane configuration which yields a 5-brane web for $SU(2)+8\mathbf{F}$ whose UV completion is realized as the E-string theory. There are several different ways of representing the E-string theory on a circle using Type IIB 5-brane web. As $SU(2) + 8\mathbf{F}$, the corresponding 5-brane web is given by a Tao web diagram which does not involve any orientifolds [9]. As $Sp(1) + 8\mathbf{F}$, one can represent it with two $O7^-$ -planes [60] or with two $O5$ -planes [49]. In particular, as an affine D_4 -quiver

$$\begin{array}{ccc}
SU(1) & & SU(1) \\
& \diagdown & / \\
& SU(2) & \\
& / & \diagdown \\
SU(1) & & SU(1)
\end{array}, \tag{3.21}$$

one can use a 5-brane with two ON-planes as depicted in Figure 15. We use this 5-brane web to compute the partition function by our proposal of topological vertex with ON-planes. As its partition function is non-trivial, this case would be another good example for testing our proposal.

As one can see, Figure 15 is similar to the $SU(2) + 4\mathbf{F}$ web diagrams discussed in the previous section, the left and right hand sides of Figure 15 are two copies of the right hand side of the diagram in Figure 12(a). The eight mass parameters $M_i = e^{-\beta m_i}, i = 1, \dots, 8$ can be accordingly labelled in the 5-brane web diagram, where two $C^{\mathbf{R}}$ are introduced to the vertex nearest to each ON-plane. By using our proposal with ON-planes, we write the topological string partition function for

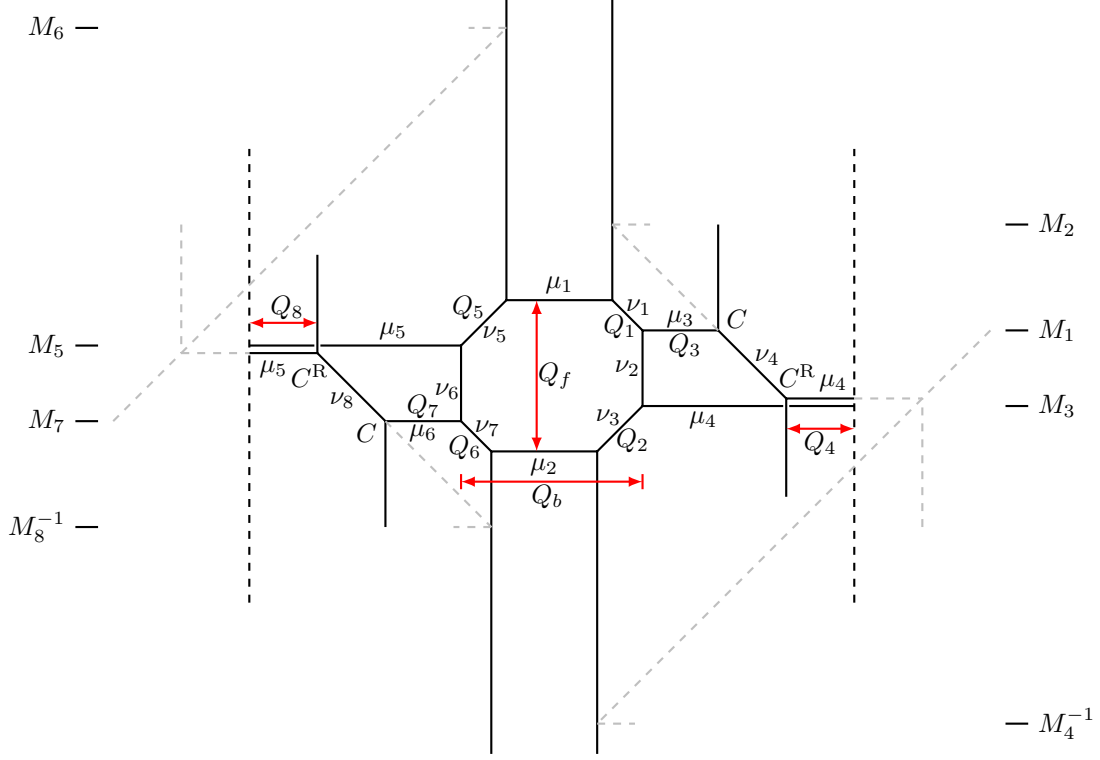


Figure 15. A 5-brane web for E-string theory on a circle as affine D_4 -quiver.

$SU(2)+8\mathbf{F}$ as

$$\begin{aligned}
Z^{\text{SU}(2)+8\mathbf{F}} &= \sum_{\mu, \nu} C_{\emptyset \nu_1^t \mu_1}(\mathbf{t}, \mathbf{q}) C_{\nu_2^t \nu_1 \mu_3^t}(\mathbf{q}, \mathbf{t}) C_{\nu_3^t \nu_2 \mu_4^t}(\mathbf{q}, \mathbf{t}) C_{\nu_3 \emptyset \mu_2}(\mathbf{t}, \mathbf{q}) C_{\emptyset \nu_4^t \mu_3}(\mathbf{t}, \mathbf{q}) \\
&\times C_{\emptyset \nu_4 \mu_4^t}^{\text{R}}(\mathbf{q}, \mathbf{t}) C_{\nu_5^t \emptyset \mu_1^t}(\mathbf{q}, \mathbf{t}) C_{\nu_5 \nu_6^t \mu_5}(\mathbf{t}, \mathbf{q}) C_{\nu_6 \nu_7^t \mu_6}(\mathbf{t}, \mathbf{q}) C_{\emptyset \nu_7 \mu_2^t}(\mathbf{q}, \mathbf{t}) \\
&\times C_{\emptyset \nu_8^t \mu_5}^{\text{R}}(\mathbf{t}, \mathbf{q}) C_{\emptyset \nu_8 \mu_6^t}(\mathbf{q}, \mathbf{t}) (-Q_1)^{|\nu_1|} \left(-\frac{Q_f}{Q_{1,2}}\right)^{|\nu_2|} \tilde{f}_{\nu_2}(\mathbf{q}, \mathbf{t}) (-Q_2)^{|\nu_3|} \\
&\times \left(-\frac{Q_f}{Q_{1,2}} \sqrt{\frac{\mathbf{q}}{\mathbf{t}}}\right)^{|\nu_4|} (-Q_5)^{|\nu_5|} \left(-\frac{Q_f}{Q_{5,6}}\right)^{|\nu_6|} \tilde{f}_{\nu_6}^{-1}(\mathbf{q}, \mathbf{t}) (-Q_6)^{|\nu_7|} \left(-\frac{Q_f}{Q_{5,6}} \sqrt{\frac{\mathbf{t}}{\mathbf{q}}}\right)^{|\nu_8|} \\
&\times \left(-\frac{Q_b}{Q_{1,5}}\right)^{|\mu_1|} f_{\mu_1}(\mathbf{t}, \mathbf{q}) \left(-\frac{Q_b}{Q_{2,6}}\right)^{|\mu_2|} f_{\mu_2}(\mathbf{t}, \mathbf{q})^{-1} (-Q_3)^{|\mu_3|} \left(+\frac{Q_{3,f,4^2}}{Q_{1,2}}\right)^{|\mu_4|} f_{\mu_4^t}(\mathbf{q}, \mathbf{t}) \\
&\times \frac{\tilde{Z}_{\mu_4}(\mathbf{t}, \mathbf{q})}{\tilde{Z}_{\mu_4^t}(\mathbf{q}, \mathbf{t})} \left(+\frac{Q_{8^2,f,7}}{Q_{5,6}}\right)^{|\mu_5|} f_{\mu_5}(\mathbf{t}, \mathbf{q}) \frac{\tilde{Z}_{\mu_5^t}(\mathbf{q}, \mathbf{t})}{\tilde{Z}_{\mu_5}(\mathbf{t}, \mathbf{q})} (-Q_7)^{|\mu_6|}. \tag{3.22}
\end{aligned}$$

After simplifying the sum over ν , we express the partition function as

$$\begin{aligned}
Z^{\text{SU}(2)+8\mathbf{F}} &= \sum_{\mu} \frac{\mathcal{R}_{\mu_1^t \mu_3}(\mathbf{Q}_1) \mathcal{R}_{\mu_1^t \mu_4}(\frac{\mathbf{Q}_f}{\mathbf{Q}_2}) \mathcal{R}_{\mu_1^t \mu_5}(\mathbf{Q}_5) \mathcal{R}_{\mu_1^t \mu_6}(\frac{\mathbf{Q}_f}{\mathbf{Q}_6}) \mathcal{R}_{\mu_3^t \mu_2}(\frac{\mathbf{Q}_f}{\mathbf{Q}_1}) \mathcal{R}_{\mu_4 \mu_2}(\mathbf{Q}_2) \mathcal{R}_{\mu_5^t \mu_2}(\frac{\mathbf{Q}_f}{\mathbf{Q}_5}) \mathcal{R}_{\mu_6^t \mu_2}(\mathbf{Q}_6)}{\mathcal{R}_{\mu_1^t \mu_2}(\mathbf{Q}_f \sqrt{\frac{\mathbf{q}}{\mathbf{t}}}) \mathcal{R}_{\mu_1^t \mu_2}(\mathbf{Q}_f \sqrt{\frac{\mathbf{t}}{\mathbf{q}}})} \\
&\times (-Q_3)^{|\mu_3|} (-Q_7)^{|\mu_6|} \left(\frac{Q_b}{Q_{1,5}}\right)^{|\mu_1|} \left(\frac{Q_b}{Q_{2,6}}\right)^{|\mu_2|} \left(-\frac{Q_{3,4^2,f}}{Q_{1,2}}\right)^{|\mu_4|} \left(-\frac{Q_{7,8^2,f}}{Q_{5,6}}\right)^{|\mu_5|}
\end{aligned}$$

$$\times \mathfrak{q}^{|\mu_2|^2 + \frac{1}{2} \sum_{i=3}^6 \|\mu_i\|^2} \mathfrak{t}^{|\mu_1^\dagger|^2 + \frac{1}{2} \sum_{i=3}^6 \|\mu_i^\dagger\|^2} \prod_{i=1}^6 \tilde{Z}_{\mu_i}(\mathfrak{t}, \mathfrak{q}) \tilde{Z}_{\mu_i^\dagger}(\mathfrak{q}, \mathfrak{t}) . \quad (3.23)$$

From the web diagram in Figure 15, the map between the Kähler parameters and the gauge theory parameters is given as follows:

$$\begin{aligned} Q_b &= A^2 u \sqrt{\frac{M_3 M_7}{M_1 M_2 M_4 M_5 M_6 M_8}}, & Q_f &= A^2, \\ Q_1 &= \frac{A}{M_1}, & Q_2 &= A M_3, & Q_3 &= \frac{M_2}{A}, & Q_4 &= \sqrt{\frac{M_3 M_4}{M_1 M_2}}, \\ Q_5 &= \frac{A}{M_5}, & Q_6 &= A M_7, & Q_7 &= \frac{M_8}{A}, & Q_8 &= \sqrt{\frac{M_6 M_7}{M_5 M_8}}, \end{aligned} \quad (3.24)$$

where A is the Coulomb branch parameter and u is the instanton factor. After extracting the \mathcal{M} factors and factorizing the remaining parts, as demonstrated in the previous subsection, we can write the partition function as

$$\begin{aligned} Z^{\text{SU}(2)+8\mathbf{F}} &= Z_{\mathbf{M}}^{N_f=8} \sum_{\mu_1 \mu_2} Z_{\mu_1 \mu_2}^{N_f=8} \sum_{\mu_3} Z_{\mu_1 \mu_2 \mu_3}(M_1, M_2) \sum_{\mu_4} Z_{\mu_1 \mu_2 \mu_4}(M_3, M_4) \\ &\quad \times \sum_{\mu_5} Z_{\mu_1 \mu_2 \mu_5}(M_5, M_6) \sum_{\mu_6} Z_{\mu_1 \mu_2 \mu_6}(M_7, M_8) , \end{aligned} \quad (3.25)$$

where

$$\begin{aligned} Z_{\mathbf{M}}^{N_f=8} &= \mathcal{M}(A^2) \mathcal{M}\left(A^2 \frac{\mathfrak{t}}{\mathfrak{q}}\right) \left[\mathcal{M}\left(\frac{A}{M_1} \sqrt{\frac{\mathfrak{t}}{\mathfrak{q}}}\right) \mathcal{M}\left(A M_1 \sqrt{\frac{\mathfrak{t}}{\mathfrak{q}}}\right) \mathcal{M}\left(\frac{A}{M_3} \sqrt{\frac{\mathfrak{t}}{\mathfrak{q}}}\right) \mathcal{M}\left(A M_3 \sqrt{\frac{\mathfrak{t}}{\mathfrak{q}}}\right) \right. \\ &\quad \left. \times \mathcal{M}\left(\frac{A}{M_5} \sqrt{\frac{\mathfrak{t}}{\mathfrak{q}}}\right) \mathcal{M}\left(A M_5 \sqrt{\frac{\mathfrak{t}}{\mathfrak{q}}}\right) \mathcal{M}\left(\frac{A}{M_7} \sqrt{\frac{\mathfrak{t}}{\mathfrak{q}}}\right) \mathcal{M}\left(A M_7 \sqrt{\frac{\mathfrak{t}}{\mathfrak{q}}}\right) \right]^{-1}, \end{aligned} \quad (3.26)$$

$$Z_{\mu_1 \mu_2}^{N_f=8} = \frac{\mathfrak{q}^{|\mu_2|^2} \mathfrak{t}^{|\mu_1^\dagger|^2} \tilde{Z}_{\mu_1}(\mathfrak{t}, \mathfrak{q}) \tilde{Z}_{\mu_1^\dagger}(\mathfrak{q}, \mathfrak{t}) \tilde{Z}_{\mu_2}(\mathfrak{t}, \mathfrak{q}) \tilde{Z}_{\mu_2^\dagger}(\mathfrak{q}, \mathfrak{t}) u^{|\mu_1|+|\mu_2|}}{\mathcal{N}_{\mu_1 \mu_2}(A^2) \mathcal{N}_{\mu_1 \mu_2}(A^2 \frac{\mathfrak{t}}{\mathfrak{q}})}, \quad (3.27)$$

and $Z_{\mu_1 \mu_2 \mu_i}(M_j, M_k)$ are the same as those defined in (3.7) and (3.8) ,

$$\begin{aligned} Z_{\mu_1 \mu_2 \mu_i}(M_j, M_k) &= \mathfrak{q}^{\frac{\|\mu_j\|^2}{2}} \mathfrak{t}^{\frac{\|\mu_k^\dagger\|^2}{2}} Z_{\mu_i}(\mathfrak{t}, \mathfrak{q}) Z_{\mu_i^\dagger}(\mathfrak{q}, \mathfrak{t}) \mathcal{N}_{\mu_1 \mu_i}\left(\frac{A}{M_j} \sqrt{\frac{\mathfrak{t}}{\mathfrak{q}}}\right) \mathcal{N}_{\mu_i \mu_2}\left(A M_j \sqrt{\frac{\mathfrak{t}}{\mathfrak{q}}}\right) \\ &\quad \times \left(-\frac{M_k}{A}\right)^{|\mu_i|} \left(\frac{1}{\sqrt{M_j M_k}}\right)^{|\mu_2|} \left(\sqrt{\frac{M_j}{M_k}}\right)^{|\mu_1|} . \end{aligned} \quad (3.28)$$

The perturbative part of the partition function then takes the form

$$Z_{\text{pert}}^{\text{SU}(2)+8\mathbf{F}} = Z_{\mathbf{M}}^{N_f=8} \sum_{\mu_3} Z_{\emptyset \emptyset \mu_3}(M_1, M_2) \sum_{\mu_4} Z_{\emptyset \emptyset \mu_4}(M_3, M_4)$$

$$\times \sum_{\mu_5} Z_{\emptyset\emptyset\mu_5}(M_5, M_6) \sum_{\mu_6} Z_{\emptyset\emptyset\mu_6}(M_7, M_8) . \quad (3.29)$$

Plugging in (3.9), dropping the extra factors and flopping necessary factors, we obtain the perturbative part in terms of the gauge theory parameters:

$$Z_{\text{pert}}^{\text{SU}(2)+8\mathbf{F}} = \frac{\mathcal{M}(A^2)\mathcal{M}(A^2\frac{\mathfrak{t}}{\mathfrak{q}})}{\prod_{i=1}^8 \mathcal{M}\left(\frac{A}{M_i}\sqrt{\frac{\mathfrak{t}}{\mathfrak{q}}}\right)\mathcal{M}\left(AM_i\sqrt{\frac{\mathfrak{t}}{\mathfrak{q}}}\right)} . \quad (3.30)$$

Expressed as the Plethystic exponential, it is given by

$$Z_{\text{pert}}^{\text{SU}(2)+8\mathbf{F}} = \text{PE}\left[\frac{1}{(1-\mathfrak{t})(1-\mathfrak{q})} \left((\mathfrak{q}+\mathfrak{t})A^2 - \chi_{16}\sqrt{\mathfrak{q}\mathfrak{t}}A\right)\right] , \quad (3.31)$$

where we denote by $\chi_{\mathbf{n}}$ the characters of the \mathbf{n} -dimensional irreducible representation of $\text{SO}(16)$. See also Appendix A for their explicit forms.

By extracting the perturbative part from (3.25), we find the instanton part has the following structure:

$$Z_{\text{inst+extra}}^{\text{SU}(2)+8\mathbf{F}} = \sum_{\mu_1, \mu_2} \left(Z_{\mu_1\mu_2}^{N_f=8} \frac{\sum_{\mu_3} Z_{\mu_1\mu_2\mu_3}(M_1, M_2) \sum_{\mu_4} Z_{\mu_1\mu_2\mu_4}(M_3, M_4)}{\sum_{\mu_3} Z_{\emptyset\emptyset\mu_3}(M_1, M_2) \sum_{\mu_4} Z_{\emptyset\emptyset\mu_4}(M_3, M_4)} \right. \\ \left. \times \frac{\sum_{\mu_5} Z_{\mu_1\mu_2\mu_5}(M_5, M_6) \sum_{\mu_6} Z_{\mu_1\mu_2\mu_6}(M_7, M_8)}{\sum_{\mu_5} Z_{\emptyset\emptyset\mu_5}(M_5, M_6) \sum_{\mu_6} Z_{\emptyset\emptyset\mu_6}(M_7, M_8)} \right) , \quad (3.32)$$

where extra factors are included. From Figure 15 we can see that there are four upper and four lower parallel external branes which are also parallel to the two ON-planes, so there will be infinitely many different strings connecting these external parallel branes. They contribute to the extra factors in (3.32) if the corresponding distances between the branes depend on the instanton factor. With the definition in (3.13), (3.32) is rewritten as

$$Z_{\text{inst+extra}}^{\text{SU}(2)+8\mathbf{F}} = \sum_{\mu_1, \mu_2} Z_{\mu_1\mu_2}^{N_f=8} \mathcal{Z}_{\mu_1\mu_2}(M_1, M_2) \mathcal{Z}_{\mu_1\mu_2}(M_3, M_4) \mathcal{Z}_{\mu_1\mu_2}(M_5, M_6) \mathcal{Z}_{\mu_1\mu_2}(M_7, M_8) . \quad (3.33)$$

By plugging in the expressions of $\mathcal{Z}_{\mu_1\mu_2}$'s, for up to two-instanton, (3.15) and (3.16), we can obtain the instanton partition function which includes the extra factors.

As the Omega deformation parameters capture the left-right spin content $[j_l, j_r]$ of the theory under $\text{SU}(2)_l \times \text{SU}(2)_r$, which is [28, 62, 63] defined as

$$[j_l, j_r] := \frac{(-1)^{2j_l+2j_r+1} \left((\mathfrak{t}\mathfrak{q})^{-j_l} + \dots + (\mathfrak{t}\mathfrak{q})^{j_l} \right) \left(\left(\frac{\mathfrak{t}}{\mathfrak{q}}\right)^{-j_r} + \dots + \left(\frac{\mathfrak{t}}{\mathfrak{q}}\right)^{j_r} \right)}{(\mathfrak{t}^{1/2} - \mathfrak{t}^{-1/2})(\mathfrak{q}^{1/2} - \mathfrak{q}^{-1/2})} , \quad (3.34)$$

we express the partition function as the GV invariant with $[j_l, j_r]$ and the characters χ for the flavor symmetry. The perturbative part is then re-expressed as

$$Z_{\text{pert}}^{\text{SU}(2)+8\mathbf{F}} = \text{PE}\left[\left[0, \frac{1}{2}\right] A^2 + \chi_{16} [0, 0] A\right] . \quad (3.35)$$

The instanton partition function which includes the extra factors can be written as

$$Z_{\text{inst+extra}}^{\text{SU}(2)+8\mathbf{F}} = \text{PE} \left[\sum_{n=1}^{\infty} d_n(A, M_i, \mathbf{t}, \mathbf{q}) u^n \right], \quad (3.36)$$

with

$$d_n(A, M_i, \mathbf{t}, \mathbf{q}) = \sum_{m=0}^{\infty} d_{n,m}(M_i, \mathbf{t}, \mathbf{q}) A^m, \quad (3.37)$$

where the mass M_i terms are organized as the characters $\chi_{\mathbf{n}}$ of $\text{SO}(16)$, whose explicit forms are given in Appendix A. As the extra factor is the part that does not depend on the Coulomb branch parameter A , the extra factor is expressed as $Z_{\text{extra}} = \text{PE} \left[\sum_{n=1}^{\infty} d_{n,0} u^n \right]$. Discarding this extra factor, we find the instanton part is given by

$$Z_{\text{inst}}^{\text{SU}(2)+8\mathbf{F}} = \text{PE} \left[\sum_{n,m=1}^{\infty} d_{n,m} A^m u^n \right], \quad (3.38)$$

where, up to u^3 and A^2 , the explicit forms of $d_{n,m}$ with $n \leq 3, m \leq 2$ are given as follows:

$$\begin{aligned} d_{1,1} &= \chi_{\overline{128}} [0, 0], \\ d_{1,2} &= \chi_{128} [0, \frac{1}{2}], \\ d_{2,1} &= \chi_{16} [\frac{1}{2}, \frac{1}{2}] + (\chi_{560} + \chi_{16}) [0, 0], \\ d_{2,2} &= [1, \frac{3}{2}] + (\chi_{120} + 1) [\frac{1}{2}, 1] + [\frac{1}{2}, 0] + (\chi_{1820} + \chi_{120} + 2) [0, \frac{1}{2}], \\ d_{3,1} &= \chi_{\overline{128}} [\frac{1}{2}, \frac{1}{2}] + (\chi_{\overline{1920}} + \chi_{\overline{128}}) [0, 0], \\ d_{3,2} &= \chi_{128} [1, \frac{3}{2}] + (\chi_{1920} + 2\chi_{128}) [\frac{1}{2}, 1] + \chi_{128} [\frac{1}{2}, 0] + (\chi_{13312} + \chi_{1920} + 3\chi_{128}) [0, \frac{1}{2}]. \end{aligned} \quad (3.39)$$

The result completely agrees with the known refined partition function [9, 39, 64]. We note that there has been several partition function computations for $\text{SU}(2)+8\mathbf{F}$ based the topological vertex [9, 49, 65], but all these attempts are computed in the unrefined limit $\mathbf{t} = \mathbf{q}$. The result (3.38) is the first example that correctly reproduces the refined result based on topological vertex formalism.

3.3 5d $\text{SU}(3)$ theory at CS level 7

In this subsection, we consider yet another non-trivial theory of rank-2. It was proposed in [14] that pure $\text{SU}(3)$ theories at various Chern-Simons (CS) level κ can have 5-brane webs with ON-plane(s). Such 5-brane webs can be understood as a Higgsing from D-type quivers. We first consider the example of $\kappa = 7$, denoted as

$SU(3)_7$. It is obtained by Higgsing the D_4 -type quiver

$$\begin{array}{c}
 \text{SU}(2) \\
 \diagup \\
 \text{SU}(2) \text{ --- } \text{SU}(3)_1 \\
 \diagdown \\
 \text{SU}(2)
 \end{array}
 \tag{3.40}$$

where the middle node is an $SU(3)$ theory at the CS level 1, the corresponding

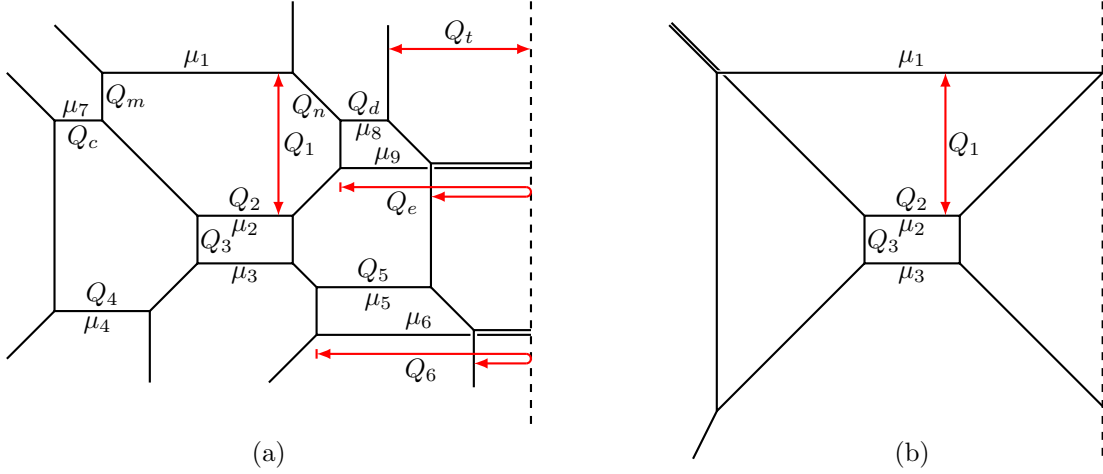


Figure 16. (a) The D_4 -type quiver theory. (b) $SU(3)$ theory at CS level 7.

web diagram is illustrated in Figure 16(a). Here, the Higgsing procedure is as follows: A Higgsing of an $SU(2)$ gives rise to an antisymmetric hypermultiplet (**AS**) to $SU(3)$, increasing the CS level of $SU(3)$ by $\frac{3}{2}$ [14]. As we have three $SU(2)$, we get $SU(3)_{\frac{11}{2}} + 3\mathbf{AS}$ after the Higgsing, in Figure 16(a) it corresponds to shrink $Q_m, Q_c, Q_n, Q_d, Q_t, Q_e$. Finally, since an antisymmetric hypermultiplet transforms as $\mathbf{3}$, the decoupling of an antisymmetric hypermultiplet further increases the CS level of $SU(3)$ by $\frac{1}{2}$. Hence, decoupling all the **AS** which means flopping Q_4, Q_5, Q_6 downward to infinity yields $SU(3)_7$ whose web diagram is illustrated in Figure 16(b).

However, if we start from Figure 16(a) to compute the topological string partition function, the two $SU(2)$ sub webs on the right side are overlapping. In order to use our ON proposal, we have to swap the positions of the brane μ_9 and μ_5 in the web diagram to make the sub webs of the two $SU(2)$ nodes separated which corresponds to Figure 17. Due to this swapping, the Kähler parameters in Figure 16(a) change into the Kähler parameters in Figure 17. Then, by our proposal of topological vertex with ON-planes, the input data of topological vertex for Figure 17 is:

$$Z'^{D_4} = \sum_{\mu, \nu} C_{\emptyset \nu_1^t \mu_1}(\mathbf{t}, \mathbf{q}) C_{\nu_2^t \nu_1^t \mu_8^t}(\mathbf{q}, \mathbf{t}) C_{\nu_3^t \nu_2^t \mu_5^t}(\mathbf{q}, \mathbf{t}) C_{\nu_3^t \nu_4^t \mu_2}(\mathbf{t}, \mathbf{q}) C_{\nu_4^t \nu_5^t \mu_3}(\mathbf{t}, \mathbf{q}) C_{\nu_6^t \nu_5^t \mu_9^t}(\mathbf{q}, \mathbf{t}) C_{\emptyset \nu_6^t \mu_6^t}(\mathbf{q}, \mathbf{t})$$

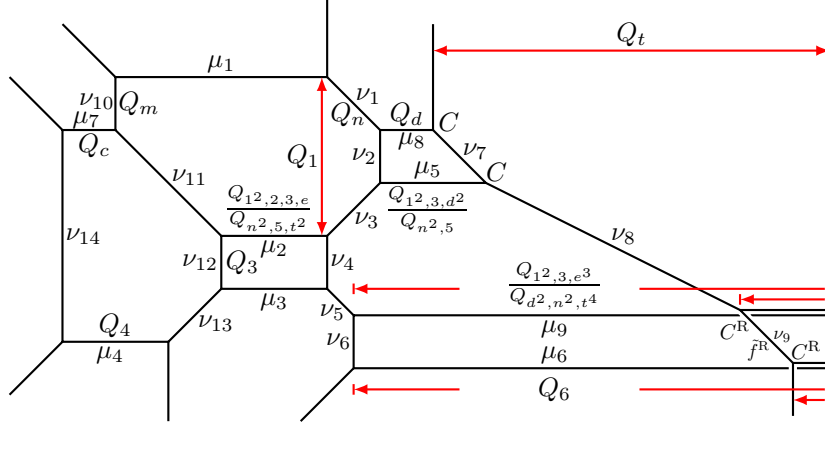


Figure 17. The D_4 -type quiver theory with separated $SU(2)$ sub webs on the right.

$$\begin{aligned}
& \times C_{\emptyset\nu_7^t\mu_8}(\mathbf{t}, \mathbf{q}) C_{\nu_7\nu_8^t\mu_5}(\mathbf{t}, \mathbf{q}) C_{\nu_9^t\nu_8\mu_9}^R(\mathbf{q}, \mathbf{t}) C_{\emptyset\nu_9\mu_6}^R(\mathbf{q}, \mathbf{t}) C_{\nu_{10}\emptyset\mu_1^t}(\mathbf{q}, \mathbf{t}) C_{\nu_{10}\nu_{11}^t\mu_7}(\mathbf{t}, \mathbf{q}) \\
& \times C_{\nu_{12}^t\nu_{11}\mu_2^t}(\mathbf{q}, \mathbf{t}) C_{\nu_{13}^t\nu_{12}\mu_3^t}(\mathbf{q}, \mathbf{t}) C_{\nu_{13}\emptyset\mu_4}(\mathbf{t}, \mathbf{q}) C_{\nu_{14}\emptyset\mu_7^t}(\mathbf{q}, \mathbf{t}) C_{\emptyset\nu_{14}\mu_4^t}(\mathbf{q}, \mathbf{t}) (-Q_n)^{|\nu_1|} \\
& \times \left(-\frac{Q^{1^2,3,d}}{Q_{n^2,5}}\right)^{|\nu_2|} \tilde{f}_{\nu_2}(\mathbf{q}, \mathbf{t}) \left(-\frac{Q_{n,5}}{Q_{1,3,d}}\right)^{|\nu_3|} (-Q_3)^{|\nu_4|} \tilde{f}_{\nu_4}(\mathbf{q}, \mathbf{t})^{-1} \left(-\frac{Q_{d,n,t^2}}{Q_{e,3,1}}\right)^{|\nu_5|} \left(-\frac{Q^{1^2,3,e^3}}{Q_{d^2,n^2,t^4,6}}\right)^{|\nu_6|} \\
& \times \tilde{f}_{\nu_6}(\mathbf{q}, \mathbf{t}) \left(-\frac{Q^{1^2,3,d}}{Q_{n^2,5}}\right)^{|\nu_7|} \tilde{f}_{\nu_7}(\mathbf{q}, \mathbf{t})^{-1} \left(-\frac{Q_{n^2,t^2,5}}{Q^{1^2,3,e}} \sqrt{\frac{\mathbf{q}}{\mathbf{t}}}\right)^{|\nu_8|} \left(-\frac{Q^{1^2,3,e^3}}{Q_{d^2,n^2,t^4,6}}\right)^{|\nu_9|} \tilde{f}_{\nu_9}^R(\mathbf{q}, \mathbf{t}) \\
& \times (-Q_m)^{|\nu_{10}|} \left(-\frac{Q_1}{Q_m}\right)^{\nu_{11}} (-Q_3)^{|\nu_{12}|} \tilde{f}_{\nu_{12}}(\mathbf{q}, \mathbf{t}) \left(-\frac{Q_{c,1}}{Q_{m,4}}\right)^{|\nu_{13}|} \left(-\frac{Q_{c,3,1^2}}{Q_{m^2,4}}\right)^{|\nu_{14}|} \tilde{f}_{\nu_{14}}(\mathbf{q}, \mathbf{t}) \\
& \times \left(-\frac{Q^{1^2,2,e}}{Q_{n^2,t^2,m,d}}\right)^{|\mu_1|} \left(-\frac{Q^{1^2,2,3,e}}{Q_{n^2,5,t^2}}\right)^{|\mu_2|} f_{\mu_2}(\mathbf{t}, \mathbf{q})^{-1} \left(-\frac{Q^{1^2,2,3,e}}{Q_{n^2,5,t^2}}\right)^{|\mu_3|} f_{\mu_3}(\mathbf{t}, \mathbf{q}) (-Q_d)^{|\mu_8|} \\
& \times \left(-\frac{Q^{1^2,3,d^2}}{Q_{n^2,5}}\right)^{|\mu_5|} f_{\mu_5}(\mathbf{t}, \mathbf{q})^2 \left(\frac{Q^{1^2,3,e^3}}{Q_{d^2,n^2,t^4}}\right)^{|\mu_9|} f_{\mu_9}(\mathbf{t}, \mathbf{q})^{-2} f_{\mu_9^t}(\mathbf{q}, \mathbf{t}) \frac{\tilde{Z}_{\mu_9}(\mathbf{t}, \mathbf{q})}{\tilde{Z}_{\mu_9^t}(\mathbf{q}, \mathbf{t})} Q_6^{|\mu_6|} \\
& \times f_{\mu_6^t}(\mathbf{q}, \mathbf{t}) \frac{\tilde{Z}_{\mu_6}(\mathbf{t}, \mathbf{q})}{\tilde{Z}_{\mu_6^t}(\mathbf{q}, \mathbf{t})} (-Q_c)^{|\mu_7|} (-Q_4)^{|\mu_4|} . \tag{3.41}
\end{aligned}$$

After summing over the non-preferred direction Young diagrams, the result is

$$Z'^{D_4} = \sum_{\boldsymbol{\mu}} Z'^{D_4}_{\mu_1\mu_2\mu_3} Z^{D_4}_{\mu_1\mu_2\mu_3\mu_7\mu_4} Z'^{D_4}_{\mu_1\mu_2\mu_3\mu_8\mu_5} Z'^{D_4}_{\mu_1\mu_2\mu_3\mu_9\mu_6} \tag{3.42}$$

where

$$\begin{aligned}
Z'^{D_4}_{\mu_1\mu_2\mu_3} &= W_{\mu_1}(\mathbf{t}, \mathbf{q}) \left(-\frac{Q^{1^2,2,e}}{Q_{n^2,t^2,m,d}}\right)^{|\mu_1|} W_{\mu_2}(\mathbf{t}, \mathbf{q}) \left(-\frac{Q^{1^2,2,3,e}}{Q_{n^2,5,t^2}}\right)^{|\mu_2|} f_{\mu_2}(\mathbf{t}, \mathbf{q})^{-1} W_{\mu_3}(\mathbf{t}, \mathbf{q}) \\
& \times \left(-\frac{Q^{1^2,2,3,e}}{Q_{n^2,5,t^2}}\right)^{|\mu_3|} f_{\mu_3}(\mathbf{t}, \mathbf{q}) \times \left[\mathcal{R}_{\mu_1^t\mu_2}(Q_1\sqrt{\frac{\mathbf{q}}{\mathbf{t}}}) \mathcal{R}_{\mu_1^t\mu_2}(Q_1\sqrt{\frac{\mathbf{t}}{\mathbf{q}}}) \mathcal{R}_{\mu_1^t\mu_3}(Q_{1,3}\sqrt{\frac{\mathbf{q}}{\mathbf{t}}}) \right. \\
& \left. \times \mathcal{R}_{\mu_1^t\mu_3}(Q_{1,3}\sqrt{\frac{\mathbf{t}}{\mathbf{q}}}) \mathcal{R}_{\mu_2^t\mu_3}(Q_3\sqrt{\frac{\mathbf{q}}{\mathbf{t}}}) \mathcal{R}_{\mu_2^t\mu_3}(Q_3\sqrt{\frac{\mathbf{t}}{\mathbf{q}}}) \right]^{-1} , \tag{3.43}
\end{aligned}$$

$$\begin{aligned}
Z_{\mu_1\mu_2\mu_3\mu_7\mu_4}^{D_4} &= W_{\mu_7}(\mathbf{t}, \mathbf{q})(-Q_c)^{|\mu_7|} W_{\mu_4}(\mathbf{t}, \mathbf{q})(-Q_4)^{|\mu_4|} \mathcal{R}_{\mu_1^\dagger\mu_7}(Q_m) \mathcal{R}_{\mu_7^\dagger\mu_2}\left(\frac{Q_1}{Q_m}\right) \\
&\times \mathcal{R}_{\mu_7^\dagger\mu_3}\left(\frac{Q_{1,3}}{Q_m}\right) \mathcal{R}_{\mu_1^\dagger\mu_4}\left(\frac{Q_{1^2,3,c}}{Q_{m,4}}\right) \mathcal{R}_{\mu_2^\dagger\mu_4}\left(\frac{Q_{1,3,c}}{Q_{m,4}}\right) \mathcal{R}_{\mu_3^\dagger\mu_4}\left(\frac{Q_{1,c}}{Q_{m,4}}\right) \\
&\times \left[\mathcal{R}_{\mu_7^\dagger\mu_4}\left(\frac{Q_{c,3,1^2}}{Q_{m^2,4}} \sqrt{\frac{\mathbf{q}}{\mathbf{t}}}\right) \mathcal{R}_{\mu_7^\dagger\mu_4}\left(\frac{Q_{c,3,1^2}}{Q_{m^2,4}} \sqrt{\frac{\mathbf{t}}{\mathbf{q}}}\right) \right]^{-1}, \tag{3.44}
\end{aligned}$$

$$\begin{aligned}
Z'_{\mu_1\mu_2\mu_3\mu_8\mu_5}^{D_4} &= W_{\mu_8}(\mathbf{t}, \mathbf{q})(-Q_d)^{|\mu_8|} W_{\mu_5}(\mathbf{t}, \mathbf{q}) \left(-\frac{Q_{1^2,3,d^2}}{Q_{n^2,5}}\right)^{|\mu_5|} f_{\mu_5}(\mathbf{t}, \mathbf{q})^2 \mathcal{R}_{\mu_1^\dagger\mu_8}(Q_n) \\
&\times \mathcal{R}_{\mu_8^\dagger\mu_2}\left(\frac{Q_1}{Q_n}\right) \mathcal{R}_{\mu_3^\dagger\mu_3}\left(\frac{Q_{1,3}}{Q_n}\right) \mathcal{R}_{\mu_1^\dagger\mu_5}\left(\frac{Q_{1^2,3,d}}{Q_{n,5}}\right) \mathcal{R}_{\mu_5^\dagger\mu_2}\left(\frac{Q_{n,5}}{Q_{1,3,d}}\right) \mathcal{R}_{\mu_5^\dagger\mu_3}\left(\frac{Q_{n,5}}{Q_{1,d}}\right) \\
&\times \left[\mathcal{R}_{\mu_8^\dagger\mu_5}\left(\frac{Q_{1^2,3,d}}{Q_{n^2,5}} \sqrt{\frac{\mathbf{q}}{\mathbf{t}}}\right) \mathcal{R}_{\mu_8^\dagger\mu_5}\left(\frac{Q_{1^2,3,d}}{Q_{n^2,5}} \sqrt{\frac{\mathbf{t}}{\mathbf{q}}}\right) \right]^{-1}, \tag{3.45}
\end{aligned}$$

$$\begin{aligned}
Z'_{\mu_1\mu_2\mu_3\mu_9\mu_6}^{D_4} &= W_{\mu_9}(\mathbf{t}, \mathbf{q}) \left(-\frac{Q_{1^2,3,e^3}}{Q_{d^2,n^2,t^4}}\right)^{|\mu_9|} f_{\mu_9}(\mathbf{t}, \mathbf{q})^{-2} W_{\mu_6}(\mathbf{t}, \mathbf{q})(-Q_6)^{|\mu_6|} \mathcal{R}_{\mu_1^\dagger\mu_9}\left(\frac{Q_{d,n,t^2}}{Q_e}\right) \\
&\times \mathcal{R}_{\mu_2^\dagger\mu_9}\left(\frac{Q_{d,n,t^2}}{Q_{1,e}}\right) \mathcal{R}_{\mu_3^\dagger\mu_9}\left(\frac{Q_{d,n,t^2}}{Q_{1,3,e}}\right) \mathcal{R}_{\mu_1^\dagger\mu_6}\left(\frac{Q_{1^2,3,e^2}}{Q_{d,n,t^2,6}}\right) \mathcal{R}_{\mu_2^\dagger\mu_6}\left(\frac{Q_{1,3,e^2}}{Q_{d,n,t^2,6}}\right) \\
&\times \mathcal{R}_{\mu_3^\dagger\mu_6}\left(\frac{Q_{1,e^2}}{Q_{d,n,t^2,6}}\right) \left[\mathcal{R}_{\mu_9^\dagger\mu_6}\left(\frac{Q_{1^2,3,e^3}}{Q_{d^2,n^2,t^4,6}} \sqrt{\frac{\mathbf{q}}{\mathbf{t}}}\right) \mathcal{R}_{\mu_9^\dagger\mu_6}\left(\frac{Q_{1^2,3,e^3}}{Q_{d^2,n^2,t^4,6}} \sqrt{\frac{\mathbf{t}}{\mathbf{q}}}\right) \right]^{-1}. \tag{3.46}
\end{aligned}$$

We have defined

$$W_\mu(\mathbf{t}, \mathbf{q}) \equiv \mathbf{t}^{\frac{\|\mu^\dagger\|^2}{2}} \mathbf{q}^{\frac{\|\mu\|^2}{2}} \tilde{Z}_{\mu^\dagger}(\mathbf{q}, \mathbf{t}) \tilde{Z}_\mu(\mathbf{t}, \mathbf{q}) \tag{3.47}$$

for convenience, this factor is universal for every color brane.

However, in order to do the Higgsing and decoupling, it is much more convenient to use Figure 16(a). So, we transform the result obtained from Figure 17 to the one that corresponds to Figure 16(a) by using the following formula [66]:

$$\mathcal{R}_{\mu^\dagger\nu}(Q^{-1}; \mathbf{t}, \mathbf{q}) \rightarrow (Q^{-1})^{|\mu|+|\nu|} f_\mu(\mathbf{t}, \mathbf{q})^{-1} f_\nu(\mathbf{t}, \mathbf{q}) \mathcal{R}_{\nu^\dagger\mu}(Q; \mathbf{t}, \mathbf{q}), \tag{3.48}$$

which can be derived from

$$\mathcal{N}_{\mu\nu}\left(\sqrt{\frac{\mathbf{t}}{\mathbf{q}}}Q^{-1}; \mathbf{t}, \mathbf{q}\right) = (Q^{-1})^{|\mu|+|\nu|} f_\mu(\mathbf{t}, \mathbf{q})^{-1} f_\nu(\mathbf{t}, \mathbf{q}) \mathcal{N}_{\nu\mu}\left(\sqrt{\frac{\mathbf{t}}{\mathbf{q}}}Q; \mathbf{t}, \mathbf{q}\right), \tag{3.49}$$

$$\mathcal{M}\left(\sqrt{\frac{\mathbf{t}}{\mathbf{q}}}Q^{-1}; \mathbf{t}, \mathbf{q}\right) \rightarrow \mathcal{M}\left(\sqrt{\frac{\mathbf{t}}{\mathbf{q}}}Q; \mathbf{t}, \mathbf{q}\right), \tag{3.50}$$

where \rightarrow means ‘‘equal up to a flop’’. We use (3.48) to exchange the order of indices of $\mathcal{R}_{\mu_5^\dagger\mu_2}, \mathcal{R}_{\mu_5^\dagger\mu_3}, \mathcal{R}_{\mu_5^\dagger\mu_9}$ and $\mathcal{R}_{\mu_3^\dagger\mu_9}$ which are affected by the swapping of color branes from Figure 17 to Figure 16(a). This procedure also generates Q factors and framing factors which will be rearranged into the Z 's of (3.42). We then have

$$Z^{D_4} = \sum_{\mu} Z_{\mu_1\mu_2\mu_3}^{D_4} Z_{\mu_1\mu_2\mu_3\mu_7\mu_4}^{D_4} Z_{\mu_1\mu_2\mu_3\mu_8\mu_5}^{D_4} Z_{\mu_1\mu_2\mu_3\mu_9\mu_6}^{D_4}, \tag{3.51}$$

where

$$\begin{aligned}
Z_{\mu_1\mu_2\mu_3}^{D_4} &= W_{\mu_1}(\mathbf{t}, \mathbf{q}) \left(-\frac{Q_{1^2,2,e}}{Q_{n^2,t^2,m,d}}\right)^{|\mu_1|} W_{\mu_2}(\mathbf{t}, \mathbf{q}) (-Q_2)^{|\mu_2|} f_{\mu_2}(\mathbf{t}, \mathbf{q})^{-1} W_{\mu_3}(\mathbf{t}, \mathbf{q}) \\
&\times (-Q_2)^{|\mu_3|} f_{\mu_3}(\mathbf{t}, \mathbf{q}) \times \left[\mathcal{R}_{\mu_1^\dagger\mu_2} \left(Q_1 \sqrt{\frac{\mathbf{q}}{\mathbf{t}}}\right) \mathcal{R}_{\mu_1^\dagger\mu_2} \left(Q_1 \sqrt{\frac{\mathbf{t}}{\mathbf{q}}}\right) \mathcal{R}_{\mu_1^\dagger\mu_3} \left(Q_{1,3} \sqrt{\frac{\mathbf{q}}{\mathbf{t}}}\right) \right. \\
&\times \left. \mathcal{R}_{\mu_1^\dagger\mu_3} \left(Q_{1,3} \sqrt{\frac{\mathbf{t}}{\mathbf{q}}}\right) \mathcal{R}_{\mu_2^\dagger\mu_3} \left(Q_3 \sqrt{\frac{\mathbf{q}}{\mathbf{t}}}\right) \mathcal{R}_{\mu_2^\dagger\mu_3} \left(Q_3 \sqrt{\frac{\mathbf{t}}{\mathbf{q}}}\right) \right]^{-1}, \tag{3.52}
\end{aligned}$$

$$\begin{aligned}
Z_{\mu_1\mu_2\mu_3\mu_7\mu_4}^{D_4} &= W_{\mu_7}(\mathbf{t}, \mathbf{q}) (-Q_c)^{|\mu_7|} W_{\mu_4}(\mathbf{t}, \mathbf{q}) (-Q_4)^{|\mu_4|} \mathcal{R}_{\mu_1^\dagger\mu_7} \left(Q_m\right) \mathcal{R}_{\mu_7^\dagger\mu_2} \left(\frac{Q_1}{Q_m}\right) \\
&\times \mathcal{R}_{\mu_7^\dagger\mu_3} \left(\frac{Q_{1,3}}{Q_m}\right) \mathcal{R}_{\mu_1^\dagger\mu_4} \left(\frac{Q_{1^2,3,c}}{Q_{m,4}}\right) \mathcal{R}_{\mu_2^\dagger\mu_4} \left(\frac{Q_{1,3,c}}{Q_{m,4}}\right) \mathcal{R}_{\mu_3^\dagger\mu_4} \left(\frac{Q_{1,c}}{Q_{m,4}}\right) \\
&\times \left[\mathcal{R}_{\mu_7^\dagger\mu_4} \left(\frac{Q_{c,3,1^2}}{Q_{m^2,4}} \sqrt{\frac{\mathbf{q}}{\mathbf{t}}}\right) \mathcal{R}_{\mu_7^\dagger\mu_4} \left(\frac{Q_{c,3,1^2}}{Q_{m^2,4}} \sqrt{\frac{\mathbf{t}}{\mathbf{q}}}\right) \right]^{-1}, \tag{3.53}
\end{aligned}$$

$$\begin{aligned}
Z_{\mu_1\mu_2\mu_3\mu_8\mu_5}^{D_4} &= W_{\mu_8}(\mathbf{t}, \mathbf{q}) (-Q_d)^{|\mu_8|} W_{\mu_5}(\mathbf{t}, \mathbf{q}) (-Q_5)^{|\mu_5|} \mathcal{R}_{\mu_1^\dagger\mu_8} \left(Q_n\right) \\
&\times \mathcal{R}_{\mu_8^\dagger\mu_2} \left(\frac{Q_1}{Q_n}\right) \mathcal{R}_{\mu_8^\dagger\mu_3} \left(\frac{Q_{1,3}}{Q_n}\right) \mathcal{R}_{\mu_1^\dagger\mu_5} \left(\frac{Q_{1^2,3,d}}{Q_{n,5}}\right) \mathcal{R}_{\mu_2^\dagger\mu_5} \left(\frac{Q_{1,3,d}}{Q_{n,5}}\right) \mathcal{R}_{\mu_3^\dagger\mu_5} \left(\frac{Q_{1,d}}{Q_{n,5}}\right) \\
&\times \left[\mathcal{R}_{\mu_8^\dagger\mu_5} \left(\frac{Q_{1^2,3,d}}{Q_{n^2,5}} \sqrt{\frac{\mathbf{q}}{\mathbf{t}}}\right) \mathcal{R}_{\mu_8^\dagger\mu_5} \left(\frac{Q_{1^2,3,d}}{Q_{n^2,5}} \sqrt{\frac{\mathbf{t}}{\mathbf{q}}}\right) \right]^{-1}, \tag{3.54}
\end{aligned}$$

$$\begin{aligned}
Z_{\mu_1\mu_2\mu_3\mu_9\mu_6}^{D_4} &= W_{\mu_9}(\mathbf{t}, \mathbf{q}) (-Q_e)^{|\mu_9|} W_{\mu_6}(\mathbf{t}, \mathbf{q}) (-Q_6)^{|\mu_6|} \mathcal{R}_{\mu_1^\dagger\mu_9} \left(\frac{Q_{d,n,t^2}}{Q_e}\right) \\
&\times \mathcal{R}_{\mu_9^\dagger\mu_2} \left(\frac{Q_{1,e}}{Q_{d,n,t^2}}\right) \mathcal{R}_{\mu_9^\dagger\mu_3} \left(\frac{Q_{1,3,e}}{Q_{d,n,t^2}}\right) \mathcal{R}_{\mu_1^\dagger\mu_6} \left(\frac{Q_{1^2,3,e^2}}{Q_{d,n,t^2,6}}\right) \mathcal{R}_{\mu_2^\dagger\mu_6} \left(\frac{Q_{1,3,e^2}}{Q_{d,n,t^2,6}}\right) \\
&\times \mathcal{R}_{\mu_3^\dagger\mu_6} \left(\frac{Q_{1,e^2}}{Q_{d,n,t^2,6}}\right) \left[\mathcal{R}_{\mu_9^\dagger\mu_6} \left(\frac{Q_{1^2,3,e^3}}{Q_{d^2,n^2,t^4,6}} \sqrt{\frac{\mathbf{q}}{\mathbf{t}}}\right) \mathcal{R}_{\mu_9^\dagger\mu_6} \left(\frac{Q_{1^2,3,e^3}}{Q_{d^2,n^2,t^4,6}} \sqrt{\frac{\mathbf{t}}{\mathbf{q}}}\right) \right]^{-1}. \tag{3.55}
\end{aligned}$$

We can see from the above results that the Q factors and framing factors generated through (3.48) compensate the Q factors and framing factors⁷ corresponding to the color branes μ_2, μ_3, μ_5 and μ_9 in Figure 17 to make the recombined Q factors and framing factors correspond to the original unswapped web diagram in Figure 16(a). And now, the forms of (3.54) and (3.55) are exactly like the form of (3.53). Then we take the Higgsing limit which means that $Q_m, Q_c, Q_n, Q_d, Q_t, Q_e$ in Figure 16(a) shrink and take some \mathbf{t}, \mathbf{q} related values in the limit. For Q_m, Q_c, Q_n, Q_d their limits are found in [44], which is $\sqrt{\frac{\mathbf{q}}{\mathbf{t}}}$ for all of them. As the right hand side of the middle SU(3) node in Figure 16(a) has two separate SU(2) nodes, we can find⁸ that Q_d in one node corresponds to Q_e in the other node, similarly Q_n in one node corresponds to $\frac{Q_{n,d,t^2}}{Q_e}$ in the other node, so $Q_e \rightarrow \sqrt{\frac{\mathbf{q}}{\mathbf{t}}}$ and $Q_t \rightarrow 1$ in the Higgsing limit.

⁷Here the framing factors are the \mathcal{F}_\bullet in (2.18) which are framing factors of the unreflected branes.

⁸By observation from Figure 16(a), Q_d is the length of color brane μ_8 , Q_e is the length of color brane μ_9 , Q_n is the distance between μ_1 and μ_8 , $\frac{Q_{n,d,t^2}}{Q_e}$ is the distance between μ_1 and μ_9 .

In the partition function (3.51) there are three factors which come from the three SU(3)-SU(2) bifundamental contributions:

$$\mathcal{R}_{\mu_1^t \mu_7}(Q_m) \mathcal{R}_{\mu_1^t \mu_8}(Q_n) \mathcal{R}_{\mu_1^t \mu_9}\left(\frac{Q_{d,n,t^2}}{Q_e}\right). \quad (3.56)$$

After dropping the \mathcal{M} 's from the \mathcal{R} 's, the remaining is

$$\mathcal{N}_{\mu_1 \mu_7}(Q_m \sqrt{\frac{\mathfrak{t}}{\mathfrak{q}}}) \mathcal{N}_{\mu_1 \mu_8}(Q_n \sqrt{\frac{\mathfrak{t}}{\mathfrak{q}}}) \mathcal{N}_{\mu_1 \mu_9}\left(\frac{Q_{d,n,t^2}}{Q_e} \sqrt{\frac{\mathfrak{t}}{\mathfrak{q}}}\right). \quad (3.57)$$

Then we plug in the Higgsing limit values for the Kähler parameters, we obtain

$$\mathcal{N}_{\mu_1 \mu_7}(1; \mathfrak{t}, \mathfrak{q}) \mathcal{N}_{\mu_1 \mu_8}(1; \mathfrak{t}, \mathfrak{q}) \mathcal{N}_{\mu_1 \mu_9}(1; \mathfrak{t}, \mathfrak{q}). \quad (3.58)$$

By using the following formula which is found in [44]:

$$\mathcal{N}_{\mu\alpha}(1; \mathfrak{t}, \mathfrak{q}) \neq 0, \text{ only if } \mu \succcurlyeq \alpha, \quad (3.59)$$

the non-zero contributing Young diagrams are now restricted to be $\mu_{7,8,9} \preccurlyeq \mu_1$. After taking this Higgsing limit, the partition function Z^{D_4} in (3.51) can now be written as

$$Z^{\mu D_4} = Z_M^{D_4} \sum_{\mu} \left(Z_{\mu_1 \mu_2 \mu_3}^{\kappa=7} \prod_{i=7,8,9} Z_{\mu_1 \mu_2 \mu_3 \mu_i} \prod_{j=4,5,6} Z_{\mu_1 \mu_2 \mu_3 \mu_{j+3} \mu_j}^{Q_j} \right), \quad (3.60)$$

where

$$Z_M^{D_4} = \frac{\mathcal{M}(Q_1) \mathcal{M}(Q_3) \mathcal{M}(Q_{1,3}) \mathcal{M}(Q_3 \frac{\mathfrak{t}}{\mathfrak{q}})}{\mathcal{M}(1)^3 \mathcal{M}(Q_1 \frac{\mathfrak{t}}{\mathfrak{q}})^2 \mathcal{M}(Q_{1,3} \frac{\mathfrak{t}}{\mathfrak{q}})^2} \prod_{j=4,5,6} \frac{\mathcal{M}\left(\frac{Q_{1^2,3}}{Q_j} \sqrt{\frac{\mathfrak{t}}{\mathfrak{q}}}\right) \mathcal{M}\left(\frac{Q_{1^2,3}}{Q_j} \frac{\mathfrak{t}^{3/2}}{\mathfrak{q}^{3/2}}\right)}{\mathcal{M}\left(\frac{Q_{1^2,3}}{Q_j} \sqrt{\frac{\mathfrak{t}}{\mathfrak{q}}}\right) \mathcal{M}\left(\frac{Q_{1,3}}{Q_j} \sqrt{\frac{\mathfrak{t}}{\mathfrak{q}}}\right) \mathcal{M}\left(\frac{Q_1}{Q_j} \sqrt{\frac{\mathfrak{t}}{\mathfrak{q}}}\right)}, \quad (3.61)$$

$$Z_{\mu_1 \mu_2 \mu_3}^{\kappa=7} = \frac{\mathfrak{q}^{\frac{\|\mu_1\|^2}{2} + \|\mu_2\|^2} \mathfrak{t}^{\frac{\|\mu_1^t\|^2}{2} + \|\mu_3^t\|^2} \prod_{i=1,2,3} \tilde{Z}_{\mu_i}(\mathfrak{t}, \mathfrak{q}) \tilde{Z}_{\mu_i^t}(\mathfrak{q}, \mathfrak{t}) \left(-Q_{1^2,2} \frac{\mathfrak{t}^{3/2}}{\mathfrak{q}^{3/2}}\right)^{|\mu_1|} Q_2^{|\mu_2| + |\mu_3|}}{\mathcal{N}_{\mu_1 \mu_2}(Q_1) \mathcal{N}_{\mu_1 \mu_2}(Q_1 \frac{\mathfrak{t}}{\mathfrak{q}}) \mathcal{N}_{\mu_1 \mu_3}(Q_{1,3}) \mathcal{N}_{\mu_1 \mu_3}(Q_{1,3} \frac{\mathfrak{t}}{\mathfrak{q}}) \mathcal{N}_{\mu_2 \mu_3}(Q_3) \mathcal{N}_{\mu_2 \mu_3}(Q_3 \frac{\mathfrak{t}}{\mathfrak{q}})}, \quad (3.62)$$

$$Z_{\mu_1 \mu_2 \mu_3 \mu_i} = \mathfrak{q}^{\frac{\|\mu_i\|^2}{2}} \mathfrak{t}^{\frac{\|\mu_i^t\|^2}{2}} \tilde{Z}_{\mu_i}(\mathfrak{t}, \mathfrak{q}) \tilde{Z}_{\mu_i^t}(\mathfrak{q}, \mathfrak{t}) \left(-\sqrt{\frac{\mathfrak{q}}{\mathfrak{t}}}\right)^{|\mu_i|} \mathcal{N}_{\mu_1 \mu_i}(1) \mathcal{N}_{\mu_i \mu_2}\left(Q_1 \frac{\mathfrak{t}}{\mathfrak{q}}\right) \mathcal{N}_{\mu_i \mu_3}\left(Q_{1,3} \frac{\mathfrak{t}}{\mathfrak{q}}\right) \quad (3.63)$$

for $i = 7, 8, 9$, and

$$Z_{\mu_1 \mu_2 \mu_3 \mu_{j+3} \mu_j}^{Q_j} = \mathfrak{q}^{\frac{\|\mu_j\|^2}{2}} \mathfrak{t}^{\frac{\|\mu_j^t\|^2}{2}} \tilde{Z}_{\mu_j}(\mathfrak{t}, \mathfrak{q}) \tilde{Z}_{\mu_j^t}(\mathfrak{q}, \mathfrak{t}) (-Q_j)^{|\mu_j|}$$

$$\times \frac{\mathcal{N}_{\mu_1\mu_j}\left(\frac{Q_{1^2,3}}{Q_j}\sqrt{\frac{\mathfrak{t}}{\mathfrak{q}}}\right)\mathcal{N}_{\mu_2\mu_j}\left(\frac{Q_{1,3}}{Q_j}\sqrt{\frac{\mathfrak{t}}{\mathfrak{q}}}\right)\mathcal{N}_{\mu_3\mu_j}\left(\frac{Q_1}{Q_j}\sqrt{\frac{\mathfrak{t}}{\mathfrak{q}}}\right)}{\mathcal{N}_{\mu_{j+3}\mu_j}\left(\frac{Q_{1^2,3}}{Q_j}\sqrt{\frac{\mathfrak{t}}{\mathfrak{q}}}\right)\mathcal{N}_{\mu_{j+3}\mu_j}\left(\frac{Q_{1^2,3}}{Q_j}\frac{\mathfrak{t}^{3/2}}{\mathfrak{q}^{3/2}}\right)} \quad (3.64)$$

for $j = 4, 5, 6$. We note that from the web diagram in Figure 16(b), the map from Kähler parameters to gauge theory parameters is given by

$$Q_1 = \frac{A_1^2}{A_2}, \quad Q_2 = \frac{A_2^2}{A_1^3}u, \quad Q_3 = \frac{A_2^2}{A_1}, \quad (3.65)$$

where A_1 and A_2 are the Coulomb branch parameters, u is the instanton factor.

Now we compute the perturbative part of the partition function which corresponds to $\mu_{1,2,3} = \emptyset$, and because $\mu_{7,8,9} \preceq \mu_1$, $\mu_{7,8,9}$ are also empty in this case.

$$Z_{\text{pert}}^{\mu D_4} = Z_{\text{M}}^{D_4} \sum_{\mu_4} Z_{\emptyset\emptyset\emptyset\mu_4}^{Q_4} \sum_{\mu_5} Z_{\emptyset\emptyset\emptyset\mu_5}^{Q_5} \sum_{\mu_6} Z_{\emptyset\emptyset\emptyset\mu_6}^{Q_6}. \quad (3.66)$$

We first sum over $Z_{\emptyset\emptyset\emptyset\mu_4}^{Q_4}$ from zero to some finite Young diagram boxes number of μ_4 , and then series expand it with respect to Q_1 and Q_4 . There are both negative power and positive power terms of Q_4 in the expansion, but when we increase the upper bound of the boxes number of μ_4 , lower positive power terms of Q_4 disappear, in the limit that the upper bound of boxes number of μ_4 goes to infinity, all the positive power terms of Q_4 will disappear and only negative power terms of Q_4 remain which are not changing once the upper bound exceeds some finite number, then we take the limit that Q_4 goes to ∞ , we obtain

$$\mathcal{Z}_0 \equiv \lim_{Q_4 \rightarrow \infty} \sum_{\mu_4} Z_{\emptyset\emptyset\emptyset\mu_4}^{Q_4} = \text{PE} \left[\frac{Q_1(1+Q_3)\mathfrak{t}}{(1-\mathfrak{q})(1-\mathfrak{t})} \right]. \quad (3.67)$$

Because Z^{Q_5}, Z^{Q_6} have the same form as Z^{Q_4} , they will have the same limit (3.67) when $Q_5, Q_6 \rightarrow \infty$. Substitute (3.67) into (3.66), take the decoupling limit, transform Kähler parameters into gauge theory parameters and drop the factors that do not depend on A_1 or A_2 , we obtain the perturbative part of $\text{SU}(3)_7$:

$$\begin{aligned} Z_{\text{pert}}^{\mu \text{SU}(3)_7} &= \frac{\mathcal{M}(Q_1)\mathcal{M}(Q_3)\mathcal{M}(Q_{1,3})\mathcal{M}(Q_3\frac{\mathfrak{t}}{\mathfrak{q}})}{\mathcal{M}(Q_1\frac{\mathfrak{t}}{\mathfrak{q}})^2\mathcal{M}(Q_{1,3}\frac{\mathfrak{t}}{\mathfrak{q}})^2} \mathcal{Z}_0^3 \\ &= \text{PE} \left[\frac{\mathfrak{q} + \mathfrak{t}}{(1-\mathfrak{q})(1-\mathfrak{t})} \left(\frac{A_1^2}{A_2} + A_1A_2 + \frac{A_2^2}{A_1} \right) \right]. \end{aligned} \quad (3.68)$$

The instanton part of (3.60) is

$$Z_{\text{inst}}^{\mu D_4} = \sum_{\mu_1, \mu_2, \mu_3} \left(Z_{\mu_1\mu_2\mu_3}^{\kappa=7} \prod_{j=4,5,6} \sum_{\mu_{j+3}} \left(Z_{\mu_1\mu_2\mu_3\mu_{j+3}} \frac{\sum_{\mu_j} Z_{\mu_1\mu_2\mu_3\mu_{j+3}\mu_j}^{Q_j}}{\sum_{\mu_j} Z_{\emptyset\emptyset\emptyset\mu_j}^{Q_j}} \right) \right). \quad (3.69)$$

We define

$$\mathcal{Z}_{\mu_1\mu_2\mu_3} \equiv \lim_{Q_4 \rightarrow \infty} \sum_{\mu_7} \left(Z_{\mu_1\mu_2\mu_3\mu_7} \frac{\sum_{\mu_4} Z_{\mu_1\mu_2\mu_3\mu_7\mu_4}^{Q_4}}{\sum_{\mu_4} Z_{\emptyset\emptyset\emptyset\mu_4}^{Q_4}} \right). \quad (3.70)$$

Because $\mu_7 \preccurlyeq \mu_1$, the summation over μ_7 is finite, while the summation over μ_4 is up to infinity. In order to compute $\mathcal{Z}_{\mu_1\mu_2\mu_3}$, we first sum over μ_4 up to a finite boxes number in the numerator and denominator of (3.70), then we expand the whole expression (3.70) with respect to Q_1 and Q_4 . There are both negative power and positive power terms of Q_4 appearing in the expansion, but when we increase the upper bound of the boxes number of μ_4 , lower order positive power terms of Q_4 disappear, in the limit that the upper bound of boxes number of μ_4 goes to infinity, all the positive power terms of Q_4 will disappear and only negative power terms of Q_4 remain which are not changing once the upper bound exceeds some finite number. Higher order terms of Q_1 also disappear because their coefficients contain only positive power terms of Q_4 . Then we take the limit that Q_4 goes to ∞ , we will obtain $\mathcal{Z}_{\mu_1\mu_2\mu_3}$ expanded with respect to Q_1 up to finite order. Because Z^{Q_5}, Z^{Q_6} have the same form as Z^{Q_4} , they will have the same limit (3.70) when $Q_5, Q_6 \rightarrow \infty$. Because $Z_{\mu_1\mu_2\mu_3}^{\kappa=7}$ is proportional to $Q_2^{|\mu_1|+|\mu_2|+|\mu_3|}$, Young diagram assignments that satisfy $|\mu_1| + |\mu_2| + |\mu_3| = 1$ contribute to one-instanton partition function, and the corresponding \mathcal{Z} 's are

$$\begin{aligned} \mathcal{Z}_{\{1\},\emptyset,\emptyset} &= 1 - \frac{\mathfrak{q}}{\mathfrak{t}} Q_1 (1 + Q_3), \\ \mathcal{Z}_{\emptyset,\{1\},\emptyset} &= 1 + Q_1 \left(Q_3 - \frac{\mathfrak{t}}{\mathfrak{q}} \right), \\ \mathcal{Z}_{\emptyset,\emptyset,\{1\}} &= 1 + Q_1 \left(1 - \frac{\mathfrak{t}}{\mathfrak{q}} Q_3 \right). \end{aligned} \quad (3.71)$$

Young diagram assignments that satisfy $|\mu_1| + |\mu_2| + |\mu_3| = 2$ contribute to two-instanton partition function, then the corresponding \mathcal{Z} 's are given as follows:

$$\begin{aligned} \mathcal{Z}_{\{2\},\emptyset,\emptyset} &= 1 - \frac{\mathfrak{q}(1+\mathfrak{q})}{\mathfrak{t}} Q_1 (1 + Q_3) + \frac{\mathfrak{q}^3}{\mathfrak{t}^2} Q_1^2 (1 + Q_3 + \mathfrak{q}Q_3 + Q_3^2), \\ \mathcal{Z}_{\{1,1\},\emptyset,\emptyset} &= 1 - \frac{\mathfrak{q}(1+\mathfrak{t})}{\mathfrak{t}^2} Q_1 (1 + Q_3) + \frac{\mathfrak{q}^2}{\mathfrak{t}^4} Q_1^2 (\mathfrak{t} + Q_3 + \mathfrak{t}Q_3 + \mathfrak{t}Q_3^2), \\ \mathcal{Z}_{\{1\},\{1\},\emptyset} &= 1 + Q_1 \left(1 - \frac{1}{\mathfrak{t}} - \frac{\mathfrak{t}}{\mathfrak{q}} + Q_3 - \frac{\mathfrak{q}}{\mathfrak{t}} (\mathfrak{t} + Q_3) \right) + \frac{1}{\mathfrak{t}} Q_1^2 (1 + Q_3) (\mathfrak{t} - \mathfrak{q}Q_3), \\ \mathcal{Z}_{\{1\},\emptyset,\{1\}} &= 1 + Q_1 \left(1 - \frac{\mathfrak{q}}{\mathfrak{t}} + Q_3 \left(1 - \mathfrak{q} - \frac{1}{\mathfrak{t}} - \frac{\mathfrak{t}}{\mathfrak{q}} \right) \right) - \frac{1}{\mathfrak{t}} Q_1^2 (1 + Q_3) (\mathfrak{q} - \mathfrak{t}Q_3), \\ \mathcal{Z}_{\emptyset,\{1\},\{1\}} &= 1 + \frac{\mathfrak{q} - \mathfrak{t}}{\mathfrak{q}} Q_1 (1 + Q_3) + Q_1^2 \left(\mathfrak{t}Q_3 + \frac{\mathfrak{t}^2}{\mathfrak{q}^2} Q_3 - \frac{\mathfrak{t} + (\mathfrak{t} - 1)Q_3 + \mathfrak{t}Q_3^2}{\mathfrak{q}} \right), \\ \mathcal{Z}_{\emptyset,\{2\},\emptyset} &= 1 + \frac{1+\mathfrak{q}}{\mathfrak{q}^2} Q_1 (\mathfrak{q}^2 Q_3 - \mathfrak{t}) + Q_1^2 \left(Q_3^2 - \frac{(1+\mathfrak{q})\mathfrak{t}}{\mathfrak{q}^2} Q_3 + \frac{\mathfrak{t}^2}{\mathfrak{q}^3} \right), \end{aligned}$$

$$\begin{aligned}
Z_{\emptyset, \{1,1\}, \emptyset} &= 1 + \frac{1+t}{qt} Q_1(qQ_3 - t^2) + Q_1^2 \left(\frac{t^3}{q^2} + Q_3^2 - \frac{(t+t^2)Q_3}{q} \right), \\
Z_{\emptyset, \emptyset, \{2\}} &= 1 + \frac{1+q}{q^2} Q_1(q^2 - tQ_3) + Q_1^2 \left(1 - \frac{t}{q^2} Q_3 - \frac{t}{q} Q_3 + \frac{t^2}{q^3} Q_3^2 \right), \\
Z_{\emptyset, \emptyset, \{1,1\}} &= 1 + \frac{1+t}{qt} Q_1(q - t^2 Q_3) + Q_1^2 \left(1 + \frac{t^3}{q^2} Q_3^2 - \frac{t(1+t)Q_3}{q} \right). \tag{3.72}
\end{aligned}$$

So the instanton partition function of $SU(3)_7$ is

$$Z_{\text{inst}}^{\text{SU}(3)_7} = \sum_{\mu_1, \mu_2, \mu_3} Z_{\mu_1 \mu_2 \mu_3}^{\kappa=7} Z_{\mu_1 \mu_2 \mu_3}^3, \tag{3.73}$$

where $Z_{\mu_1 \mu_2 \mu_3}^{\kappa=7}$ is defined in (3.62). Summing over the Young diagrams, one can express the instanton partition function as an expansion of Q_2 . Here we write it as a PE:

$$Z_{\text{inst}}^{\text{SU}(3)_7} = 1 + \sum_{n=1} Z_n Q_2^n = \text{PE} \left[\sum_{n=1} f_n^{\kappa=7}(Q_1, Q_3; t, q) Q_2^n \right], \tag{3.74}$$

where Z_n is the n -instanton partition function up to an overall factor $(A_2^2/A_1^3)^n$ due to (3.65). By substituting (3.62) and (3.71) into (3.73), we can obtain the one-instanton partition function, then by (3.74), we have the exact form of the one-instanton part:

$$\begin{aligned}
f_1^{\kappa=7} &= \frac{t}{(1-q)(1-t)q} \left(\frac{Q_1^2(qQ_1(1+Q_3) - t)^3}{(1-Q_1)(1-Q_1Q_3)(qQ_1 - t)(qQ_1Q_3 - t)} \right. \\
&\quad + \frac{(q + qQ_1Q_3 - Q_1t)^3}{(1-Q_1)(1-Q_3)(qQ_3 - t)(Q_1t - q)} \\
&\quad \left. + \frac{(q + qQ_1 - Q_1Q_3t)^3}{(1-Q_3)(1-Q_1Q_3)(q - Q_3t)(q - Q_1Q_3t)} \right). \tag{3.75}
\end{aligned}$$

To compare this with the known result from the blowup [39], we expand (3.75) with respect to Q_1 and Q_3 , which gives

$$\begin{aligned}
f_1^{\kappa=7} &= \frac{q+t}{(q-1)(t-1)} \left[1 + Q_1 + \left(\frac{q}{t} + \frac{t}{q} \right) Q_3 + Q_1^2 + \left(\frac{q}{t} + \frac{t}{q} + 1 \right) Q_1 Q_3 + \left(\frac{q^2}{t^2} + \frac{t^2}{q^2} + 1 \right) Q_3^2 \right. \\
&\quad + Q_1^3 + \left(\frac{q}{t} + \frac{t}{q} + 1 \right) Q_1^2 Q_3 + \left(\frac{q^2}{t^2} + \frac{t^2}{q^2} + \frac{q}{t} + \frac{t}{q} + 1 \right) Q_1 Q_3^2 + \left(\frac{q^2}{t^2} + \frac{t^2}{q^2} + \frac{q}{t} + \frac{t}{q} + 2 \right) Q_1^2 Q_3^2 \\
&\quad + \left(\frac{q^3}{t^3} + \frac{t^3}{q^3} + \frac{q}{t} + \frac{t}{q} \right) Q_3^3 + \left(\frac{q}{t} + \frac{t}{q} + 1 \right) Q_1^3 Q_3 + \left(\frac{q^3}{t^3} + \frac{q^2}{t^2} + \frac{t^3}{q^3} + \frac{t^2}{q^2} + \frac{q}{t} + \frac{t}{q} + 1 \right) Q_1 Q_3^3 \\
&\quad + \left(\frac{q^2}{t^2} + \frac{t^2}{q^2} + \frac{q}{t} + \frac{t}{q} + 2 \right) Q_1^3 Q_3^2 + \left(\frac{q^3}{t^3} + \frac{q^2}{t^2} + \frac{t^3}{q^3} + \frac{t^2}{q^2} + \frac{2q}{t} + \frac{2t}{q} + 1 \right) Q_1^2 Q_3^3 \\
&\quad \left. + \left(\frac{q^3}{t^3} + \frac{q^2}{t^2} + \frac{t^3}{q^3} + \frac{t^2}{q^2} + \frac{2q}{t} + \frac{2t}{q} + 2 \right) Q_1^3 Q_3^3 \right] + \mathcal{O}(Q_1^4, Q_3^4), \tag{3.76}
\end{aligned}$$

where $\mathcal{O}(Q_1^4, Q_3^4)$ denotes terms either of order Q_1^4 or higher or of Q_3^4 or higher. We express this in terms of the spin state $[j_l, j_r]$ defined in (3.34),

$$\begin{aligned}
f_1^{\kappa=7} = & [0, \frac{1}{2}] + [0, \frac{3}{2}]Q_3 + [0, \frac{5}{2}]Q_3^2 + [0, \frac{1}{2}]Q_1 + \left([0, \frac{1}{2}] + [0, \frac{3}{2}]\right)Q_1Q_3 \\
& + \left([0, \frac{3}{2}] + [0, \frac{5}{2}]\right)Q_1Q_3^2 + [0, \frac{1}{2}]Q_1^2 + \left([0, \frac{1}{2}] + [0, \frac{3}{2}]\right)Q_1^2Q_3 \\
& + \left([0, \frac{1}{2}] + [0, \frac{3}{2}] + [0, \frac{5}{2}]\right)Q_1^2Q_3^2 \\
& + [0, \frac{7}{2}]Q_3^3 + \left([0, \frac{5}{2}] + [0, \frac{7}{2}]\right)Q_1Q_3^3 + \left([0, \frac{3}{2}] + [0, \frac{5}{2}] + [0, \frac{7}{2}]\right)Q_1^2Q_3^3 \\
& + [0, \frac{1}{2}]Q_1^3 + \left([0, \frac{1}{2}] + [0, \frac{3}{2}]\right)Q_1^3Q_3 + \left([0, \frac{1}{2}] + [0, \frac{3}{2}] + [0, \frac{5}{2}]\right)Q_1^3Q_3^2 \\
& + \left([0, \frac{1}{2}] + [0, \frac{3}{2}] + [0, \frac{5}{2}] + [0, \frac{7}{2}]\right)Q_1^3Q_3^3 + \mathcal{O}(Q_1^4, Q_3^4). \tag{3.77}
\end{aligned}$$

This agrees with the blowup result in [39].

By substituting (3.72) into (3.73), we can obtain the two-instanton partition function. As a PE form (3.74), we can obtain the exact form $f_2^{\kappa=7}$.⁹ Here, we expand $f_2^{\kappa=7}$ to order $Q_1^2Q_3^2$:

$$\begin{aligned}
f_2^{\kappa=7} = & \frac{1}{(1-q)(1-t)} \left[\left(\frac{q^3}{t^2} + \frac{t^3}{q^2} + \frac{q^2}{t} + \frac{t^2}{q} + q + t \right) Q_3 + \left(\frac{q^3}{t^2} + \frac{t^3}{q^2} + \frac{2q^2}{t} + \frac{2t^2}{q} + 2q \right. \right. \\
& + 2t \left. \right) Q_1Q_3 + \left(\frac{q^5}{t^3} + \frac{q^4}{t^2} + \frac{q^4}{t^3} + \frac{q^4}{t^4} + \frac{2q^3}{t^2} + \frac{q^3}{t^3} + \frac{q^2}{t^2} + \frac{t^5}{q^3} + \frac{t^4}{q^2} + \frac{t^4}{q^3} + \frac{t^4}{q^4} + \frac{2t^3}{q^2} \right. \\
& + \frac{t^3}{q^3} + \frac{t^2}{q^2} + \frac{q^3}{t} + \frac{2q^2}{t} + q^2 + \frac{t^3}{q} + \frac{2t^2}{q} + qt + \frac{q}{t} + \frac{t}{q} + 2q + t^2 + 2t + 1 \left. \right) Q_3^2 \\
& + \left(\frac{q^3}{t^2} + \frac{t^3}{q^2} + \frac{2q^2}{t} + \frac{2t^2}{q} + 3q + 3t \right) Q_1^2Q_3 + \left(\frac{q^5}{t^3} + \frac{2q^4}{t^2} + \frac{2q^4}{t^3} + \frac{q^4}{t^4} + \frac{5q^3}{t^2} + \frac{2q^3}{t^3} \right. \\
& + \frac{2q^2}{t^2} + \frac{t^5}{q^3} + \frac{2t^4}{q^2} + \frac{2t^4}{q^3} + \frac{t^4}{q^4} + \frac{5t^3}{q^2} + \frac{2t^3}{q^3} + \frac{2t^2}{q^2} + \frac{2q^3}{t} + \frac{6q^2}{t} + 2q^2 + \frac{2t^3}{q} + \frac{6t^2}{q} \\
& + 2qt + \frac{2q}{t} + \frac{2t}{q} + 6q + 2t^2 + 6t + 2 \left. \right) Q_1Q_3^2 + \left(\frac{q^5}{t^3} + \frac{2q^4}{t^2} + \frac{2q^4}{t^3} + \frac{q^4}{t^4} + \frac{6q^3}{t^2} + \frac{2q^3}{t^3} \right. \\
& + \frac{3q^2}{t^2} + \frac{t^5}{q^3} + \frac{2t^4}{q^2} + \frac{2t^4}{q^3} + \frac{t^4}{q^4} + \frac{6t^3}{q^2} + \frac{2t^3}{q^3} + \frac{3t^2}{q^2} + \frac{3q^3}{t} + \frac{9q^2}{t} + 3q^2 + \frac{3t^3}{q} + \frac{9t^2}{q} \\
& \left. + 3qt + \frac{3q}{t} + \frac{3t}{q} + 10q + 3t^2 + 10t + 3 \right) Q_1^2Q_3^2 \Big] + \mathcal{O}(Q_1^3, Q_3^3). \tag{3.78}
\end{aligned}$$

In terms of the spin state, it is given by

$$\begin{aligned}
f_2^{\kappa=7} = & [0, \frac{5}{2}]Q_3 + \left([0, \frac{5}{2}] + [0, \frac{7}{2}] + [\frac{1}{2}, 4]\right)Q_3^2 + \left([0, \frac{3}{2}] + [0, \frac{5}{2}]\right)Q_1Q_3 \tag{3.79} \\
& + \left([0, \frac{3}{2}] + 3[0, \frac{5}{2}] + 2[0, \frac{7}{2}] + [\frac{1}{2}, 3] + [\frac{1}{2}, 4]\right)Q_1Q_3^2 + \left([0, \frac{1}{2}] + [0, \frac{3}{2}] + [0, \frac{5}{2}]\right)Q_1^2Q_3 \\
& + \left([0, \frac{1}{2}] + 3[0, \frac{3}{2}] + 4[0, \frac{5}{2}] + 2[0, \frac{7}{2}] + [\frac{1}{2}, 2] + [\frac{1}{2}, 3] + [\frac{1}{2}, 4]\right)Q_1^2Q_3^2 + \mathcal{O}(Q_1^3, Q_3^3),
\end{aligned}$$

which agrees with the two-instanton part from the blowup result [39].

⁹As the exact form $f_2^{\kappa=7}$ is rather long, we put the exact form into a Mathematica file attached as an ancillary file.

3.4 5d SU(3) theory at CS level 9

We consider 5d SU(3) theory at CS level 9 without flavor, denoted as $SU(3)_9$, which is a KK theory arising from 6d SU(3) theory on a circle with a \mathbb{Z}_2 twist [67–69]. Its refined partition function is computed in [39] via bootstrapping the BPS spectrum based on the blowup equation [31, 70, 71]. From the perspective of topological vertex, the partition function for 6d SU(3) theory with a \mathbb{Z}_2 -twist is obtained in [52] based on 5-brane web with two $\widetilde{O5}$ -planes, and that for the 5d $SU(3)_9$ is also obtained in the S-dual frame [50]. However these partition functions based on topological vertex are limited to the unrefined case where $\epsilon_1 + \epsilon_2 = 0$.¹⁰ We here, however, compute the refined Nekrasov partition function for 5d $SU(3)_9$ theory, using our proposal for the refined topological vertex with ON-planes. The corresponding 5-brane web requires two ON-planes and can be obtained from the Higgsing of the following affine D_4 -type quiver [14],

$$\begin{array}{c}
 \text{SU}(2) \quad \quad \quad \text{SU}(2) \\
 \quad \quad \quad \diagdown \quad \diagup \\
 \quad \quad \quad \text{SU}(3)_1 \\
 \quad \quad \quad \diagup \quad \diagdown \\
 \text{SU}(2) \quad \quad \quad \text{SU}(2)
 \end{array} \tag{3.80}$$

Here, the middle node is the SU(3) theory at the CS level 1 and the corresponding

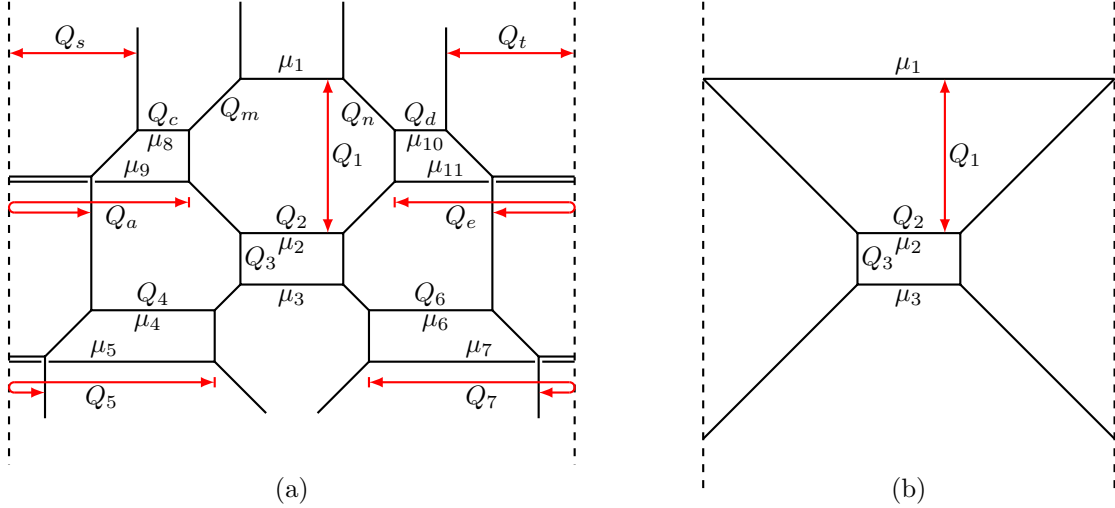


Figure 18. (a) A 5-brane web for the affine D_4 -type quiver with two ON-planes on the left and right. (b) $SU(3)$ with CS 9 obtained by Higgsing and decoupling.

web diagram is depicted in Figure 18(a). The Higgsing procedure is similar to the

¹⁰In [52], the refined elliptic genus for 6d SU(3) theory with a \mathbb{Z}_2 twist is also computed via the ADHM method.

SU(3)₇ case discussed in the previous section: A Higgsing of an SU(2) gives rise to an antisymmetric hypermultiplet (**AS**) to SU(3), increasing the CS level of SU(3) by $\frac{3}{2}$ [14]. As we have four SU(2), we get SU(3)₇+4**AS** after the Higgsing. Finally, since an antisymmetric hypermultiplet transforms as $\bar{\mathbf{3}}$, the decoupling of an antisymmetric hypermultiplet further increases the CS level of SU(3) by $\frac{1}{2}$. Hence, decoupling all the **AS** yields SU(3)₉ whose web diagram is shown in Figure 18(b).

As in the previous section where we have computed the partition function of SU(3)₇ theory, we start from the web diagram in Figure 18(a). The two SU(2) sub webs on the right and the two SU(2) sub webs on the left are both overlapping, in order to compute by our proposal for topological vertex with ON-planes, we need to swap the positions of relevant branes to make the SU(2) sub webs separated. From the Higgsing and decoupling processes of obtaining the SU(3)₇ theory, we know that in the Higgsing limit of Figure 18(a), $Q_m, Q_c, Q_a, Q_n, Q_d, Q_e \rightarrow \sqrt{\frac{q}{t}}$ and $Q_s, Q_t \rightarrow 1$, in the decoupling limit, $Q_4, Q_5, Q_6, Q_7 \rightarrow \infty$. As the procedures are exactly like the procedures done in the previous section on SU(3)₇, we omit the detailed computation process and just list the results. From the web diagram in Figure 18(b), the Kähler parameters are expressed in terms of the gauge theory parameters as

$$Q_1 = \frac{A_1^2}{A_2}, \quad Q_2 = \frac{A_2^2}{A_1^4}u, \quad Q_3 = \frac{A_2^2}{A_1}, \quad (3.81)$$

where A_1 and A_2 are the Coulomb branch parameters and u is the instanton factor. Notice that $Q_1^2 Q_2 = u$ and hence any terms with $(Q_1^2 Q_2)^n$ do not explicitly depend on the Coulomb branch parameters and they are the extra factor, which will be modded out when expressing the partition function.

The perturbative part of the partition function is

$$\begin{aligned} Z_{\text{pert}}^{\text{SU}(3)_9} &= \frac{\mathcal{M}(Q_1)\mathcal{M}(Q_3)\mathcal{M}(Q_{1,3})\mathcal{M}(Q_{3\frac{t}{q}})}{\mathcal{M}(Q_{1\frac{t}{q}})^3\mathcal{M}(Q_{1,3\frac{t}{q}})^3} \mathcal{Z}_0^4 \\ &= \text{PE} \left[\frac{\mathbf{q} + \mathbf{t}}{(1 - \mathbf{q})(1 - \mathbf{t})} \left(\frac{A_1^2}{A_2} + A_1 A_2 + \frac{A_2^2}{A_1} \right) \right]. \end{aligned} \quad (3.82)$$

The instanton part of the partition function with extra factors included is

$$Z_{\text{inst+extra}}^{\text{SU}(3)_9} = \sum_{\mu_1, \mu_2, \mu_3} Z_{\mu_1 \mu_2 \mu_3}^{\kappa=9} \mathcal{Z}_{\mu_1 \mu_2 \mu_3}^4, \quad (3.83)$$

where

$$Z_{\mu_1 \mu_2 \mu_3}^{\kappa=9} \equiv \frac{\mathbf{q}^{|\mu_2|^2} \mathbf{t}^{|\mu_1^t|^2 + |\mu_3^t|^2} \prod_{i=1,2,3} \tilde{Z}_{\mu_i}(\mathbf{t}, \mathbf{q}) \tilde{Z}_{\mu_i^t}(\mathbf{q}, \mathbf{t}) \left(Q_{12,2} \frac{t^2}{q^2} \right)^{|\mu_1|} Q_2^{|\mu_2| + |\mu_3|}}{\mathcal{N}_{\mu_1 \mu_2}(Q_1) \mathcal{N}_{\mu_1 \mu_2}(Q_{1\frac{t}{q}}) \mathcal{N}_{\mu_1 \mu_3}(Q_{1,3}) \mathcal{N}_{\mu_1 \mu_3}(Q_{1,3\frac{t}{q}}) \mathcal{N}_{\mu_2 \mu_3}(Q_3) \mathcal{N}_{\mu_2 \mu_3}(Q_{3\frac{t}{q}})}, \quad (3.84)$$

and $\mathcal{Z}_{\mu_1\mu_2\mu_3}$ is the same one that appears in (3.73). We now expand this instanton part with respect to Q_2 which is the Kähler parameter proportional to the instanton factor u . As discussed in the previous section, $Z_{\mu_1\mu_2\mu_3}^{\kappa=9}$ is proportional to $Q_2^{|\mu_1|+|\mu_2|+|\mu_3|}$ (or $u^{|\mu_1|+|\mu_2|+|\mu_3|}$) and leads to the instanton expansion. We then organize the sum of the n -instanton part Z_n as a PE:

$$Z_{\text{inst+extra}}^{\text{SU}(3)_9} = 1 + \sum_{n=1} Z_n Q_2^n = \text{PE} \left[\sum_{n=1} f_n^{\kappa=9}(Q_1, Q_3; \mathfrak{t}, \mathfrak{q}) Q_2^n \right]. \quad (3.85)$$

By summing over the Young diagram assignments in (3.83) with the corresponding \mathcal{Z} 's defined in (3.70), order by order in Q_2 , one can obtain f_n . We list a few f_n below. In particular, the exact one-instanton part f_1 is given as follows:

$$f_1^{\kappa=9} = \frac{\mathfrak{t}}{(1-\mathfrak{q})(1-\mathfrak{t})\mathfrak{q}^2} \left(\frac{Q_1^2(-\mathfrak{q}Q_1(1+Q_3)+\mathfrak{t})^4}{(1-Q_1)(1-Q_1Q_3)(\mathfrak{q}Q_1-\mathfrak{t})(\mathfrak{q}Q_1Q_3-\mathfrak{t})} \right. \\ \left. + \frac{(\mathfrak{q}+\mathfrak{q}Q_1Q_3-Q_1\mathfrak{t})^4}{(1-Q_1)(1-Q_3)(\mathfrak{q}Q_3-\mathfrak{t})(\mathfrak{t}Q_1-\mathfrak{q})} \right. \\ \left. + \frac{(\mathfrak{q}+\mathfrak{q}Q_1-\mathfrak{t}Q_1Q_3)^4}{(1-Q_3)(1-Q_1Q_3)(\mathfrak{t}Q_3-\mathfrak{q})(\mathfrak{t}Q_1Q_3-\mathfrak{q})} \right). \quad (3.86)$$

To compare this with the result from the blowup [39], we expand f_1 with respect to Q_1, Q_3 , which gives

$$f_1^{\kappa=9} = \frac{\mathfrak{q}+\mathfrak{t}}{(1-\mathfrak{q})(1-\mathfrak{t})} \left[1 + Q_1 + \left(\frac{\mathfrak{q}}{\mathfrak{t}} + \frac{\mathfrak{t}}{\mathfrak{q}} \right) Q_3 + \left(1 + \frac{\mathfrak{q}^2}{\mathfrak{t}^2} + \frac{\mathfrak{t}^2}{\mathfrak{q}^2} \right) Q_3^2 \right. \\ \left. + \left(1 + \frac{\mathfrak{q}}{\mathfrak{t}} + \frac{\mathfrak{t}}{\mathfrak{q}} \right) Q_1Q_3 + \left(1 + \frac{\mathfrak{q}^2}{\mathfrak{t}^2} + \frac{\mathfrak{q}}{\mathfrak{t}} + \frac{\mathfrak{t}}{\mathfrak{q}} + \frac{\mathfrak{t}^2}{\mathfrak{q}^2} \right) Q_1Q_3^2 + \left(1 + 2\frac{\mathfrak{t}}{\mathfrak{q}} + \frac{\mathfrak{t}^2}{\mathfrak{q}^2} \right) Q_1^2 \right. \\ \left. + \left(1 + \frac{\mathfrak{q}}{\mathfrak{t}} + \frac{\mathfrak{t}}{\mathfrak{q}} \right) Q_1^2Q_3 + \left(2 + \frac{\mathfrak{q}^2}{\mathfrak{t}^2} + \frac{\mathfrak{q}}{\mathfrak{t}} + \frac{\mathfrak{t}}{\mathfrak{q}} + \frac{\mathfrak{t}^2}{\mathfrak{q}^2} \right) Q_1^2Q_3^2 \right. \\ \left. + Q_1^3 + \left(\frac{\mathfrak{q}}{\mathfrak{t}} + \frac{\mathfrak{t}}{\mathfrak{q}} + \frac{\mathfrak{q}^3}{\mathfrak{t}^3} + \frac{\mathfrak{t}^3}{\mathfrak{q}^3} \right) Q_3^3 + \left(1 + \frac{\mathfrak{q}}{\mathfrak{t}} + \frac{\mathfrak{t}}{\mathfrak{q}} \right) Q_1^3Q_3 \right. \\ \left. + \left(1 + \frac{\mathfrak{q}^3}{\mathfrak{t}^3} + \frac{\mathfrak{q}^2}{\mathfrak{t}^2} + \frac{\mathfrak{q}}{\mathfrak{t}} + \frac{\mathfrak{t}}{\mathfrak{q}} + \frac{\mathfrak{t}^2}{\mathfrak{q}^2} + \frac{\mathfrak{t}^3}{\mathfrak{q}^3} \right) Q_3^3Q_1 + \left(2 + \frac{\mathfrak{q}^2}{\mathfrak{t}^2} + \frac{\mathfrak{q}}{\mathfrak{t}} + \frac{\mathfrak{t}}{\mathfrak{q}} + \frac{\mathfrak{t}^2}{\mathfrak{q}^2} \right) Q_1^3Q_3^2 \right. \\ \left. + \left(1 + \frac{\mathfrak{q}^3}{\mathfrak{t}^3} + \frac{\mathfrak{q}^2}{\mathfrak{t}^2} + \frac{2\mathfrak{q}}{\mathfrak{t}} + \frac{2\mathfrak{t}}{\mathfrak{q}} + \frac{\mathfrak{t}^2}{\mathfrak{q}^2} + \frac{\mathfrak{t}^3}{\mathfrak{q}^3} \right) Q_3^3Q_1^2 \right. \\ \left. + \left(2 + \frac{\mathfrak{q}^3}{\mathfrak{t}^3} + \frac{\mathfrak{q}^2}{\mathfrak{t}^2} + \frac{2\mathfrak{q}}{\mathfrak{t}} + \frac{2\mathfrak{t}}{\mathfrak{q}} + \frac{\mathfrak{t}^2}{\mathfrak{q}^2} + \frac{\mathfrak{t}^3}{\mathfrak{q}^3} \right) Q_1^3Q_3^3 \right] + \mathcal{O}(Q_1^4, Q_3^4). \quad (3.87)$$

As $Q_1^2Q_2 = u$ does not depend on the Coulomb branch parameters, the term proportional to Q_1^2 in (3.87) contributes to the extra factor. Separating out such extra factor, we rewrite (3.87) in terms of the spin state $[j_l, j_r]$ defined in (3.34),

$$f_1^{\kappa=9} = [0, \frac{1}{2}] + [0, \frac{3}{2}]Q_3 + [0, \frac{5}{2}]Q_3^2 + [0, \frac{1}{2}]Q_1 + \left([0, \frac{1}{2}] + [0, \frac{3}{2}] \right) Q_1Q_3$$

$$\begin{aligned}
& + \left([0, \frac{3}{2}] + [0, \frac{5}{2}] \right) Q_1 Q_3^2 + \left([0, \frac{1}{2}] + [0, \frac{3}{2}] \right) Q_1^2 Q_3 + \left([0, \frac{1}{2}] + [0, \frac{3}{2}] + [0, \frac{5}{2}] \right) Q_1^2 Q_3^2 \\
& + [0, \frac{7}{2}] Q_3^3 + \left([0, \frac{5}{2}] + [0, \frac{7}{2}] \right) Q_1 Q_3^3 + \left([0, \frac{3}{2}] + [0, \frac{5}{2}] + [0, \frac{7}{2}] \right) Q_1^2 Q_3^3 \\
& + [0, \frac{1}{2}] Q_1^3 + \left([0, \frac{1}{2}] + [0, \frac{3}{2}] \right) Q_1^3 Q_3 + \left([0, \frac{1}{2}] + [0, \frac{3}{2}] + [0, \frac{5}{2}] \right) Q_1^3 Q_3^2 \\
& + \left([0, \frac{1}{2}] + [0, \frac{3}{2}] + [0, \frac{5}{2}] + [0, \frac{7}{2}] \right) Q_1^3 Q_3^3 + \mathcal{O}(Q_1^4, Q_3^4) + (\text{extra factor}) . \quad (3.88)
\end{aligned}$$

This agrees with the blowup result in [39] where the terms up to $Q_1^2 Q_3^2$ are presented at the first order of Q_2 .

The contribution at order Q_2^2 leads to two-instanton partition function. Summing over Young diagrams in (3.83) with the corresponding \mathcal{Z} 's in (3.72) and combining (3.85) and (3.86), we can obtain the exact form of f_2 . As the exact form of f_2 is rather long¹¹, we expand the form with respect to Q_1, Q_3 up to $Q_1^2 Q_3^2$ to compare it with the known result, as follows:

$$\begin{aligned}
f_2^{\kappa=9} = & \frac{1}{(1-q)(1-t)} \left[\left(q + \frac{q^3}{t^2} + \frac{q^2}{t} + t + \frac{t^2}{q} + \frac{t^3}{q^2} \right) Q_3 + \left(1 + 2q + q^2 + \frac{q^4}{t^4} + \frac{q^3}{t^3} \right. \right. \\
& + \frac{q^4}{t^3} + \frac{q^5}{t^3} + \frac{q^2}{t^2} + 2\frac{q^3}{t^2} + \frac{q^4}{t^2} + \frac{q}{t} + 2\frac{q^2}{t} + \frac{q^3}{t} + 2t + \frac{t}{q} + qt + t^2 + \frac{t^2}{q^2} + 2\frac{t^2}{q} + \frac{t^3}{q^3} \\
& + 2\frac{t^3}{q^2} + \frac{t^3}{q} + \frac{t^4}{q^4} + \frac{t^4}{q^3} + \frac{t^4}{q^2} + \frac{t^5}{q^3} \left. \right) Q_3^2 + \left(2q + \frac{q^3}{t^2} + 2\frac{q^2}{t} + 2t + 2\frac{t^2}{q} + \frac{t^3}{q^2} \right) Q_1 Q_3 \\
& + \left(2 + 6q + 2q^2 + \frac{q^4}{t^4} + 2\frac{q^3}{t^3} + 2\frac{q^4}{t^3} + \frac{q^5}{t^3} + 2\frac{q^2}{t^2} + 5\frac{q^3}{t^2} + 2\frac{q^4}{t^2} + 2\frac{q}{t} + 6\frac{q^2}{t} + 2\frac{q^3}{t} \right. \\
& + 6t + 2\frac{t}{q} + 2qt + 2t^2 + 2\frac{t^2}{q^2} + 6\frac{t^2}{q} + 2\frac{t^3}{q^3} + 5\frac{t^3}{q^2} + 2\frac{t^3}{q} + \frac{t^4}{q^4} + 2\frac{t^4}{q^3} + 2\frac{t^4}{q^2} + \frac{t^5}{q^3} \left. \right) Q_1 Q_3^2 \\
& + \left(3q + \frac{q^3}{t^2} + 2\frac{q^2}{t} + 3t + 2\frac{t^2}{q} + \frac{t^3}{q^2} \right) Q_1^2 Q_3 + \left(3 + 10q + 3q^2 + \frac{q^4}{t^4} + 2\frac{q^3}{t^3} + 2\frac{q^4}{t^3} \right. \\
& + \frac{q^5}{t^3} + 3\frac{q^2}{t^2} + 6\frac{q^3}{t^2} + 2\frac{q^4}{t^2} + 3\frac{q}{t} + 9\frac{q^2}{t} + 3\frac{q^3}{t} + 10t + 3\frac{t}{q} + 3qt + 3t^2 + 3\frac{t^2}{q^2} + 9\frac{t^2}{q} \\
& \left. + 2\frac{t^3}{q^3} + 6\frac{t^3}{q^2} + 3\frac{t^3}{q} + \frac{t^4}{q^4} + 2\frac{t^4}{q^3} + 2\frac{t^4}{q^2} + \frac{t^5}{q^3} \right) Q_1^2 Q_3^2 \Big] + \mathcal{O}(Q_1^3, Q_3^3) , \quad (3.89)
\end{aligned}$$

which can be rewritten as

$$\begin{aligned}
f_2^{\kappa=9} = & [0, \frac{5}{2}] Q_3 + \left([0, \frac{5}{2}] + [0, \frac{7}{2}] + [\frac{1}{2}, 4] \right) Q_3^2 + \left([0, \frac{3}{2}] + [0, \frac{5}{2}] \right) Q_1 Q_3 \quad (3.90) \\
& + \left([0, \frac{3}{2}] + 3[0, \frac{5}{2}] + 2[0, \frac{7}{2}] + [\frac{1}{2}, 3] + [\frac{1}{2}, 4] \right) Q_1 Q_3^2 + \left([0, \frac{1}{2}] + [0, \frac{3}{2}] + [0, \frac{5}{2}] \right) Q_1^2 Q_3 \\
& + \left([0, \frac{1}{2}] + 3[0, \frac{3}{2}] + 4[0, \frac{5}{2}] + 2[0, \frac{7}{2}] + [\frac{1}{2}, 2] + [\frac{1}{2}, 3] + [\frac{1}{2}, 4] \right) Q_1^2 Q_3^2 + \mathcal{O}(Q_1^3, Q_3^3) ,
\end{aligned}$$

which agrees with the two-instanton part from the blowup result [39]. Notice that there is no extra factor in (3.90), which is because the extra factor at order Q_2^2 comes from terms proportional to Q_1^4 .

¹¹The exact form of f_2 for the $SU(3)_9$ theory is presented in a Mathematica file attached as an ancillary file.

The instanton partition function at higher order $n \geq 3$ can be obtained in the same way. It is to repeat the same computation with $|\mu_1| + |\mu_2| + |\mu_3| = n$. One can also express the partition function in terms of the gauge theory parameters by substituting the Kähler parameters with the Coulomb branch parameters and instanton factor in (3.81), after dropping the extra factors.

4 Conclusion

In this paper, we generalized refined topological vertex formalism so that it is applicable for 5-brane webs with ON-planes. 5-brane system with an ON-plane describes a D-type quiver gauge theory. In order for a 5-brane web with an ON-plane to correctly account for a D-type quiver, there should be no bifundamental contributions between two gauge theories belonging to bivalent nodes of a D-type quiver. To this end, we proposed a new vertex factor C^R for the reflected vertices over an ON-plane and also new associated edge factors. Such new vertex and edge factors ensures the resulting partition functions correctly capture the BPS spectrum of a D-type quiver gauge theory. It is also worthy of noting that one can use only this new vertex factor and edge factor for usual 5-brane webs to obtain the same partition function obtained with the conventional vertex and edge factors as shown in Appendix B. This means that there are two different types of vertex and edge factors, yielding the same partition function. It may also support our proposal that introducing the new vertex and edge factors associated with the 5-brane web reflected over an ON-plane would be a natural procedure to distinguish original domain from the reflected domain of 5-brane system with an ON-plane.

Through the Higgsing, 5-brane configurations with ON-plane(s) can give rise to 5-brane webs for $SU(3)$ gauge theories at higher Chern-Simons level. We computed the refined partition function for $SU(3)_7$ and $SU(3)_9$ theories and confirmed that the results perfectly agree with the blowup computation [39]. We also checked our proposal against 6d E-string theory on a circle, which requires two ON-planes, which also agree with other known results. These are the first examples that the refined partition functions are obtained based on 5-brane webs with ON-plane. We also present the exact form of one- and two-instanton partition functions of these theories. For theories of higher rank gauge groups or of more complicated matter that can be described by a 5-brane web with an ON-plane [46], one can apply our new vertex and edge factors to obtain their partition functions in a straightforward way.

From the perspective of the S-duality, 5-brane configuration with an O5-plane can be understood as an S-dual configuration of that with an ON-plane. It is natural to generalize our proposal to 5-brane systems with an O5-plane, which describes 5d SO/Sp gauge theories. Though our new C^R is compatible with O5-plane, the preferred direction is assigned along the edges associated with W-bosons, and the

resulting partition function become an expansion of Coulomb branch parameters, rather than an instanton expansion. A naive attempt for refining topological vertex with an O5-plane seems more challenging because those branes which are reflected over an O5-plane are of the same Ω background parameters along the same edge. Hence, it is an interesting direction to pursue to generalize the refined topological vertex so that it is applicable to 5-brane system with an O5-plane. These would shed some light on the partition functions from newly obtained 5-brane webs which involve G_2 gauge theories, SO gauge theories with spinor matter, and Sp or SU gauge theories of hypermultiplets in the rank-3 antisymmetric representations.

It would be also interesting to study the relation between our proposal for a D -type quiver theory and algebraic constructions based on Ding-Iohara-Miki algebra where the presence of an ON-plane is discussed either from the point of view of the reflection states [56] or as the introduction of a new twisted vertex [57].

Acknowledgments

We thank Jean-Emile Bourguine, Shi Cheng, Hirotaka Hayashi, Songling He, Hee-Cheol Kim, Minsung Kim, Kimyeong Lee, Xiaobin Li, Satoshi Nawata, Yuji Sugimoto, Ryo Suzuki, Futoshi Yagi, and Ruidong Zhu for useful discussions. We are also grateful to Shi Cheng and Songling He for providing useful Mathematica codes and Futoshi Yagi and Yuji Sugimoto for their comments on the draft. SSK thanks APCTP, Fundan university, KIAS, POSTECH and YMSC Tsinghua university for the hospitality during his visit where part of this work is done. SSK is partially supported by the Fundamental Research Funds for the Central Universities 2682021ZTPY043. XYW is partially supported by NSFC grant No. 11950410490.

A Characters

The characters for the fundamental weights of $SO(8)$ $\chi_{\mathbf{dim}}^{SO(8)}$ are given as follows:

$$\begin{aligned}
\chi_{\mathbf{8v}}^{SO(8)} &= \sum_{i=1}^8 X_i^2, \\
\chi_{\mathbf{28}}^{SO(8)} &= \sum_{i=1}^8 \sum_{j>i}^8 X_i^2 X_j^2, \\
\chi_{\mathbf{8s}}^{SO(8)} &= \frac{1}{2} \left(\prod_{i=1}^4 (X_i + X_{i+4}) + \prod_{i=1}^4 (X_i - X_{i+4}) \right), \\
\chi_{\mathbf{8c}}^{SO(8)} &= \frac{1}{2} \left(\prod_{i=1}^4 (X_i + X_{i+4}) - \prod_{i=1}^4 (X_i - X_{i+4}) \right), \tag{A.1}
\end{aligned}$$

where $X_i \in \{M_1^{1/2}, \dots, M_4^{1/2}, M_1^{-1/2}, \dots, M_4^{-1/2}\}$ with the flavor mass fugacities $M_i = e^{-\beta m_i}$.

The characters for the fundamental weights of $\text{SO}(16)$ $\chi_{\mathbf{dim}}$ are given as follows:

$$\begin{aligned}
\chi_{\mathbf{16}} &= \sum_{i=1}^{16} Y_i^2, \\
\chi_{\mathbf{120}} &= \sum_{i=1}^{16} \sum_{j>i}^{16} Y_i^2 Y_j^2, \\
\chi_{\mathbf{560}} &= \sum_{i=1}^{16} \sum_{j>i}^{16} \sum_{k>j}^{16} Y_i^2 Y_j^2 Y_k^2, \\
\chi_{\mathbf{1820}} &= \sum_{i=1}^{16} \sum_{j>i}^{16} \sum_{k>j}^{16} \sum_{l>k}^{16} Y_i^2 Y_j^2 Y_k^2 Y_l^2, \\
\chi_{\mathbf{4368}} &= \sum_{i=1}^{16} \sum_{j>i}^{16} \sum_{k>j}^{16} \sum_{l>k}^{16} \sum_{m>l}^{16} Y_i^2 Y_j^2 Y_k^2 Y_l^2 Y_m^2, \\
\chi_{\mathbf{8008}} &= \sum_{i=1}^{16} \sum_{j>i}^{16} \sum_{k>j}^{16} \sum_{l>k}^{16} \sum_{m>l}^{16} \sum_{n>m}^{16} Y_i^2 Y_j^2 Y_k^2 Y_l^2 Y_m^2 Y_n^2, \\
\chi_{\mathbf{128}} &= \frac{1}{2} \left(\prod_{i=1}^8 (Y_i + Y_{i+8}) + \prod_{i=1}^8 (Y_i - Y_{i+8}) \right), \\
\chi_{\overline{\mathbf{128}}} &= \frac{1}{2} \left(\prod_{i=1}^8 (Y_i + Y_{i+8}) - \prod_{i=1}^8 (Y_i - Y_{i+8}) \right), \tag{A.2}
\end{aligned}$$

where $Y_i \in \{M_1^{1/2}, \dots, M_8^{1/2}, M_1^{-1/2}, \dots, M_8^{-1/2}\}$.

The characters for higher dimensional irreducible representations can be expressed in terms of the product of the characters of these fundamental weights. For instance, among those that appear in (3.39),

$$\begin{aligned}
\chi_{\overline{\mathbf{1920}}} + \chi_{\overline{\mathbf{128}}} &= \chi_{\mathbf{16}} \cdot \chi_{\mathbf{128}}, \\
\chi_{\mathbf{1920}} + \chi_{\mathbf{128}} &= \chi_{\mathbf{16}} \cdot \chi_{\overline{\mathbf{128}}}, \\
\chi_{\mathbf{13312}} + \chi_{\mathbf{1920}} + \chi_{\mathbf{128}} &= \chi_{\mathbf{120}} \cdot \chi_{\mathbf{128}}. \tag{A.3}
\end{aligned}$$

B Reflected 5-brane web with $C^{\mathbf{R}}$ and $\tilde{f}^{\mathbf{R}}$.

In the main text, we have introduced new vertex factor $C^{\mathbf{R}}$ and framing factor $\tilde{f}^{\mathbf{R}}$ which account for vertex and framing factors that are reflected over an ON-plane. For a 5-brane web with an ON-plane, one needs to choose the fundamental region, as there is reflected 5-brane configuration over the ON-plane. Because of the equivalence between the original 5-brane web and the reflected image, the partition function

based on either the original 5-brane web or the reflected one should be equivalent. In other words, even though one performs the topological vertex computation based on reflected web diagram with C^R and \tilde{f}^R factors, the resulting partition function should not make any difference. The new factors C^R, \tilde{f}^R and conventional C, \tilde{f} are on an equal footing.

As a concrete example, let us consider a D_4 -type quiver with $SU(3)_1$ at the center node connected to tree $SU(2)$ nodes, which is discussed in subsection 3.3. The corresponding 5-brane configuration is presented in Figure 17. The corresponding reflected 5-brane configuration can be easily depicted as given in Figure 19, where the role of C, \tilde{f} and C^R, \tilde{f}^R exchanged, compared to the original 5-brane web in Figure 17. In particular, C, \tilde{f} only appear on the strip next to an ON-plane on the left. Note that the preferred direction framing factor f in the reflected web diagram is the same as that in the unreflected web diagram as is mentioned in the main text. One can check that the partition function based on this reflected 5-brane web is the same as the one discussed in subsection 3.3.

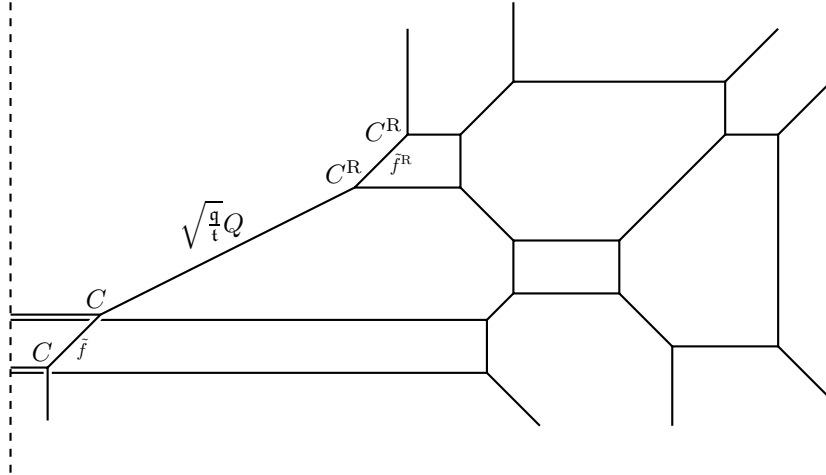


Figure 19. Reflected 5-brane configuration for a D_4 -type quiver theory discussed in Figure 17.

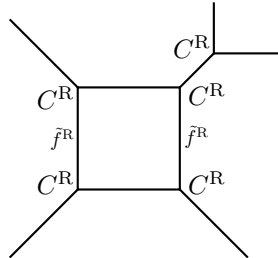


Figure 20. Web diagram of $SU(2) + 1F$ denoted by C^R and \tilde{f}^R .

It naturally follows that even for a 5-brane web without an ON-plane, one can use the new factors C^R and \tilde{f}^R , instead of using the conventional factors C and \tilde{f} . For instance, consider a 5-brane web for $SU(2)+1F$ given in Figure 20. Here in the figure, we have assigned the new vertex and framing factors C^R, \tilde{f}^R . Note that four vertex factors out of the five C^R 's in fact reduce to the usual vertex factor C because one of their legs in non-preferred direction is external, and hence effectively we have only one C^R factor presented. One can check that the partition function computation with this C^R and \tilde{f}^R is straightforward and the result is the same as the partition function obtained with C and \tilde{f} .

References

- [1] O. Aharony, A. Hanany, and B. Kol, *Webs of (p,q) five-branes, five-dimensional field theories and grid diagrams*, *JHEP* **9801** (1998) 002, [[hep-th/9710116](#)].
- [2] N. C. Leung and C. Vafa, *Branes and toric geometry*, *Adv.Theor.Math.Phys.* **2** (1998) 91–118, [[hep-th/9711013](#)].
- [3] D. R. Morrison and N. Seiberg, *Extremal transitions and five-dimensional supersymmetric field theories*, *Nucl.Phys.* **B483** (1997) 229–247, [[hep-th/9609070](#)].
- [4] M. R. Douglas, S. H. Katz, and C. Vafa, *Small instantons, Del Pezzo surfaces and type I-prime theory*, *Nucl. Phys. B* **497** (1997) 155–172, [[hep-th/9609071](#)].
- [5] K. A. Intriligator, D. R. Morrison, and N. Seiberg, *Five-dimensional supersymmetric gauge theories and degenerations of Calabi-Yau spaces*, *Nucl.Phys.* **B497** (1997) 56–100, [[hep-th/9702198](#)].
- [6] N. Seiberg, *Five-dimensional SUSY field theories, nontrivial fixed points and string dynamics*, *Phys.Lett.* **B388** (1996) 753–760, [[hep-th/9608111](#)].
- [7] E. Witten, *Small instantons in string theory*, *Nucl.Phys.* **B460** (1996) 541–559, [[hep-th/9511030](#)].
- [8] O. J. Ganor and A. Hanany, *Small $E(8)$ instantons and tensionless noncritical strings*, *Nucl.Phys.* **B474** (1996) 122–140, [[hep-th/9602120](#)].
- [9] S.-S. Kim, M. Taki, and F. Yagi, *Tao Probing the End of the World*, *PTEP* **2015** (2015), no. 8 083B02, [[arXiv:1504.03672](#)].
- [10] A. Sen, *Stable nonBPS states in string theory*, *JHEP* **06** (1998) 007, [[hep-th/9803194](#)].
- [11] A. Sen, *Stable nonBPS bound states of BPS D-branes*, *JHEP* **08** (1998) 010, [[hep-th/9805019](#)].
- [12] A. Kapustin, *$D(n)$ quivers from branes*, *JHEP* **12** (1998) 015, [[hep-th/9806238](#)].

- [13] A. Hanany and A. Zaffaroni, *Issues on orientifolds: On the brane construction of gauge theories with $SO(2n)$ global symmetry*, *JHEP* **07** (1999) 009, [[hep-th/9903242](#)].
- [14] H. Hayashi, S.-S. Kim, K. Lee, and F. Yagi, *Dualities and 5-brane webs for 5d rank 2 SCFTs*, *JHEP* **12** (2018) 016, [[arXiv:1806.10569](#)].
- [15] M. Atiyah, N. J. Hitchin, V. Drinfeld, and Y. Manin, *Construction of Instantons*, *Phys. Lett. A* **65** (1978) 185–187.
- [16] N. A. Nekrasov, *Seiberg-Witten prepotential from instanton counting*, *Adv.Theor.Math.Phys.* **7** (2004) 831–864, [[hep-th/0206161](#)].
- [17] N. Nekrasov and A. Okounkov, *Seiberg-Witten theory and random partitions*, *Prog. Math.* **244** (2006) 525–596, [[hep-th/0306238](#)].
- [18] M. Marino and N. Wyllard, *A Note on instanton counting for $N=2$ gauge theories with classical gauge groups*, *JHEP* **05** (2004) 021, [[hep-th/0404125](#)].
- [19] N. Nekrasov and S. Shadchin, *ABCD of instantons*, *Commun. Math. Phys.* **252** (2004) 359–391, [[hep-th/0404225](#)].
- [20] F. Fucito, J. F. Morales, and R. Poghossian, *Instantons on quivers and orientifolds*, *JHEP* **10** (2004) 037, [[hep-th/0408090](#)].
- [21] C. Hwang, J. Kim, S. Kim, and J. Park, *General instanton counting and 5d SCFT*, *JHEP* **07** (2015) 063, [[arXiv:1406.6793](#)]. [Addendum: *JHEP* **04**, 094 (2016)].
- [22] J.-t. Ding and K. Iohara, *Generalization and deformation of Drinfeld quantum affine algebras*, *Lett. Math. Phys.* **41** (1997) 181–193, [[q-alg/9608002](#)].
- [23] K. Miki, *$a(q, \gamma)$ analog of the $w_{1+\infty}$ algebra*, *Journal of Mathematical Physics* **48** (2007), no. 12 123520, [<https://doi.org/10.1063/1.2823979>].
- [24] H. Awata, B. Feigin, and J. Shiraishi, *Quantum Algebraic Approach to Refined Topological Vertex*, *JHEP* **03** (2012) 041, [[arXiv:1112.6074](#)].
- [25] J.-E. Bourgin, M. Fukuda, K. Harada, Y. Matsuo, and R.-D. Zhu, *(p, q) -webs of DIM representations, 5d $\mathcal{N} = 1$ instanton partition functions and qq -characters*, *JHEP* **11** (2017) 034, [[arXiv:1703.10759](#)].
- [26] M. Aganagic, M. Marino, and C. Vafa, *All loop topological string amplitudes from Chern-Simons theory*, *Commun.Math.Phys.* **247** (2004) 467–512, [[hep-th/0206164](#)].
- [27] M. Aganagic, A. Klemm, M. Marino, and C. Vafa, *The Topological vertex*, *Commun.Math.Phys.* **254** (2005) 425–478, [[hep-th/0305132](#)].
- [28] A. Iqbal, C. Kozcaz, and C. Vafa, *The Refined topological vertex*, *JHEP* **0910** (2009) 069, [[hep-th/0701156](#)].
- [29] H. Awata and H. Kanno, *Refined BPS state counting from Nekrasov’s formula and Macdonald functions*, *Int.J.Mod.Phys.* **A24** (2009) 2253–2306, [[arXiv:0805.0191](#)].
- [30] M. Aganagic and S. Shakirov, *Refined Chern-Simons Theory and Topological String*, [[arXiv:1210.2733](#)].

- [31] H. Nakajima and K. Yoshioka, *Instanton counting on blowup. 1.*, *Invent. Math.* **162** (2005) 313–355, [[math/0306198](#)].
- [32] J. Gu, M.-x. Huang, A.-K. Kashani-Poor, and A. Klemm, *Refined BPS invariants of 6d SCFTs from anomalies and modularity*, *JHEP* **05** (2017) 130, [[arXiv:1701.00764](#)].
- [33] M.-x. Huang, K. Sun, and X. Wang, *Blowup Equations for Refined Topological Strings*, *JHEP* **10** (2018) 196, [[arXiv:1711.09884](#)].
- [34] J. Gu, B. Haghighat, K. Sun, and X. Wang, *Blowup Equations for 6d SCFTs. I*, *JHEP* **03** (2019) 002, [[arXiv:1811.02577](#)].
- [35] J. Gu, A. Klemm, K. Sun, and X. Wang, *Elliptic blowup equations for 6d SCFTs. Part II. Exceptional cases*, *JHEP* **12** (2019) 039, [[arXiv:1905.00864](#)].
- [36] J. Gu, B. Haghighat, A. Klemm, K. Sun, and X. Wang, *Elliptic blowup equations for 6d SCFTs. Part III. E-strings, M-strings and chains*, *JHEP* **07** (2020) 135, [[arXiv:1911.11724](#)].
- [37] J. Gu, B. Haghighat, A. Klemm, K. Sun, and X. Wang, *Elliptic Blowup Equations for 6d SCFTs. IV: Matters*, [arXiv:2006.03030](#).
- [38] J. Kim, S.-S. Kim, K.-H. Lee, K. Lee, and J. Song, *Instantons from Blow-up*, *JHEP* **11** (2019) 092, [[arXiv:1908.11276](#)]. [Erratum: *JHEP* 06, 124 (2020)].
- [39] H.-C. Kim, M. Kim, S.-S. Kim, and K.-H. Lee, *Bootstrapping BPS spectra of 5d/6d field theories*, *JHEP* **04** (2021) 161, [[arXiv:2101.00023](#)].
- [40] H.-C. Kim, M. Kim, and S.-S. Kim, *5d/6d Wilson loops from blowups*, *JHEP* **08** (2021) 131, [[arXiv:2106.04731](#)].
- [41] A. Sen, *F theory and orientifolds*, *Nucl.Phys.* **B475** (1996) 562–578, [[hep-th/9605150](#)].
- [42] H. Hayashi, H.-C. Kim, and T. Nishinaka, *Topological strings and 5d T_N partition functions*, *JHEP* **1406** (2014) 014, [[arXiv:1310.3854](#)].
- [43] H. Hayashi and G. Zoccarato, *Partition functions of web diagrams with an $O7^-$ -plane*, *JHEP* **03** (2017) 112, [[arXiv:1609.07381](#)].
- [44] S. Cheng and S.-S. Kim, *Refined topological vertex for a 5D $Sp(N)$ gauge theories with antisymmetric matter*, *Phys. Rev. D* **104** (2021), no. 8 086004, [[arXiv:1809.00629](#)].
- [45] G. Zafrir, *Brane webs and $O5^-$ -planes*, *JHEP* **03** (2016) 109, [[arXiv:1512.08114](#)].
- [46] H. Hayashi, S.-S. Kim, K. Lee, M. Taki, and F. Yagi, *More on 5d descriptions of 6d SCFTs*, *JHEP* **10** (2016) 126, [[arXiv:1512.08239](#)].
- [47] G. Zafrir, *Brane webs in the presence of an $O5^-$ -plane and 4d class S theories of type D*, *JHEP* **07** (2016) 035, [[arXiv:1602.00130](#)].
- [48] H. Hayashi, S.-S. Kim, K. Lee, and F. Yagi, *Rank-3 antisymmetric matter on 5-brane webs*, *JHEP* **05** (2019) 133, [[arXiv:1902.04754](#)].

- [49] S.-S. Kim and F. Yagi, *Topological vertex formalism with O5-plane*, *Phys. Rev.* **D97** (2018) 026011, [[arXiv:1709.01928](#)].
- [50] H. Hayashi and R.-D. Zhu, *More on topological vertex formalism for 5-brane webs with O5-plane*, [arXiv:2012.13303](#).
- [51] X. Li and F. Yagi, *Thermodynamic limit of Nekrasov partition function for 5-brane web with O5-plane*, *JHEP* **06** (2021) 004, [[arXiv:2102.09482](#)].
- [52] H.-C. Kim, M. Kim, and S.-S. Kim, *Topological vertex for 6d SCFTs with \mathbb{Z}_2 -twist*, [arXiv:2101.01030](#).
- [53] S. Nawata and R.-D. Zhu, *Instanton counting and O-vertex*, *JHEP* **09** (2021) 190, [[arXiv:2107.03656](#)].
- [54] D. Kutasov, *Orbifolds and solitons*, *Phys. Lett.* **B383** (1996) 48–53, [[hep-th/9512145](#)].
- [55] A. Sen, *Duality and orbifolds*, *Nucl. Phys.* **B474** (1996) 361–378, [[hep-th/9604070](#)].
- [56] J.-E. Bourguine, M. Fukuda, Y. Matsuo, and R.-D. Zhu, *Reflection states in Ding-Iohara-Miki algebra and brane-web for D-type quiver*, *JHEP* **12** (2017) 015, [[arXiv:1709.01954](#)].
- [57] T. Kimura and R.-D. Zhu, *Web Construction of ABCDEFG and Affine Quiver Gauge Theories*, *JHEP* **09** (2019) 025, [[arXiv:1907.02382](#)].
- [58] L. Bao, V. Mitev, E. Pomoni, M. Taki, and F. Yagi, *Non-Lagrangian Theories from Brane Junctions*, *JHEP* **1401** (2014) 175, [[arXiv:1310.3841](#)].
- [59] F. Benini, S. Benvenuti, and Y. Tachikawa, *Webs of five-branes and $N=2$ superconformal field theories*, *JHEP* **0909** (2009) 052, [[arXiv:0906.0359](#)].
- [60] H. Hayashi, S.-S. Kim, K. Lee, M. Taki, and F. Yagi, *A new 5d description of 6d D-type minimal conformal matter*, *JHEP* **08** (2015) 097, [[arXiv:1505.04439](#)].
- [61] H.-C. Kim, S.-S. Kim, and K. Lee, *5-dim Superconformal Index with Enhanced E_n Global Symmetry*, *JHEP* **10** (2012) 142, [[arXiv:1206.6781](#)].
- [62] R. Gopakumar and C. Vafa, *M theory and topological strings. 1.*, [hep-th/9809187](#).
- [63] R. Gopakumar and C. Vafa, *M theory and topological strings. 2.*, [hep-th/9812127](#).
- [64] J. Kim, S. Kim, K. Lee, J. Park, and C. Vafa, *Elliptic Genus of E-strings*, [arXiv:1411.2324](#).
- [65] S.-S. Kim, Y. Sugimoto, and F. Yagi, *Surface defects on E-string from 5-brane webs*, *JHEP* **12** (2020) 183, [[arXiv:2008.06428](#)].
- [66] V. Mitev, E. Pomoni, M. Taki, and F. Yagi, *Fiber-Base Duality and Global Symmetry Enhancement*, *JHEP* **1504** (2015) 052, [[arXiv:1411.2450](#)].
- [67] P. Jefferson, H.-C. Kim, C. Vafa, and G. Zafrir, *Towards Classification of 5d SCFTs: Single Gauge Node*, [arXiv:1705.05836](#).

- [68] P. Jefferson, S. Katz, H.-C. Kim, and C. Vafa, *On Geometric Classification of 5d SCFTs*, *JHEP* **04** (2018) 103, [[arXiv:1801.04036](#)].
- [69] S. S. Razamat and G. Zafrir, *Compactification of 6d minimal SCFTs on Riemann surfaces*, *Phys. Rev. D* **98** (2018), no. 6 066006, [[arXiv:1806.09196](#)].
- [70] H. Nakajima and K. Yoshioka, *Instanton counting on blowup. II. K-theoretic partition function*, [math/0505553](#).
- [71] L. Gottsche, H. Nakajima, and K. Yoshioka, *K-theoretic Donaldson invariants via instanton counting*, *Pure Appl. Math. Quart.* **5** (2009) 1029–1111, [[math/0611945](#)].